

Telescope & Instrument Fundamentals

Luc Simard

Astronomy 511
Spring 2018

Outline

- Apertures, surfaces, stops and pupils
- Aberrations and telescope designs
- Imaging
- Spectroscopy
- Observing Strategies and Calibrations
- Data Reduction

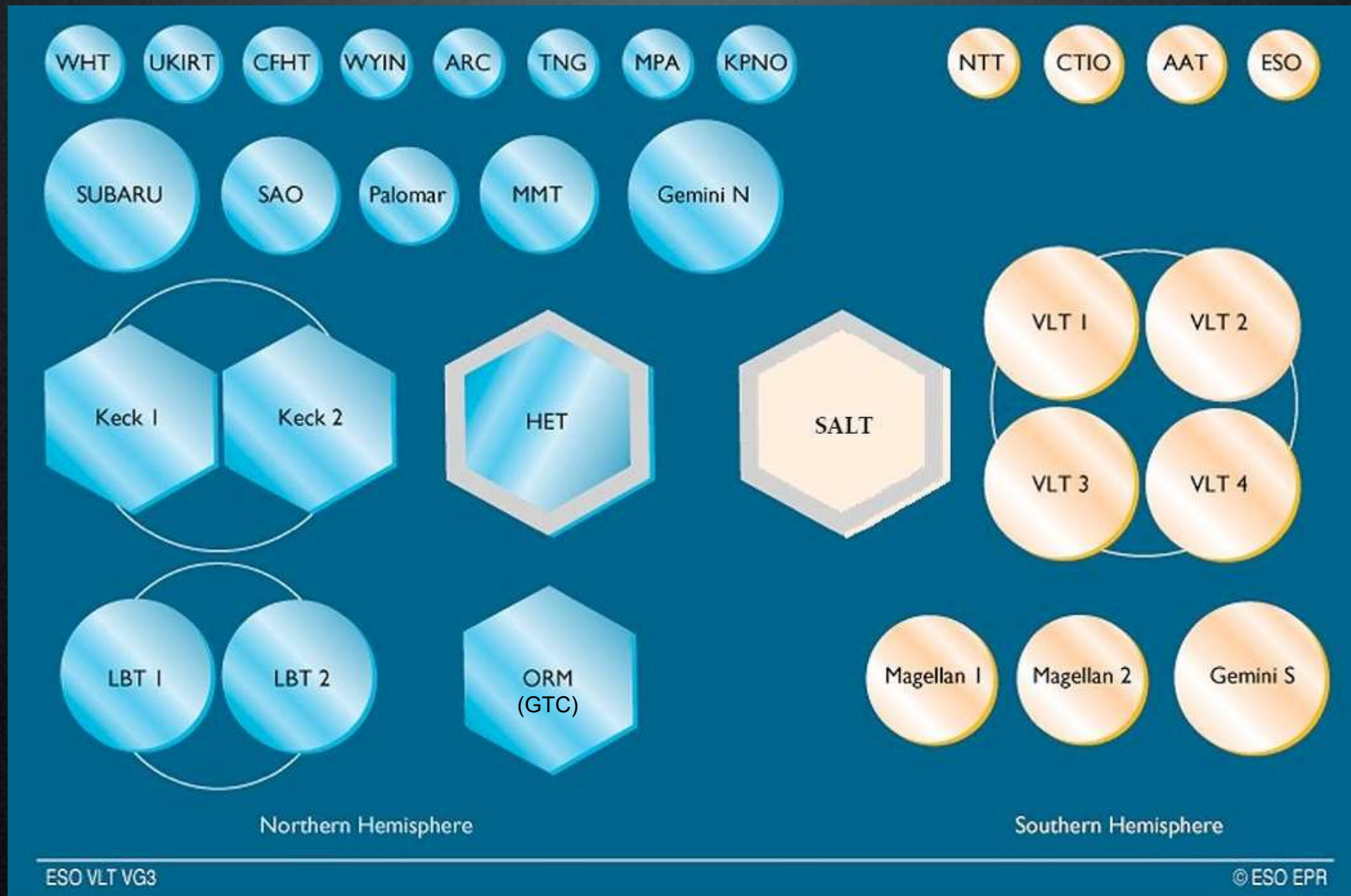
What makes a good telescope site?

- Number of clear and photometric nights (> 300)
- Larger isoplanatic angle
- Longer coherence time
- Low water vapor content
- Small pressure broadening (mid-IR)



Hawaii and Chile are considered to be the best sites on Earth thanks to a combination of geographical factors. Do you know what they are?
(Hint: Proximity to a beach is not one of them.)

Collecting Area of the Large Telescopes



All 4-meter class primary mirrors are monolithic

8-10-meter class primary mirrors are either monolithic or segmented -
dividing line is between 8 and 10 meters.

Primary Aperture - Monolithic



Gemini

Thin meniscus (thickness = 20 cm)

D = 8.1m

120 actuators

Lower mass = lower thermal inertia



Magellan 1+2/LBT1+2/GMT

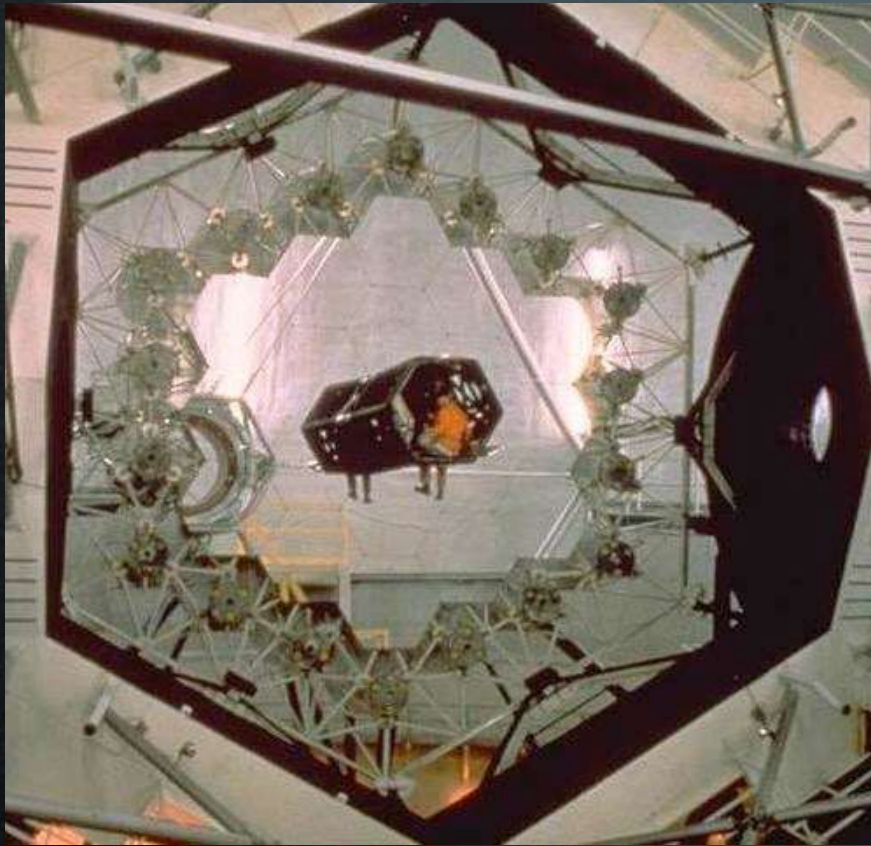
Honeycomb (thickness = 80-110 cm)

D = 8.4m

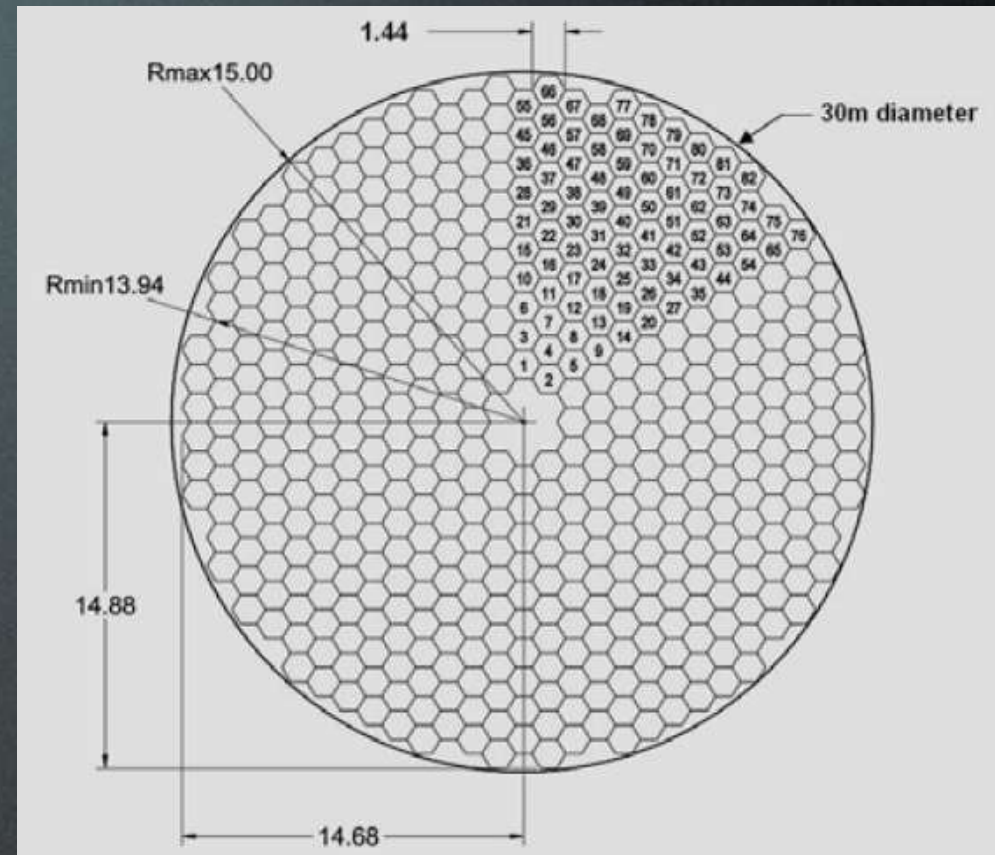
1750 alumina silica cores (D = 20 cm)

Total mass = 15% mass of a solid blank

Primary Aperture - Segmented



Keck
36 hexagonal segments
Diameter = 1.8 m
Thickness = 75 mm
Weight = 400 kg
Gap = 3 mm

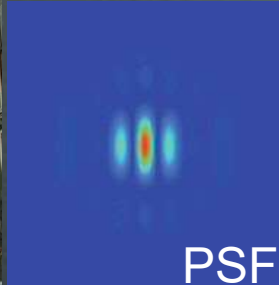


TMT
492 hexagonal segments
(82 distinct segments)
Diameter = 1.44 m
Thickness = 45 mm

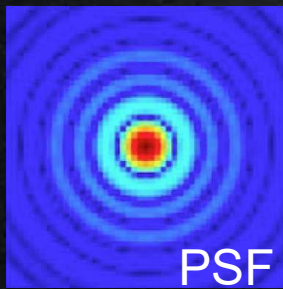
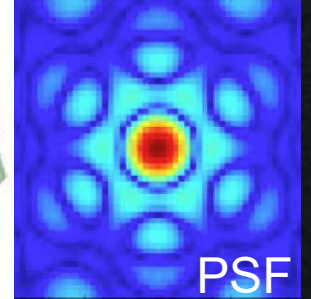
Primary Aperture - "Diluteness"



Large Binocular Telescope



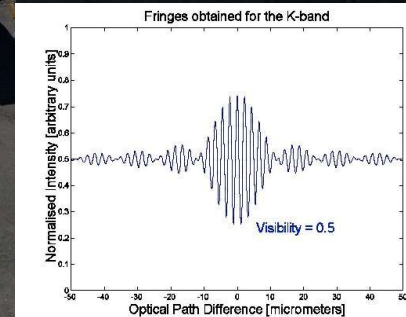
Giant Magellan Telescope



Monolithic,
unobscured,
circular aperture



VLT Interferometer



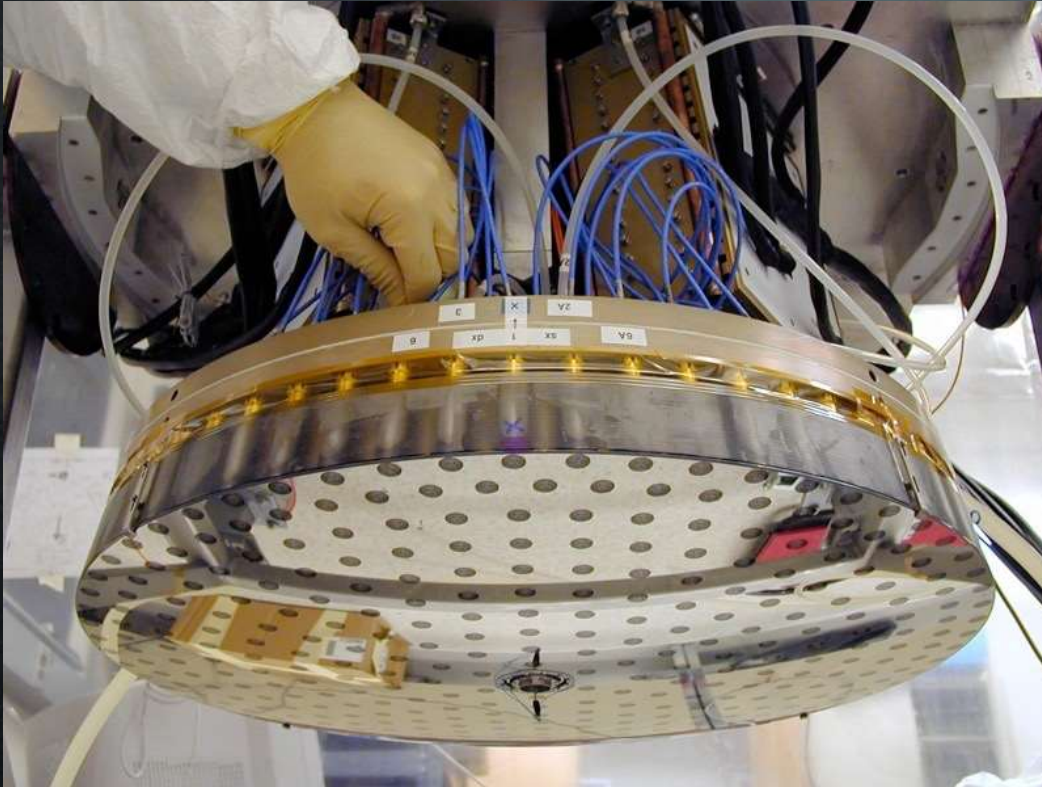
Secondary Aperture - Conventional Optical Reflector



Gemini Secondary
D = 1.023m
Central Hole D = 0.168m
Convex hyperboloid
Weight = 65 kg
Material: Schott Zerodur
Tip-tilt Frequency = 20 Hz
Light structure to minimize IR emissivity

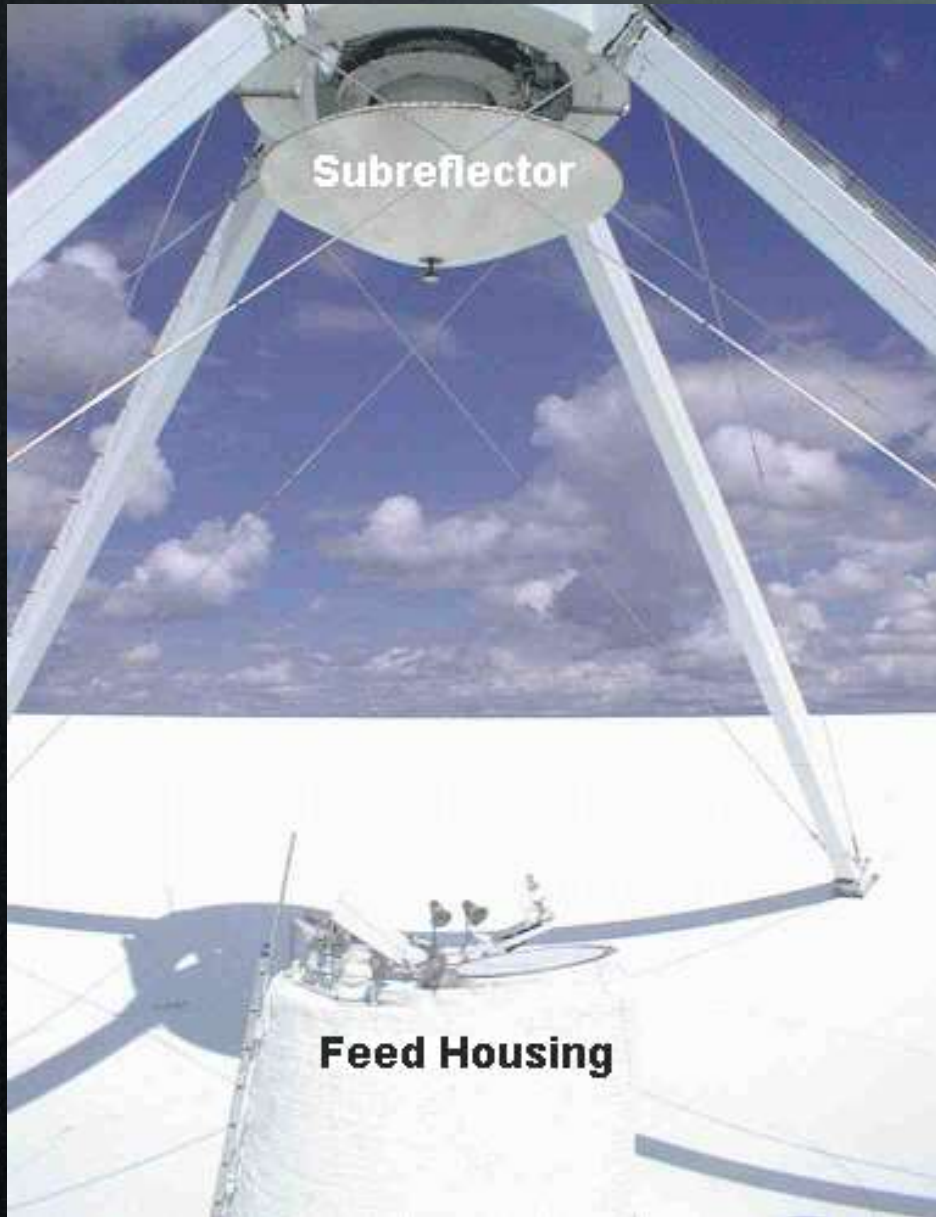


Secondary Aperture - Adaptive



MMT Adaptive Secondary
D = 640 mm
Glass shell 2 mm thick
30 microns above reference plate
336 actuators

Secondary Aperture - Subreflector



Antenna subreflectors can be jittered around for on/offsource chopping

VLBA Antenna Subreflector

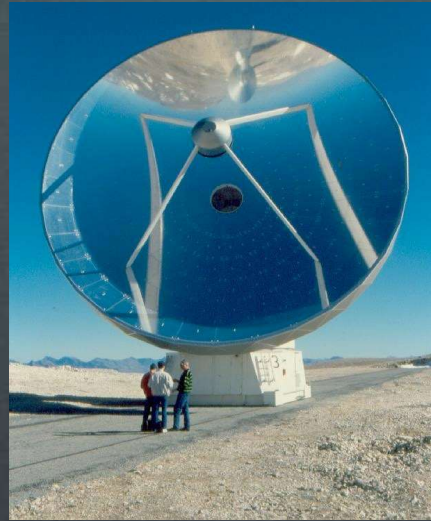


Surface Tolerance

Parkes



Plateau du Bure



HST



Reflector surface tolerance is dictated by the observing wavelength, and it is usually quoted as a fraction of the observing wavelength.

For example, the HST primary mirror had to meet a tolerance of $1/70 \lambda$. For an observing wavelength of 500 nm, this means that the rms surface errors (i.e., “bumps”) had to be less than 7 nm. The HST mirror is one of the most precise polished surface ever produced. It just had the wrong figure.

In comparison, a radio dish would have to have bumps smaller than 3 mm to be of equal optical quality. This requirement is a factor of $\sim 5 \times 10^5$ looser! This is why one can build 100-m radio dish, but an optical mirror of that size is a completely different story. This is also the reason why synthetic apertures are easier to produce at radio/submm wavelengths than in the optical.

Stops and Pupils

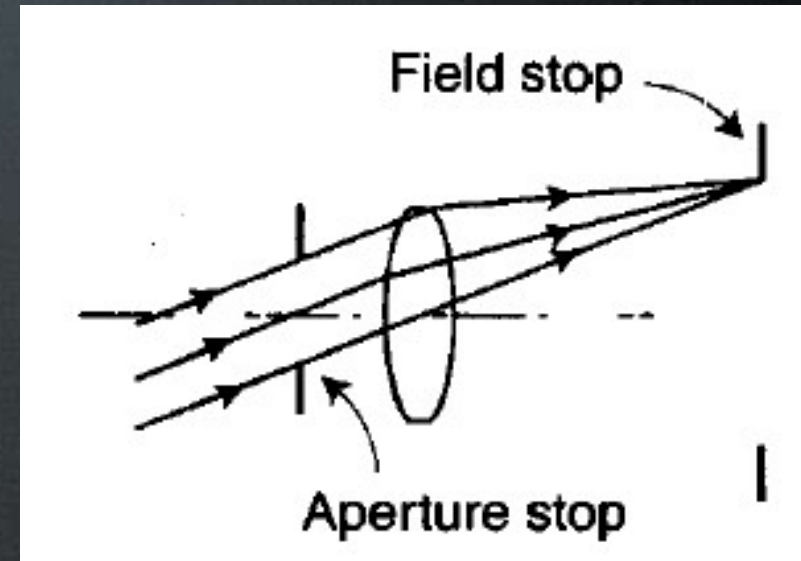
The amount of light transmitted by a telescope or an astronomical instrument depends on the dimension of the optical elements and the stops.

A stop is an aperture in an opaque screen i.e., primary mirrors are aperture stops.

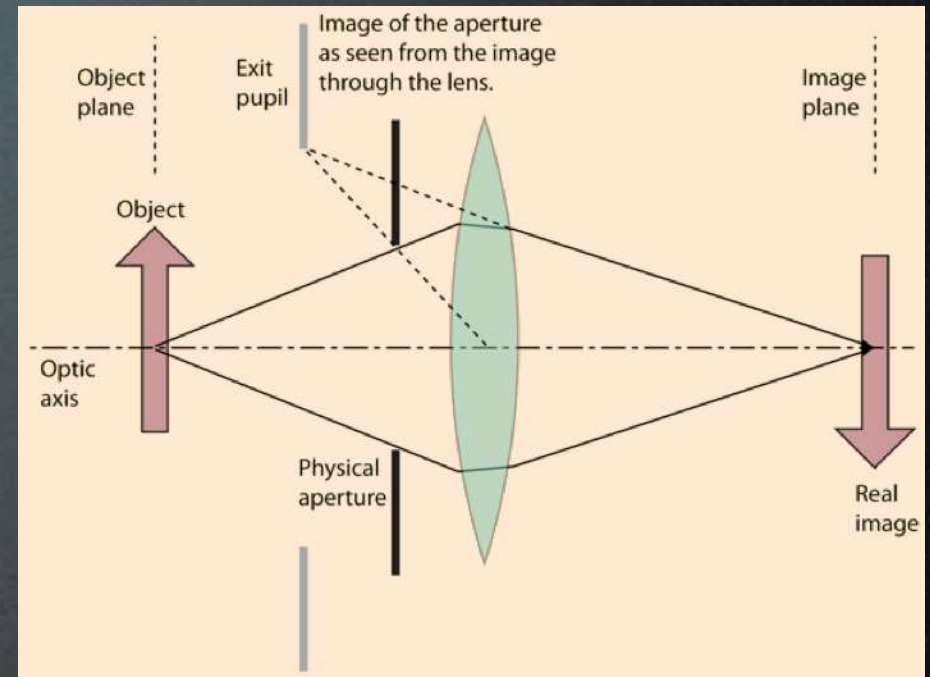
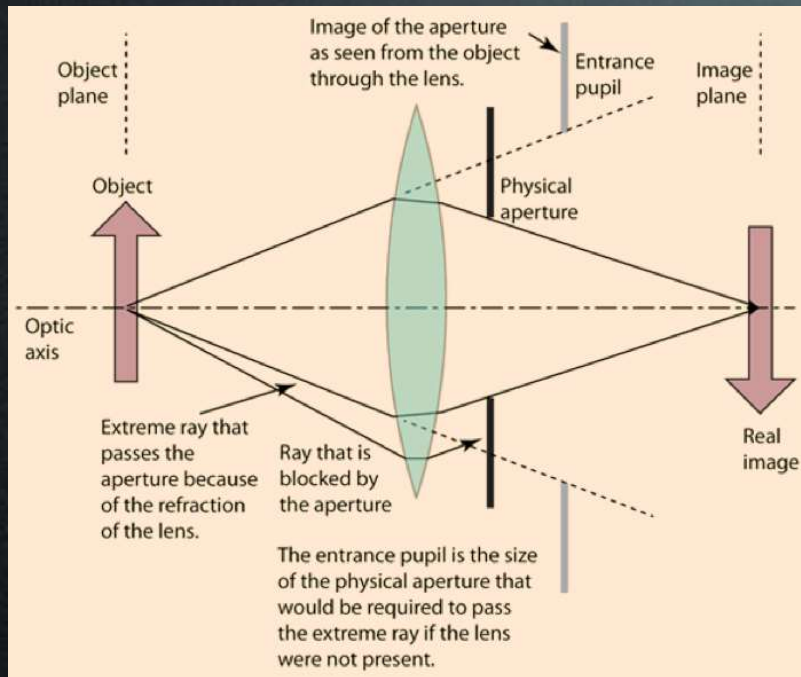
A field stop is an element that determines the angular size of the field that is imaged by the system, i.e. the boundaries of the detector.

The image of the aperture stop formed by that part of the system preceding it in the optical train is called the entrance pupil. In other words, the entrance pupil is the limiting aperture that the light rays “see” looking into the optical system from the object.

For most telescopes, the entrance pupil is the primary mirror (exception: LAMOST).



Stops and Pupils (continued)



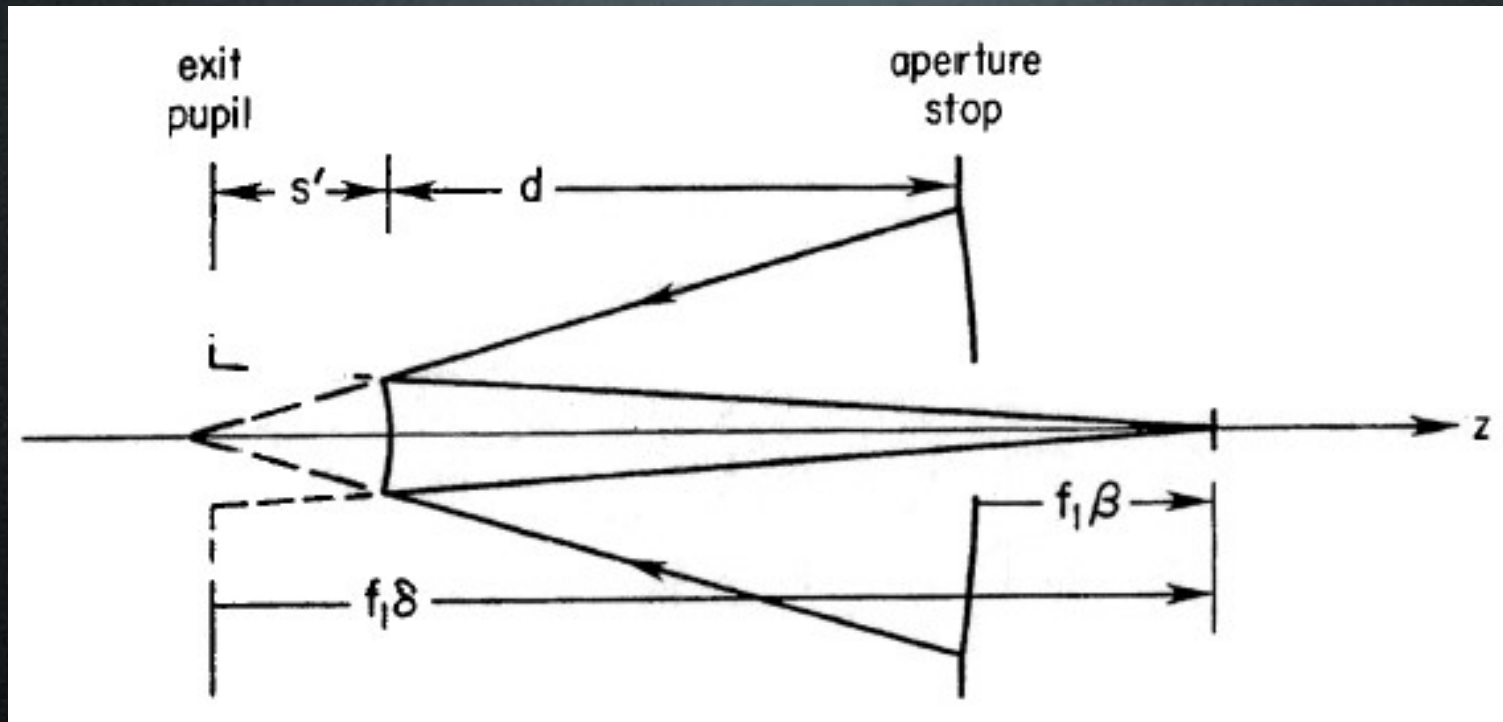
The entrance pupil of a system is the image of the aperture stop as seen from a point on the optical axis in the object plane.

The exit pupil of a system is the image of the aperture stop as seen from a point on the optical axis in the image plane.

The significance of the exit pupil is that rays from the boundary of the aperture stop approach the final image as if coming from the boundary of the exit pupil for all angles of incidence at the aperture stop.

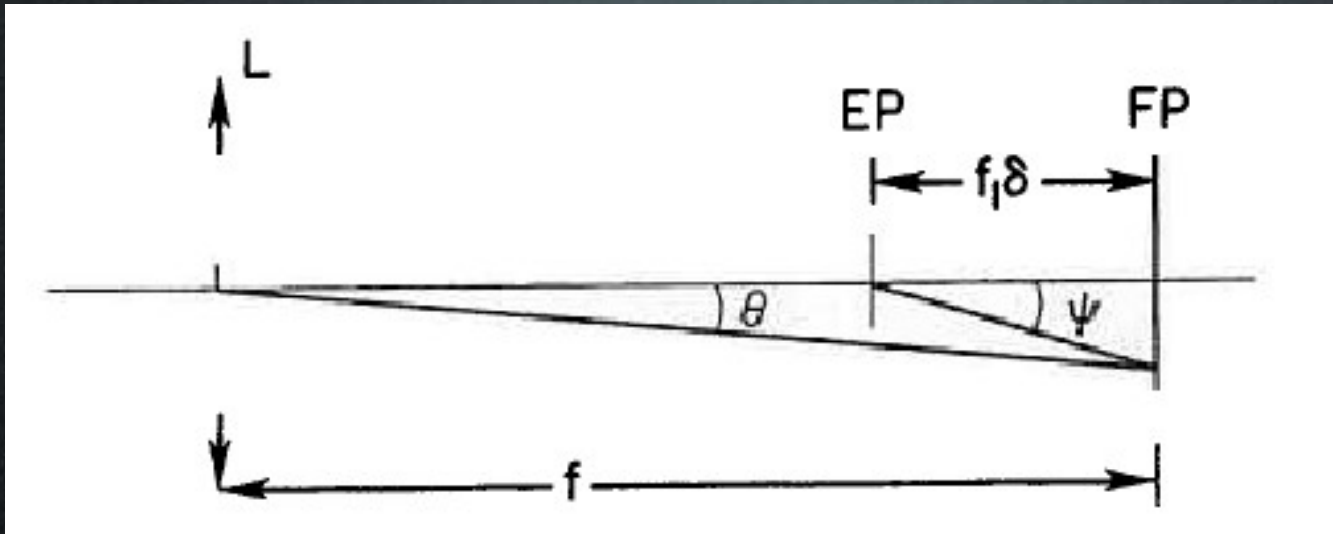
Thus a pupil can be defined as the cross-section of a bundle of rays where light from all parts of the object pass through, in equal amounts, completely mixed, with no preferential spatial separation.

Stops and Pupils (continued)



If the aperture stop of a telescope is the primary mirror, the exit pupil is the image of the primary formed by the secondary.

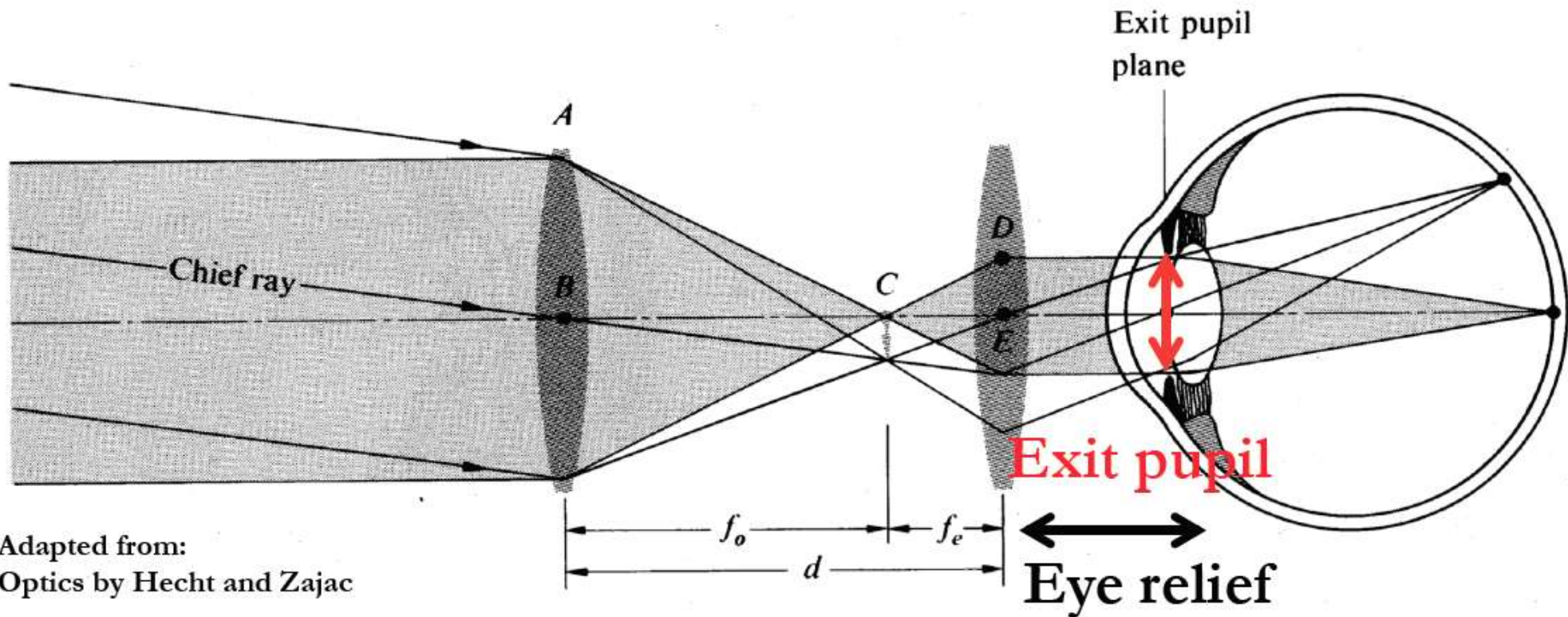
Plate Scale and Field of View



From the definition of the exit pupil (EP), the plate scale S of the telescope at the focal plane (FP) depends solely on the focal length f , i.e.

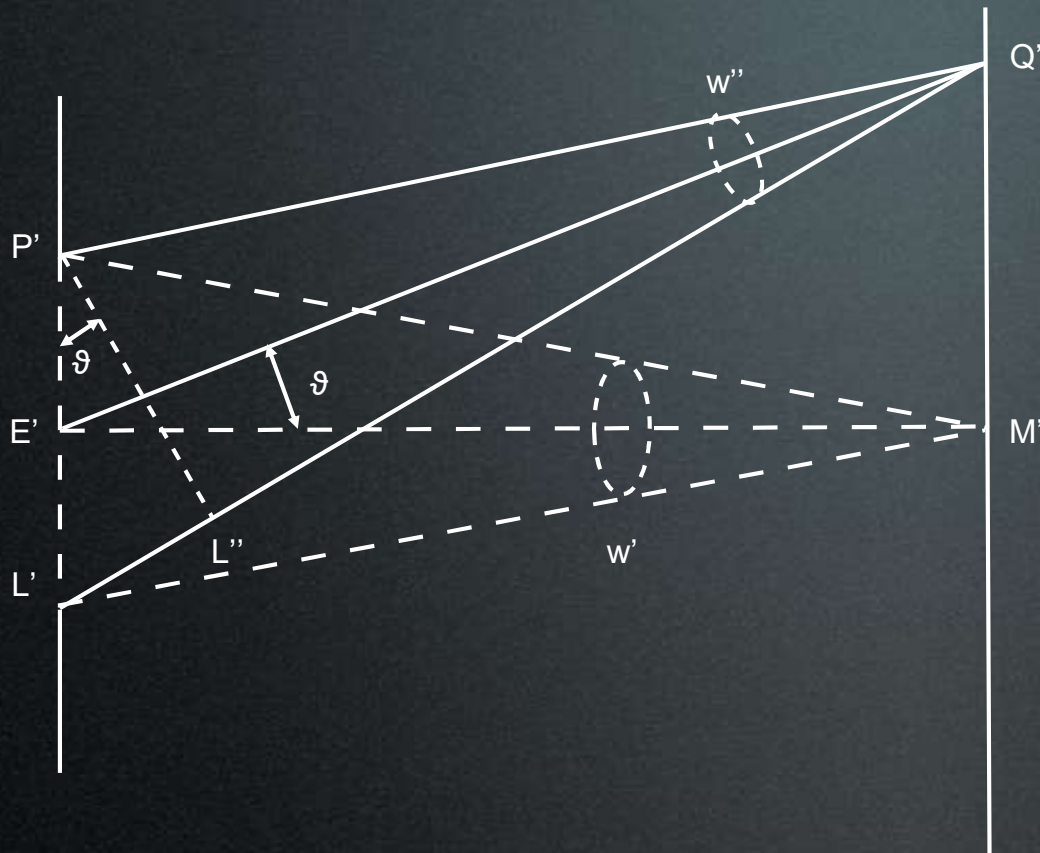
$$S = \frac{180 \times 60 \times 60}{\pi f} \simeq \frac{206264.8}{f(\text{mm})} (\text{arcseconds/mm})$$

The field of view is set by the detector size in mm.



Adapted from:
 Optics by Hecht and Zajac

Illuminance and Vignetting



P'E'L' represent the exit pupil, which has the uniform brightness B' equal to that of the source

At the axial point M' , the illuminance is equal to $B'w'$

For a point such Q' , illuminance is decreased due to:

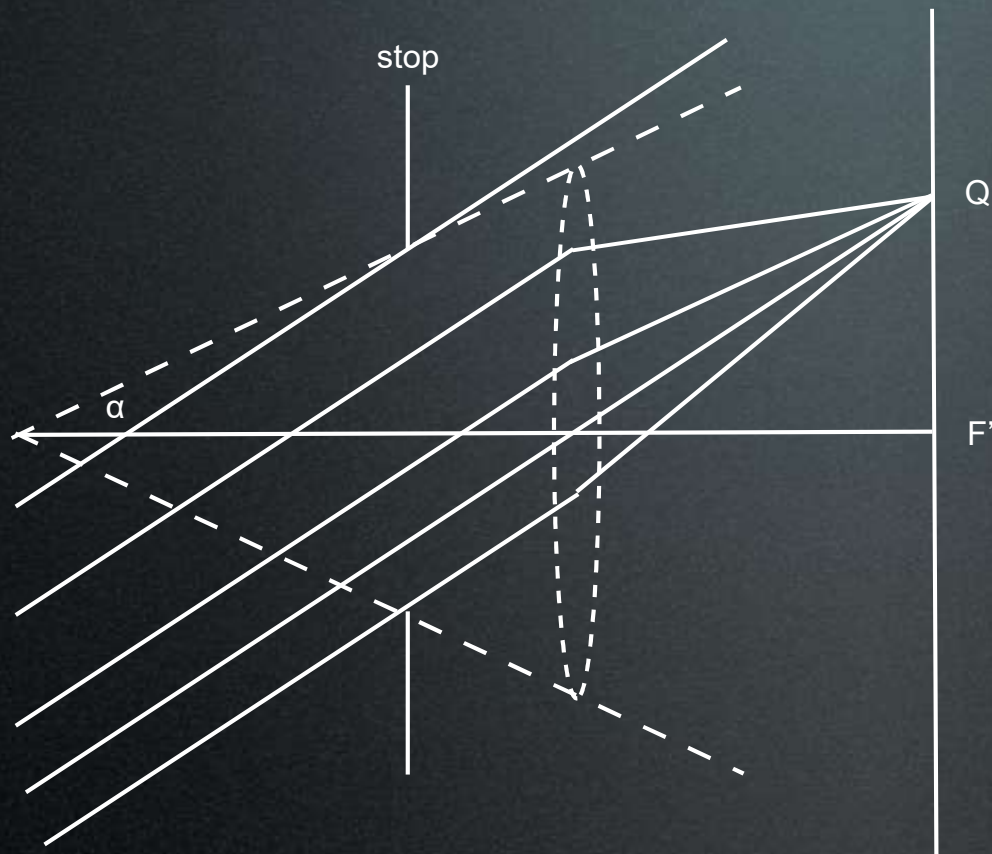
- (1) a factor $w''/w' = \cos^2\theta$
- (2) a factor $P'L''/P'L' = \cos\theta$ representing the decrease in area of the exit pupil from Q' compared with that seen from M' .
- (3) another $\cos\theta$ factor coming from the fact that the light is not normally incident at Q'

Therefore, the illuminance at Q' is

$$E'' = B'w' \cos^4 \theta$$

This is known as the “cosine fourth” law

Illuminance and Vignetting (continued)

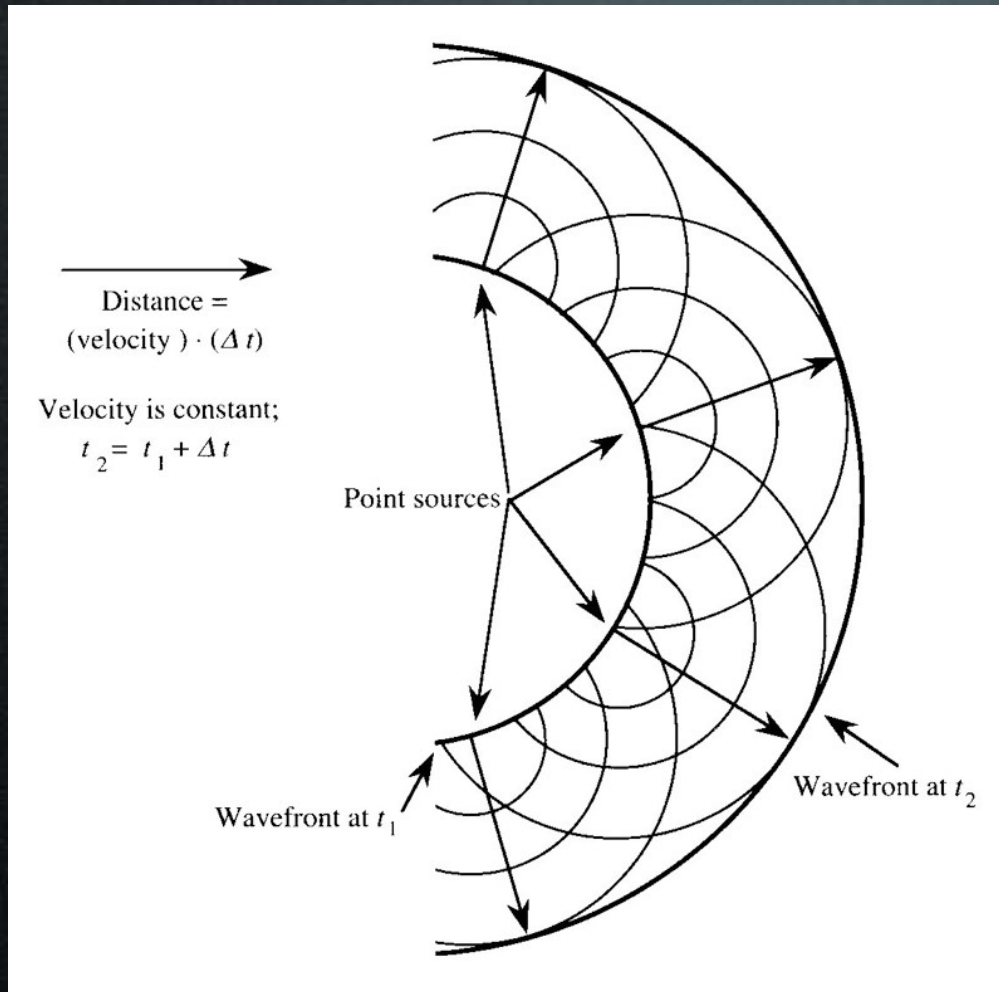


However, some optical configurations will lead to the illuminance falling off from axis faster than the cosine fourth law would predict. This is known as vignetting.

The aperture of the stop (such a telescope tube) is smaller than that of the lens at the angle of incidence shown. Some of the rays at the top miss the lens altogether, and the bottom of the lens receives no light.

For distant object points, the field that is reproduced without vignetting covers angles up to the value of α .

Huygen's Principle



Important point:
Waves from a single point are in phase.

Devices such as slits or antennae are
our tools to isolate these points for any
type of interference.

Now, let us see what happens when the Huygens
principle is applied to a circular aperture ...

Fresnel Number

This is a dimensionless parameter given by

$$F \equiv \frac{a^2}{\lambda R}$$

where a is the characteristic size (“radius”) of the aperture, λ is the wavelength and R is the distance from the aperture.

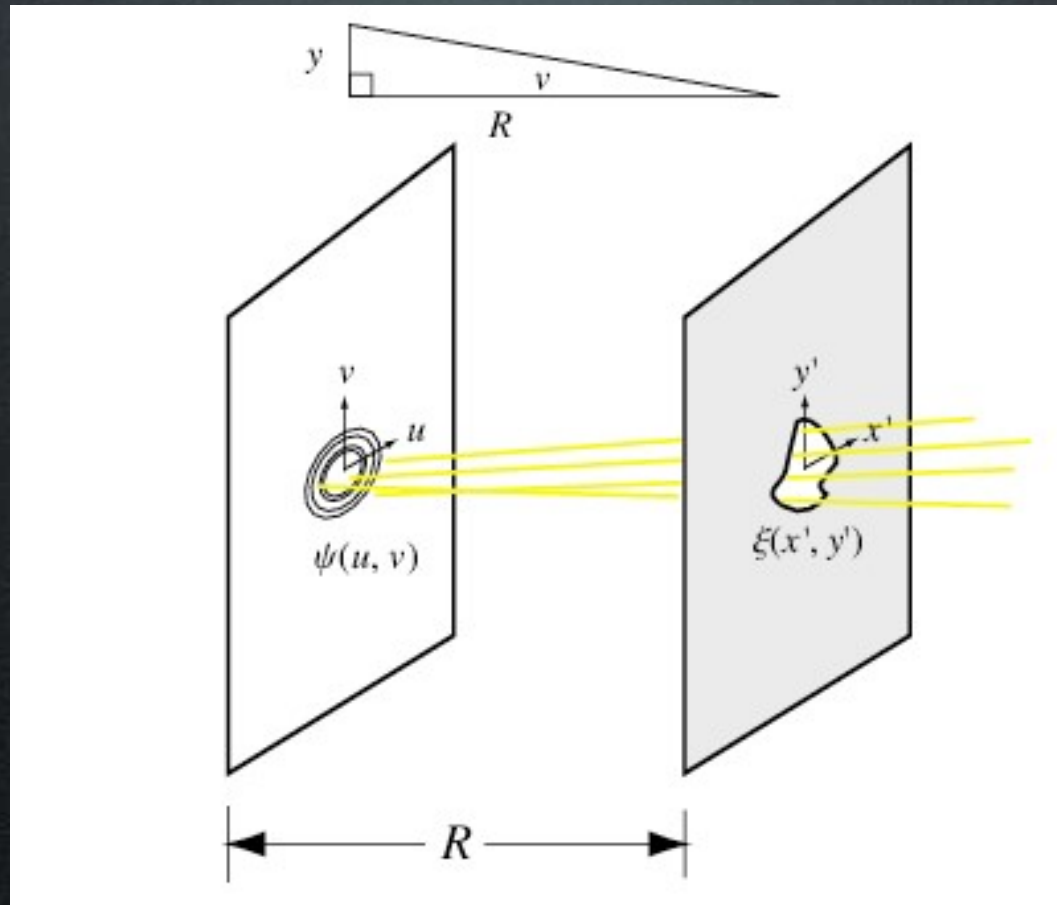
The Fresnel number is used to distinguish between two regimes: $F \ll 1$ (Fraunhofer diffraction) and $F \geq 1$ (Fresnel diffraction).

Astronomical systems operate mostly in the Fraunhofer regime.

Diffraction From a Circular Aperture

(<http://scienceworld.wolfram.com/physics/FraunhoferDiffraction.html>)

In Fraunhofer diffraction, the diffraction pattern is independent of the distance to the screen. It depends only on the angles from the aperture to the screen.



$$\psi(x, y) = C \int_{\text{aperture}} \xi(x', y') e^{-ik(xx' + yy')/R} dx' dy'$$

where C is a constant and k is the wavenumber. This is the Fraunhofer-Kirchhoff diffraction integral.

Diffraction From a Circular Aperture (continued)

For $x/R \ll 1$ and $y/R \ll 1$, we can approximate the integral by the **Fourier transform**

$$\psi(u, v) = C \int_{\text{aperture}} \xi(x', y') e^{-ik(ux' + vy')} dx' dy'$$

where $u \approx x/R$ and $v \approx y/R$ are the angular coordinates. Now, consider an elliptical aperture with semi-major axis a and semi-minor axis b . Define scaled coordinates $X = x'/a$ and $Y = y'/b$. Then

$$dx' dy' = \frac{1}{ab} dX dY$$

$$\psi(u, v) = ab \int \int_D e^{-ik(auX + bvY)} dX dY$$

Integration
over unit disk
D

Switching to polar coordinates

$$\psi(u, v) = ab \int_0^1 \int_0^{2\pi} e^{-ikr(au\cos\theta + bv\sin\theta)} r d\theta dr$$

Linear combination of a cosine and sine with the same period can be re-written as a single sinusoid, so

$$au\cos\theta + bv\sin\theta = \beta\cos(\theta + \delta) \quad \delta = \tan^{-1}\left(-\frac{bv}{au}\right)$$

$$\beta = \sqrt{a^2u^2 + b^2v^2}$$

Diffraction From a Circular Aperture (continued)

Therefore,

$$\psi(u, v) = ab \int_0^1 \int_0^{2\pi} e^{-ik\beta r \cos(\theta + \delta)} r d\theta dr$$

Using the following Bessel function integral identities

$$J_0(x) = \frac{1}{2\pi} \int_0^{2\pi} e^{-ix \cos \phi} d\phi \quad \int_0^z t J_0(t) dt = z J_1(z)$$

We get

$$\psi(u, v) = 2\pi ab \int_0^1 J_0(\beta kr) r dr$$

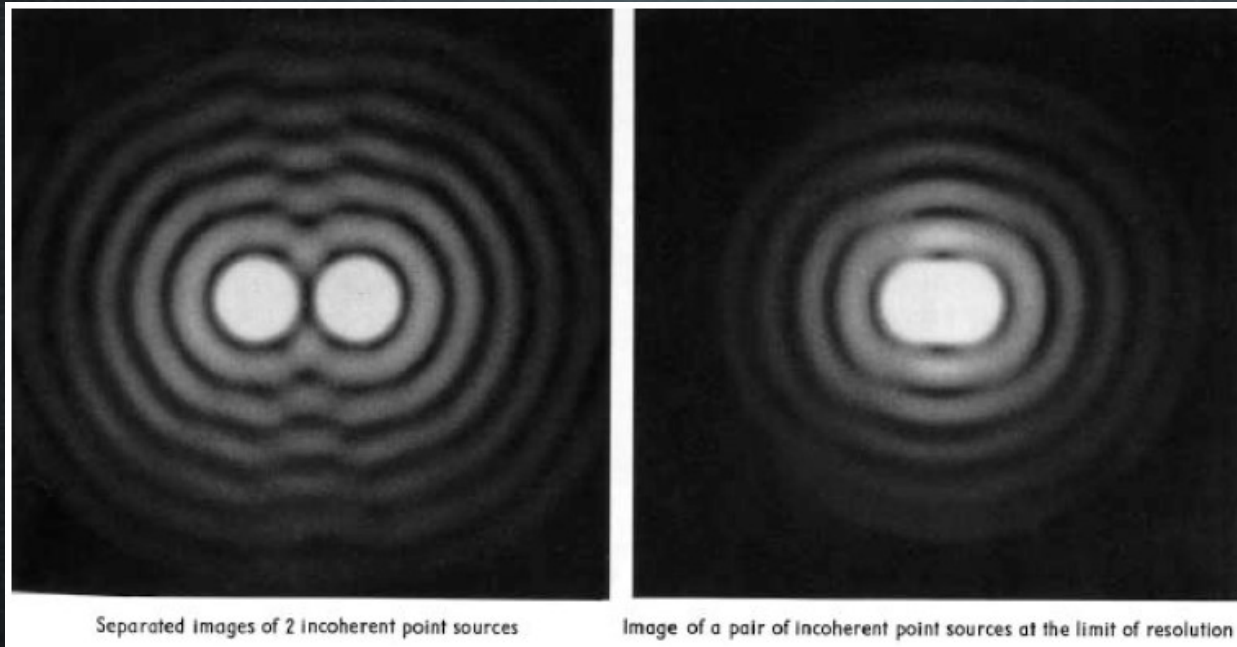
$$\psi(u, v) = 2\pi ab \frac{J_1(k\beta)}{k\beta}$$

$$\psi(u, v) = 2\pi a^2 \frac{J_1(ka\rho)}{ka\rho} \quad \rho = \sqrt{u^2 + v^2}$$

$$I \propto \psi^2(u, v) \propto \left[\frac{J_1(x)}{x} \right]^2$$

“Airy Disk”

Rayleigh's Resolution Criterion



Two sources will be resolved if the center of Source 2 is located at the first minimum in the Airy pattern of Source 1

$$\frac{J_1(x_i)}{x_i} = 0$$

Zeroes of the Airy disk pattern

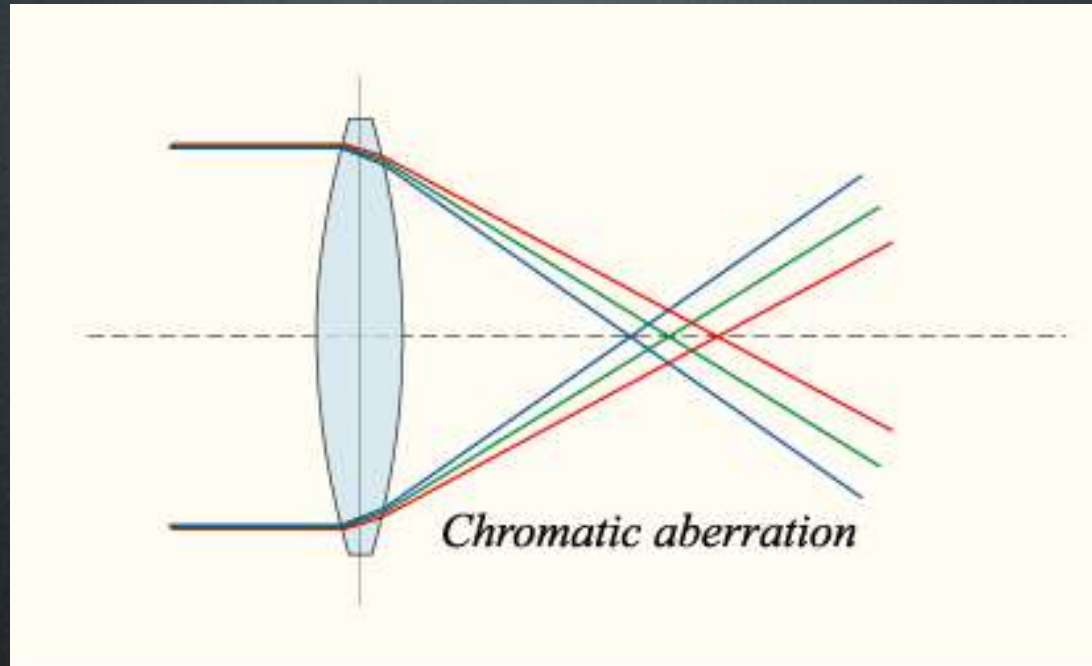
$$x_1 = k a \sin\theta = \frac{2\pi}{\lambda} a \sin\theta = \frac{\pi}{\lambda} D \sin\theta = 3.83166\dots$$

$$\theta = \sin^{-1}\left(\frac{3.83166\lambda}{\pi D}\right) \simeq \frac{3.83166\lambda}{\pi D}$$

$$\theta = 1.21967 \frac{\lambda}{D}$$

The criterion we see over and over and over and over ...

Aberration - Chromatic



A lens will not focus different colors in exactly the same place because the focal length depends on refraction, and the index of refraction is larger for bluer wavelengths.

Chromatic aberration obviously does not apply to mirrors.

Aberration - Spherical

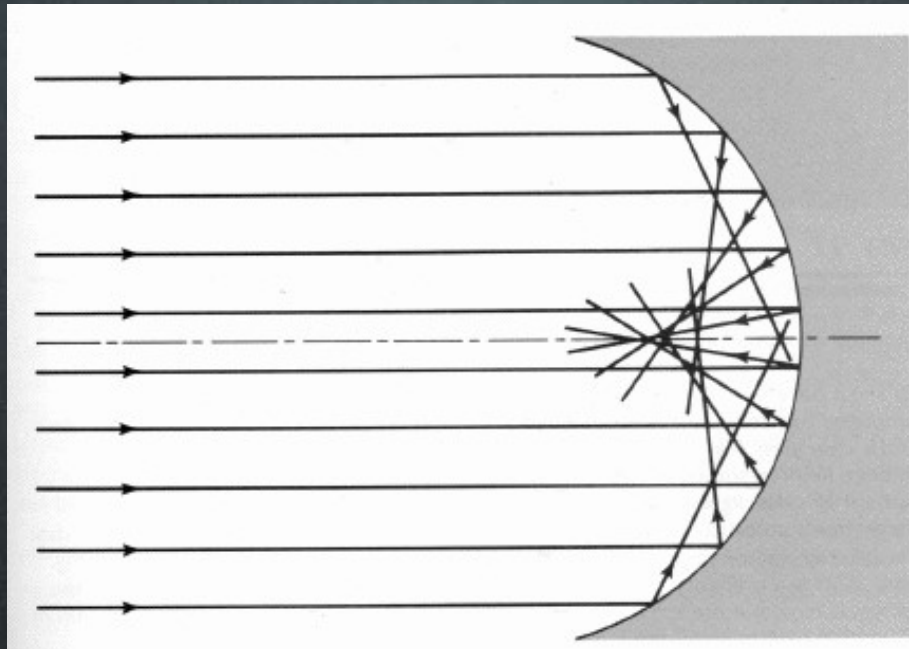
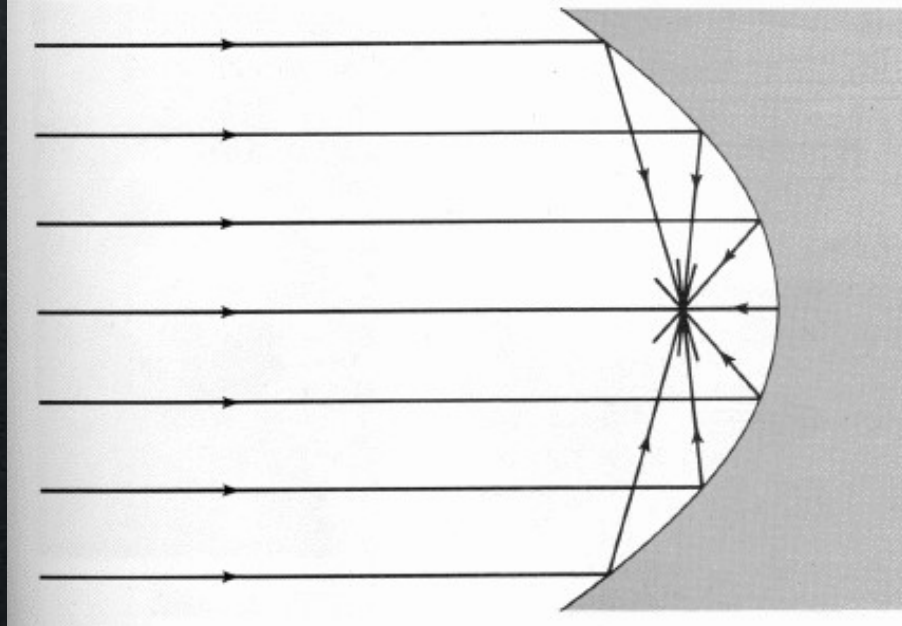


FIGURE 3.35

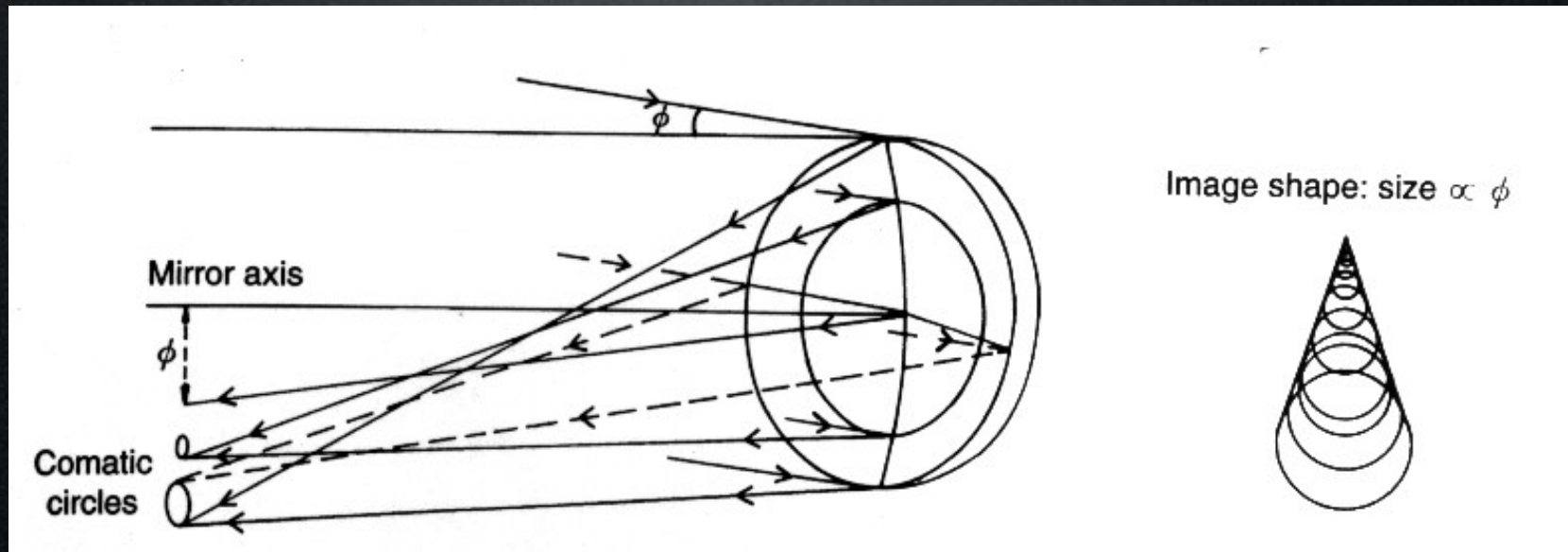
Spherical aberration in a concave mirror.



Aberration - Coma

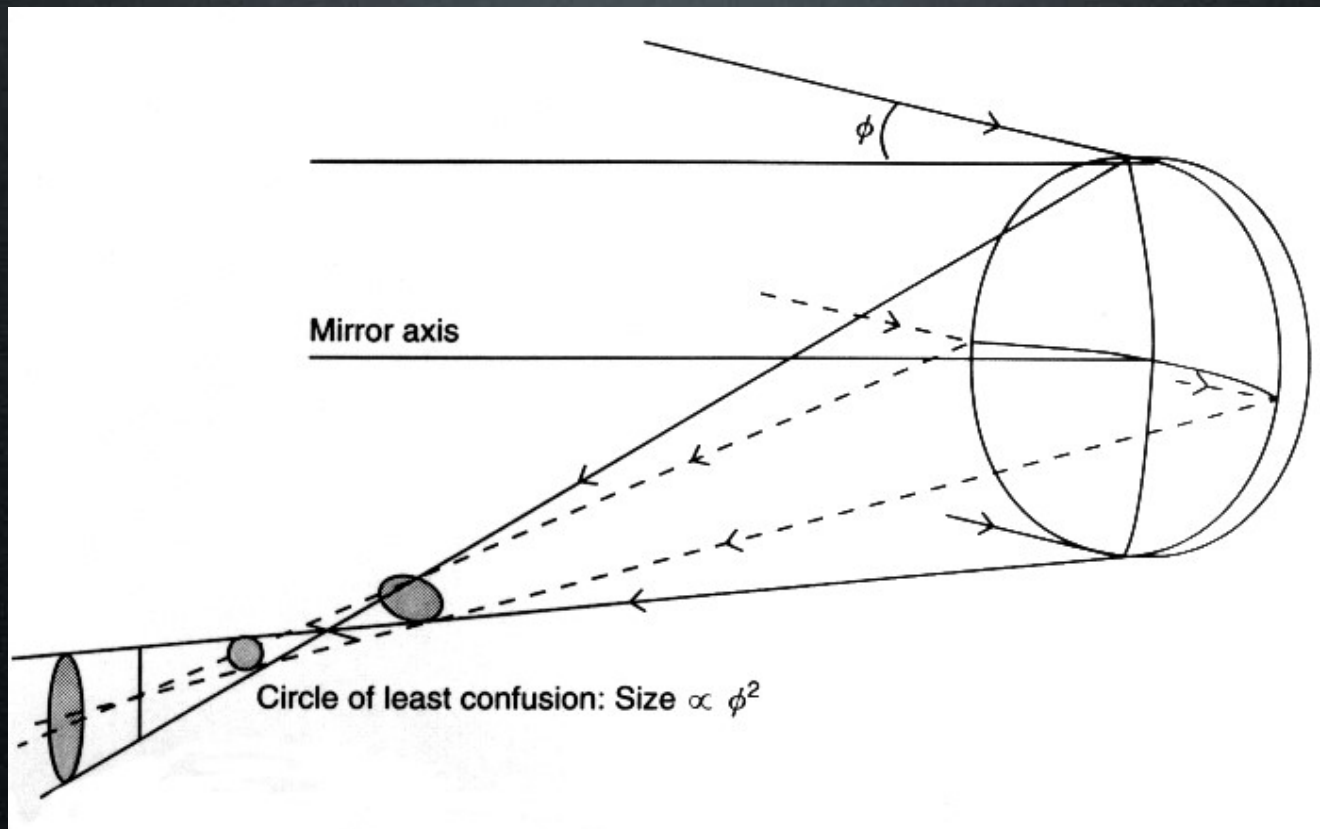
Coma is an aberration that appears as we move off the optical axis of the collector. A point source is distorted into a comet-like appearance.

Considering a lens, the off-axis ray that passes through the centre of the lens will go to a focus without deviation. Rays parallel with this ray, but a distance from it, so that they make a small circle about the central ray, will be focused to a circle that is not centered on the central ray. The sum of all such circles is the comet-shaped image. This also applies to mirrors as shown below:



Aberration - Astigmatism

Yet another kind of aberration is astigmatism. This also involves rays coming at an angle to the optical axis of the collector. Now, however, we distinguish whether the rays are off-centre "up-down" or "side-to-side". The "up-down" is called the tangential plane and the "side-to-side" is called the sagittal plane. Astigmatism is present if the rays in the two planes are focused at different points.



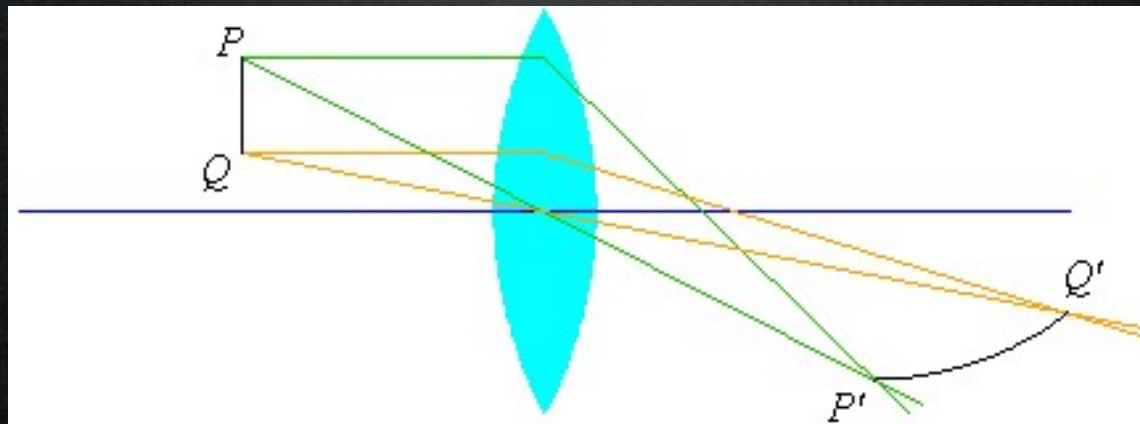
Aberration - Distortion

The shape of the image is not a true copy of the object, even though it may be in sharp focus. The two kinds of distortion are barrel, in which the image is bowed convex around the centre line, and pin cushion, in which the image is bowed concave around the centre line.

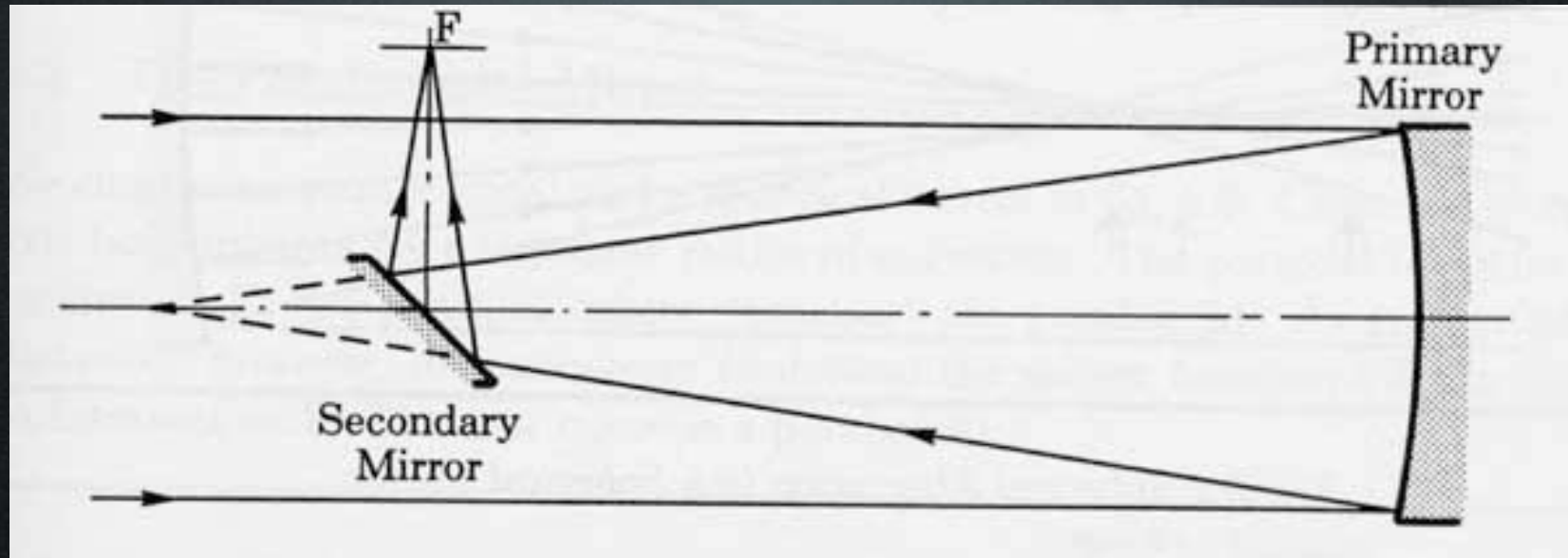


Aberration - Curvature of Field

Image does not fall on a flat plane, i.e., the focal plane is curved.



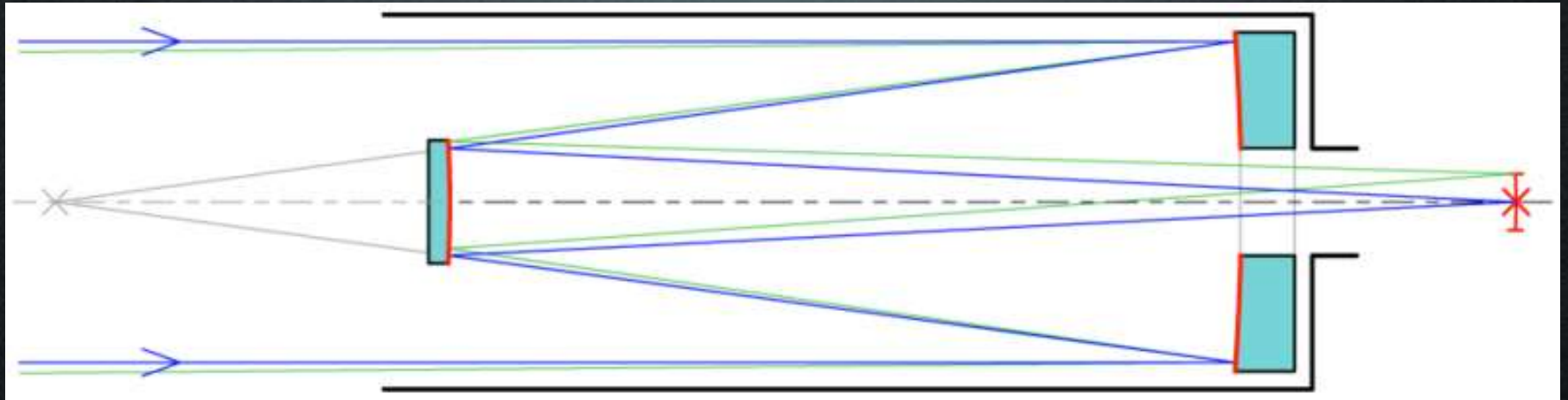
Newtonian Telescope



The Newtonian usually has a paraboloid primary mirror. A flat secondary mirror reflects the light to a focal plane at the side of the top of the telescope tube.

Essentially used only in small amateur telescopes nowadays.

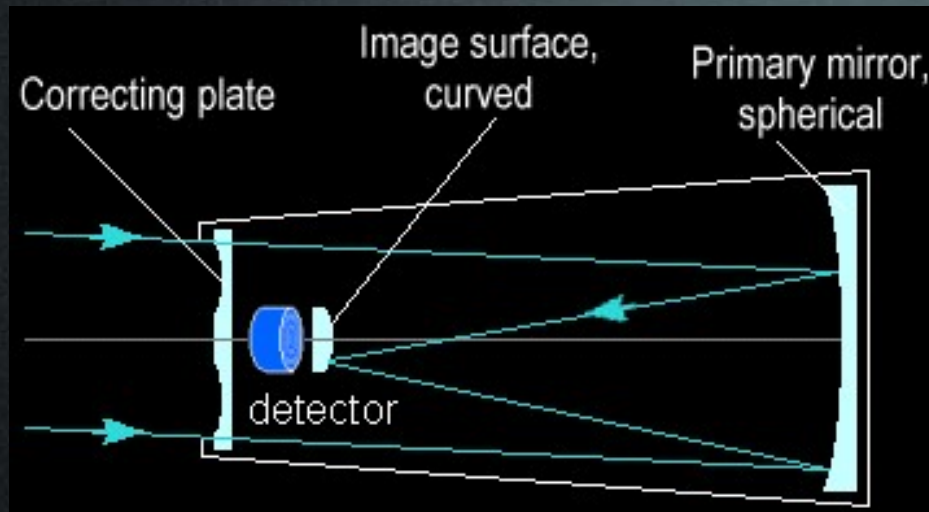
Cassegrain Telescope



The Cassegrain has a parabolic primary mirror (concave), and a hyperbolic secondary mirror (convex) that reflects the light back down through a hole in the primary. Folding the optics makes this a compact design.

Instruments are mounted at the back of the primary. This means that they are operating under a varying gravity vector.

Schmidt Telescope



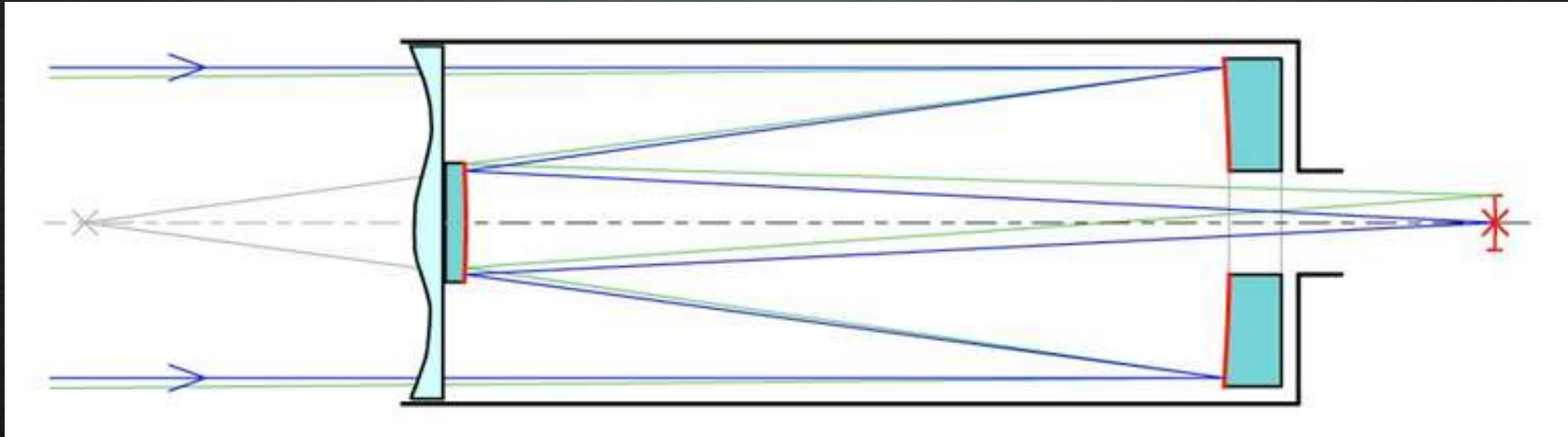
The Schmidt telescope has a spherical primary mirror, and an aspherical correcting lens, known as a corrector plate, located at the radius of curvature of the primary mirror. The detector is placed inside the telescope, at the prime focus.

A spherical mirror is easier to make, and its focus is halfway between its surface and its radius of curvature. If the tube narrows down to a small opening at the centre of curvature, then all rays entering the telescope will be nearly along a radius of the mirror, and these rays will be perpendicular to the surface. Coma is thus minimized, and images remain sharp over large fields of view.

Chromatic aberration is small because the correcting plate is thin.

However, the focal plane may be curved! One has to bend the detector.

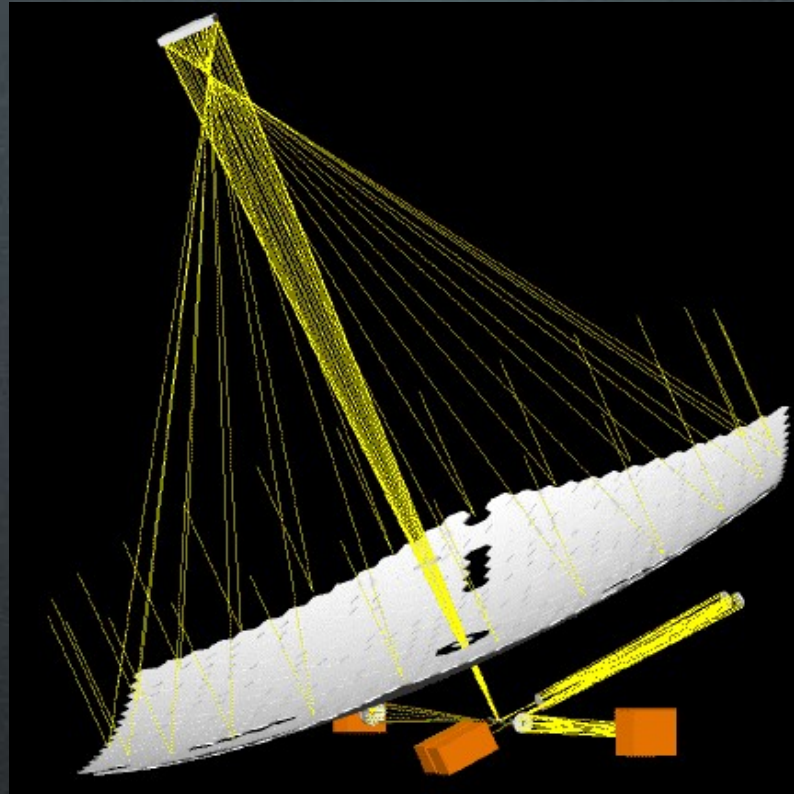
Schmidt-Cassegrain Telescope



The optical design combines elements from both the Schmidt and Cassegrain telescopes. In this system the parabolic primary mirror is replaced by a spherical mirror, which introduces spherical aberration. This is corrected by the Schmidt corrector plate, found in the Schmidt telescope. From the Cassegrain, it inherits the convex secondary mirror, perforated primary mirror, and a final focal plane located behind the primary. Some designs add additional optical elements (such as field flatteners) near the focal plane.

This design is the perfect example of a catadioptric system - it uses both lenses and mirrors

Gregorian Telescope



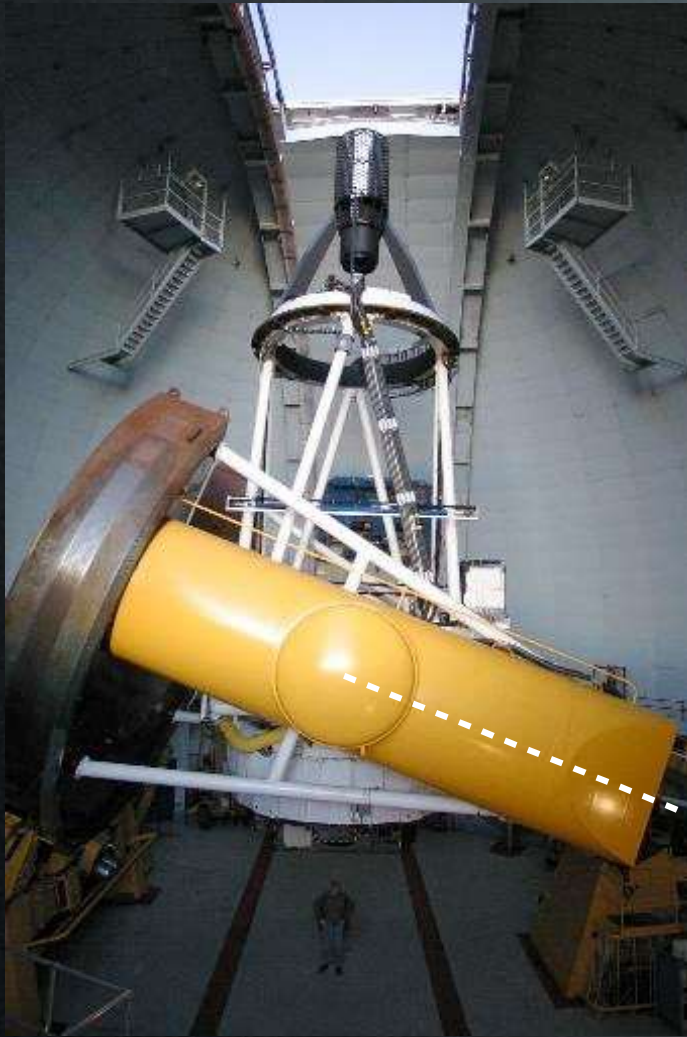
EURO50 ELT
Concept

Uses a concave (not convex) secondary. Concave surfaces are easier to figure and test.

Longer than a Cassegrain. This is bad for minimizing telescope and dome sizes unless primary mirror can have a short focal length.

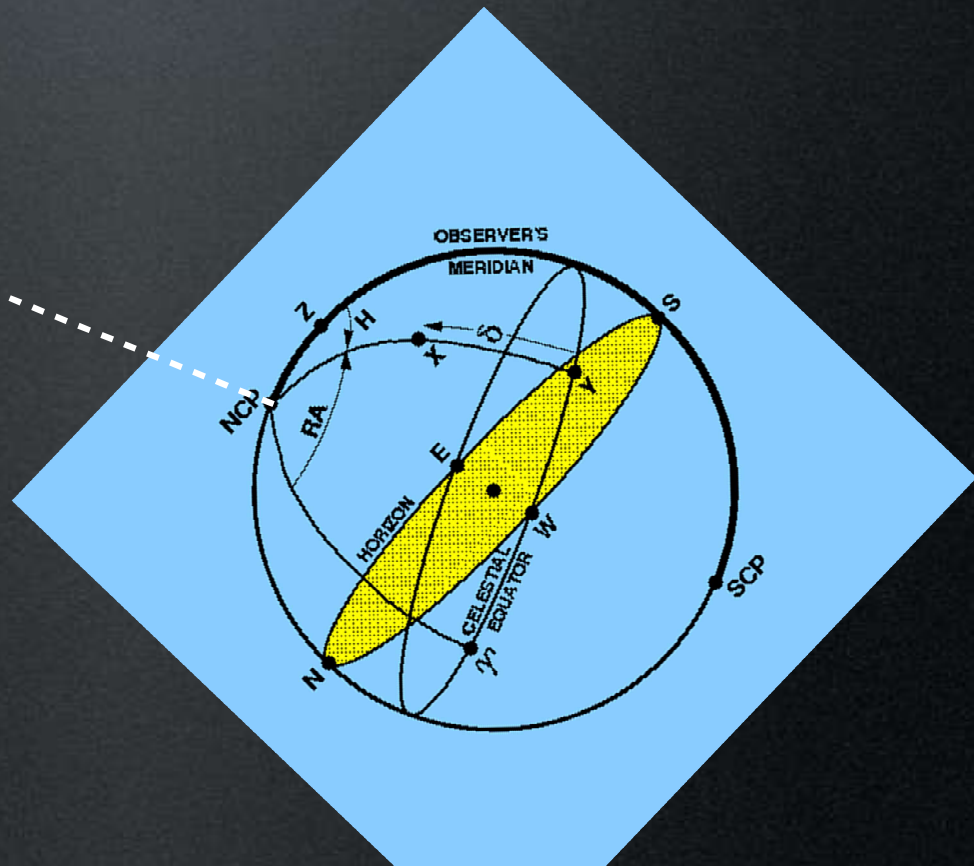
Calibration sources such as artificial stars can be inserted at the primary mirror focus. This is extremely useful for testing adaptive optics systems.

Telescope Mounts -Equatorial



3.6-m Canada-France-Hawaii
Telescope (Horseshoe)

- Pro: Follows the “natural” coordinate system of the sky - no field rotation
- Con: Heavy



Telescope Mounts - Altitude-Azimuth



Altitude



Azimuth

Every large (> 4m) telescope!

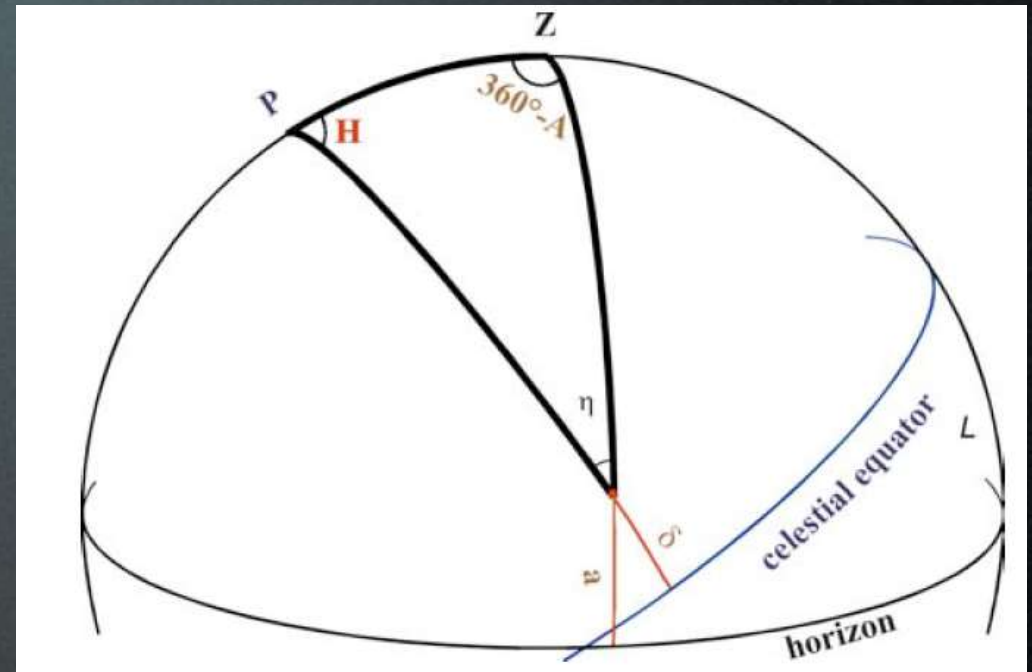
- Pro:
 - “Lightweight” (CFHT is heavier than a Keck telescope)
 - Cheaper
 - Gravity-invariant instrument foci
- Con: Field rotation
 - De-rotators needed
 - Cable wraps needed

Telescope Mounts - Altitude-Azimuth - Field Rotation

The parallactic angle η is the angle between an object's hour circle and its vertical circle.

The rate of change of parallactic angle gives the field rotation rate that must be corrected.

For an observer at latitude L , a star field centered at zenith angle z and azimuth A will rotate at a rate

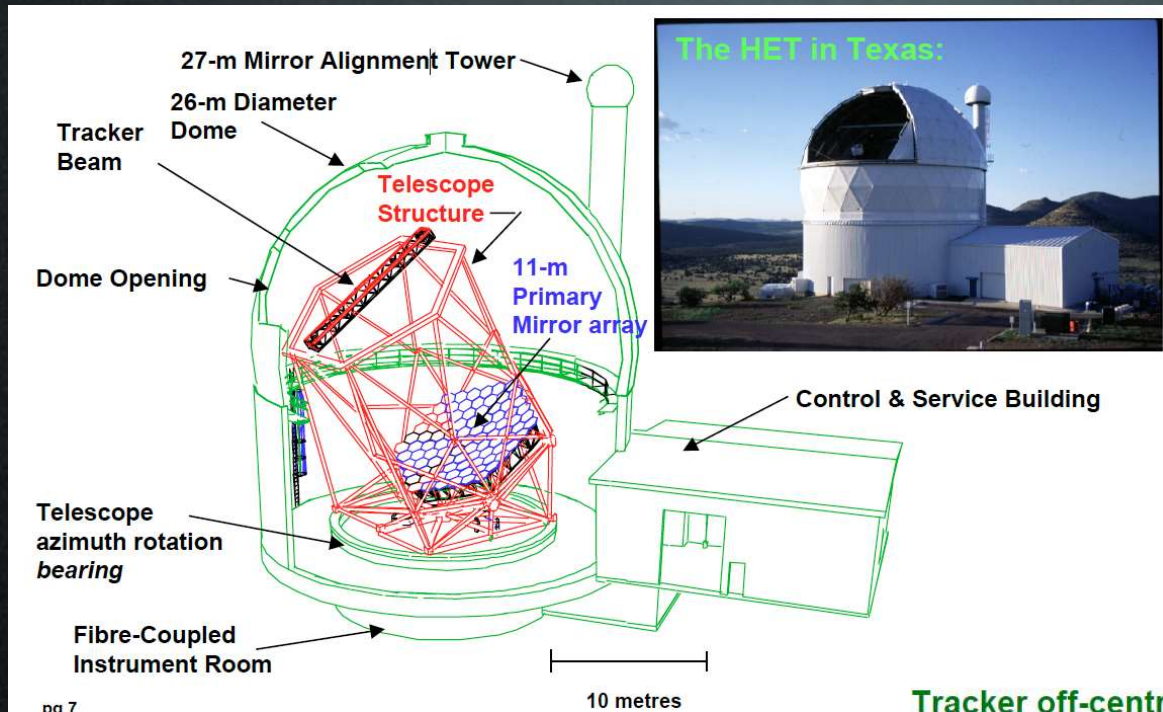


$$d\eta/dt = -0.262 \cos L \cos A \sec \alpha \quad (\text{radians/hour})$$

where $\alpha = 90^\circ - z$

Note that the rate of rotation becomes infinite for an object transiting directly through zenith ($z = 0^\circ$)!

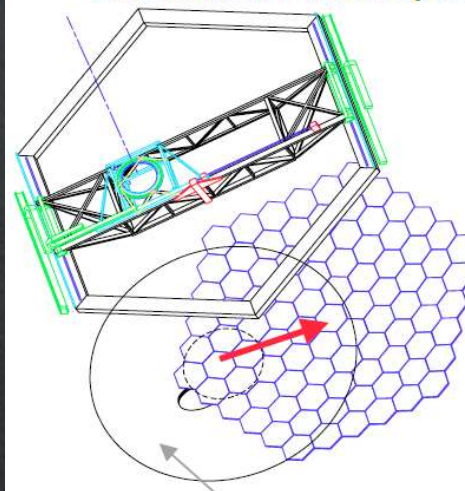
Telescope Mounts - Transit



HET (Texas)
SALT (South Africa)

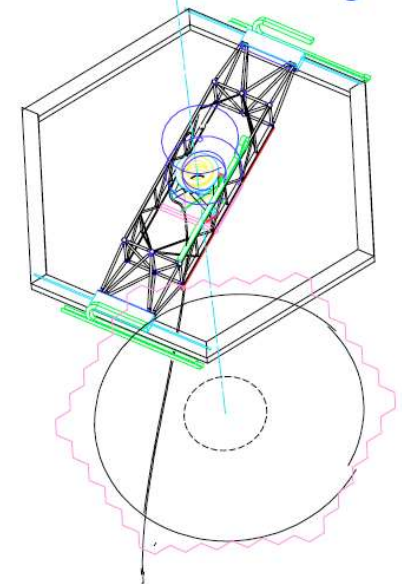
- SALT:
 - Spherical primary mirror
 - Tilted at 37°
 - $-75^\circ < \delta < +10^\circ$
 - Objects are tracked over 12° focal surface
 - Constrained scheduling

Tracker off-centre and pupil partially on primary mirror array. At worst extreme, still a 7 metre telescope!



Part of pupil off mirror is baffled at exit pupil position

Tracker centred and pupil centred on primary mirror array. Full 9.2 metre collecting area.



Large Sky Area Multi-Object Fiber Spectroscopic Telescope (LAMOST)

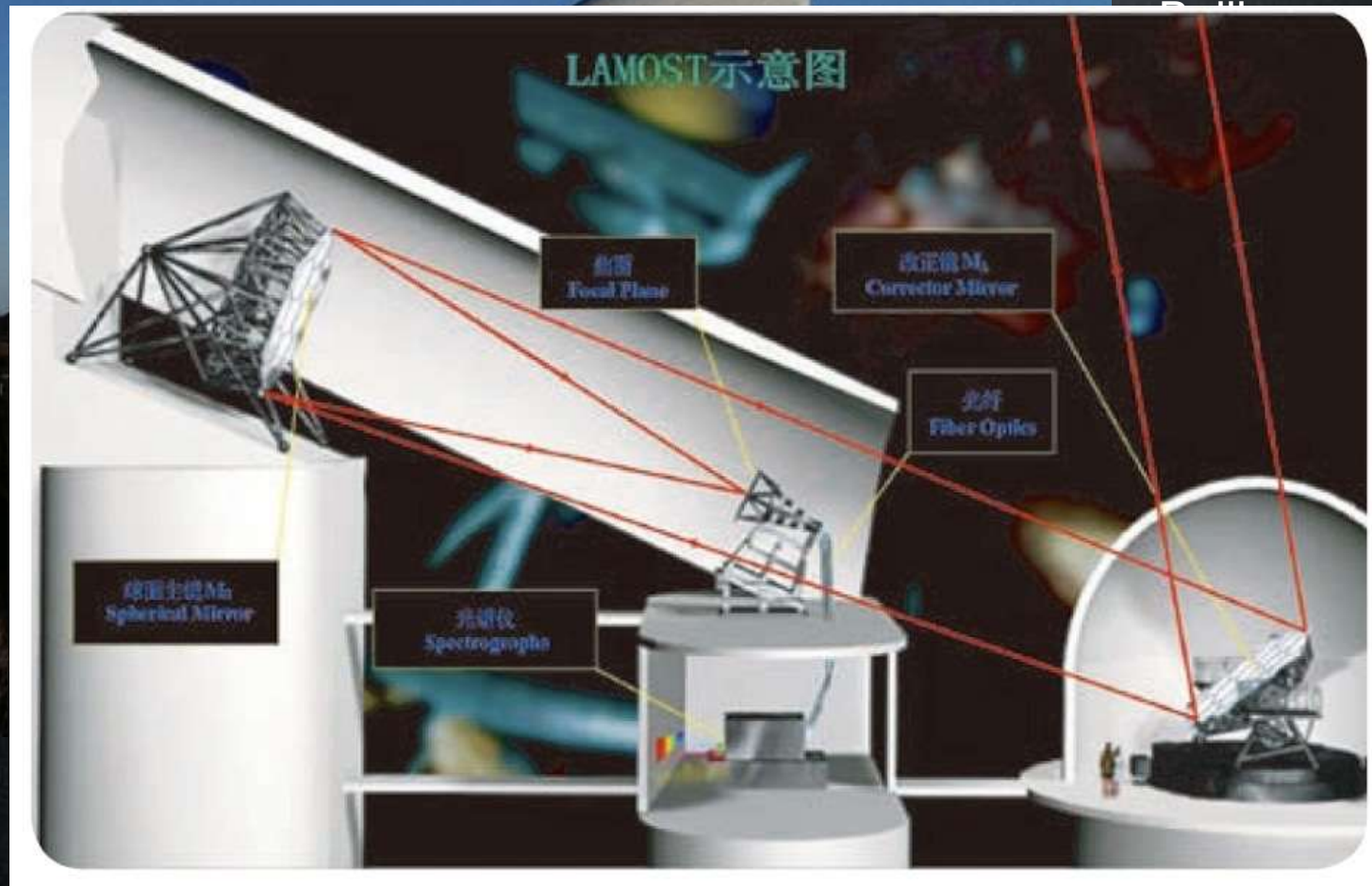


Xinglong Station,
170 km north east of
Beijing

Question: Can you guess what type of
telescope it is?

Large Sky Area Multi-Object Fiber Spectroscopic Telescope (LAMOST)

Xinglong Station,
170 km north east of

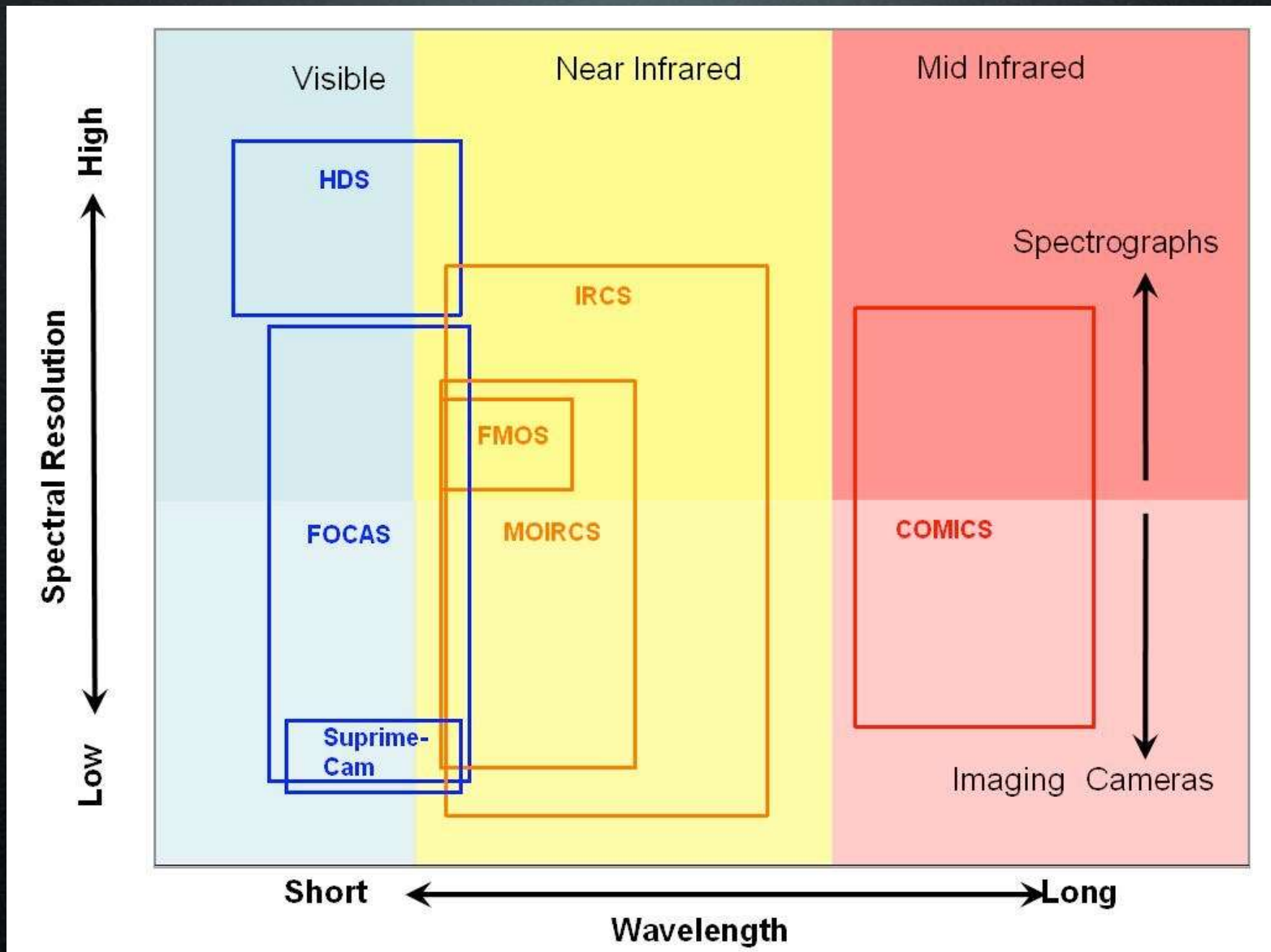


Question: Can you guess what type of telescope it is? A hint.

Some Instrument Trade-offs

- Imaging versus spectroscopy
- Seeing-limited versus Adaptive optics - assisted
- Optical versus near-infrared versus mid-infrared
- “Workhorse” instruments:
 - Aimed at a broad community of users
 - Maximizes synergy with other facilities
 - On-going science observations
- “Niche” instruments:
 - Aimed at a specific science mission with a high impact
 - Unique by definition
 - Limited useful lifetime
- Proven or new technologies?

Think "Discovery Space"



Subaru Telescope Instruments

Imaging

(Word of wisdom: Images are just very low resolution spectra
with large spatial multiplexing factors)

Sampling Theory - Resolution versus Sampling

The observed source surface brightness distribution on the sky is the convolution of the intrinsic source surface brightness distribution and the telescope point-spread-function (i.e., beam).

$$O(x, y) = I(x, y) * PSF(x, y)$$

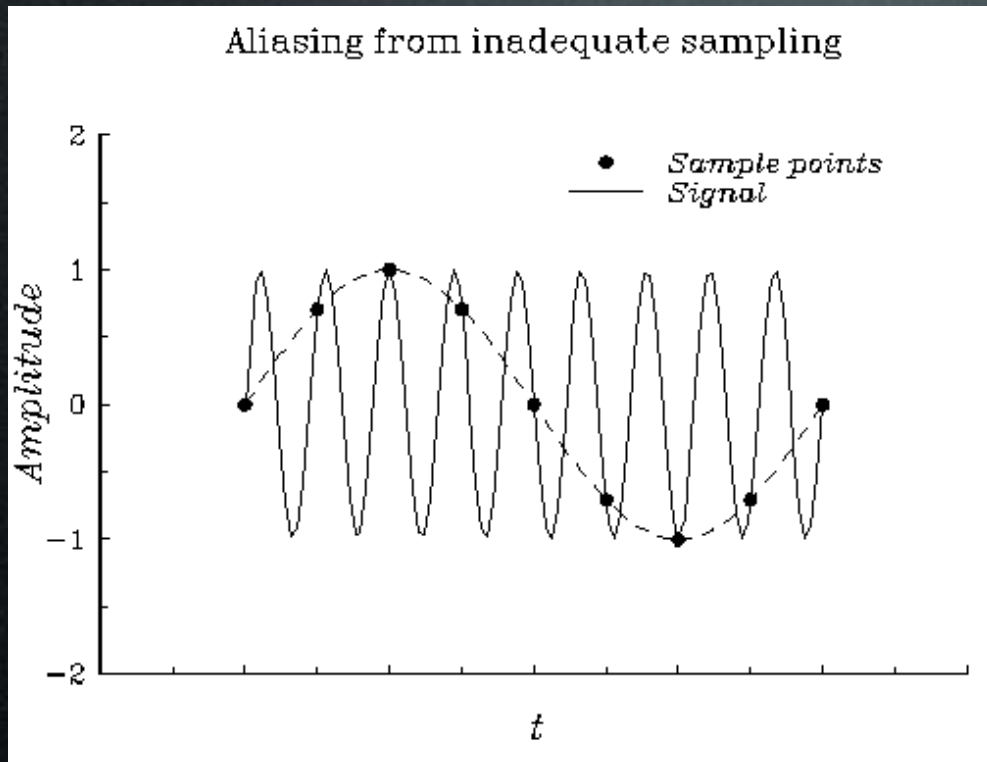
The PSF is therefore the fundamental spatial resolution element of an imager as it represents the response of the observing device to a point source (i.e., delta function).

Note that the resolution element is NOT the same thing as the sampling rate, i.e., the pixel size - resolution elements and pixels are too often confused.

Sampling rate is an inherent property of digital detectors.

The threshold between undersampling and oversampling depends on the width of the resolution element with respect to the sampling rate.

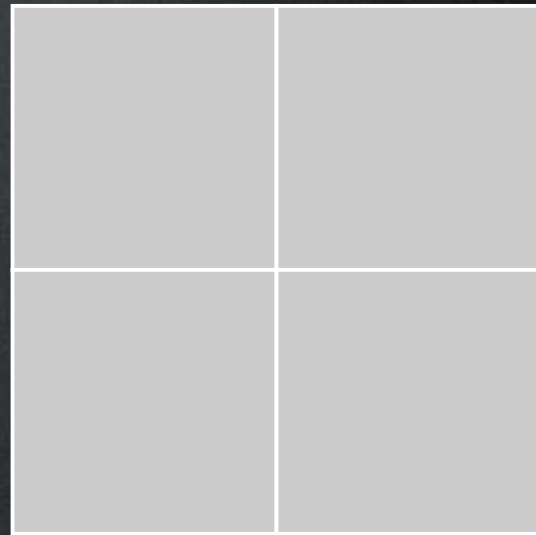
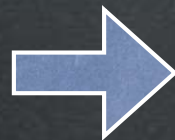
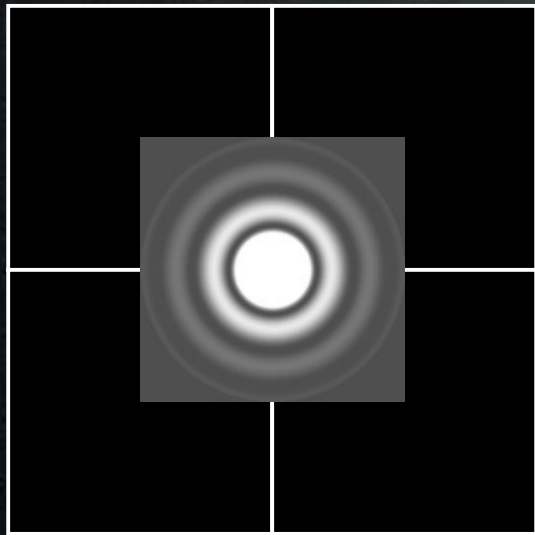
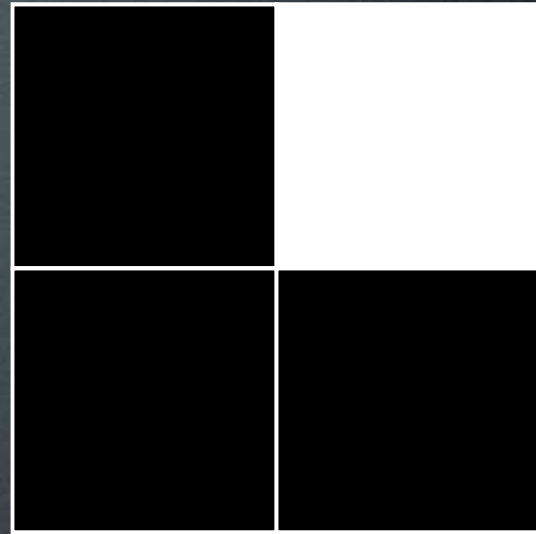
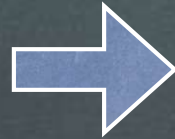
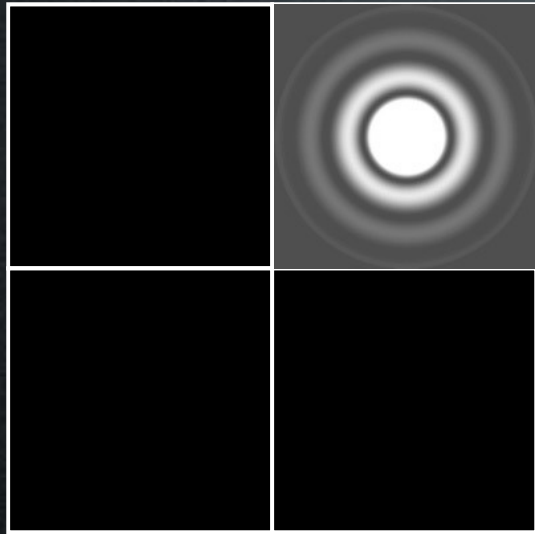
Sampling Theory - Undersampling



Aliasing applies to temporal and spatial variations as shown on the right. The Moiré pattern is caused by aliasing of the brick pattern.



Sampling Theory - Undersampling and PSFs



Sampling Theory - Nyquist Criterion

What is the best choice of sampling rate (i.e., pixel size) for an imager? The answer is not straightforward as it depends on what needs to be measured/optimized. Consider the following options:

- 1) Maximizing field-of-view: Given a limited number of pixels and a desire to image the largest possible area of sky, then undersampling your detector would be advantageous.
- 2) Optimizing signal-to-noise for faint objects: undersampling would help here as the light from a given object would be spread across a smaller number of pixels
- 3) Optimizing photometry for bright objects: oversampling would help here to make precise flux measurements in the same way that the sums of narrower strips yield better estimates of the area under a curve.

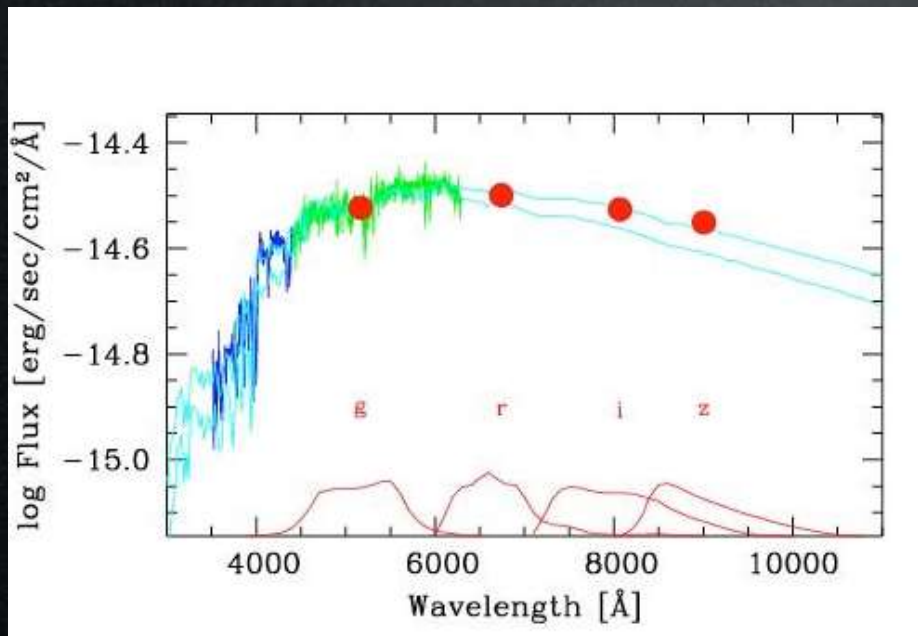
The compromise between undersampling and oversampling is to sample the resolution element (i.e., PSF FWHM) with at least 2.5 samples to remove any ambiguity as to the shape of that resolution element. This is known as the **Nyquist Sampling Criterion**.

Broadband imaging

Much of optical astronomy is preoccupied with imaging the sky with sets of filters with very broad (~ 100 nanometers) bandpasses.

This is a good approach to maximize the observed flux from faint objects if these objects have significant continuum flux.

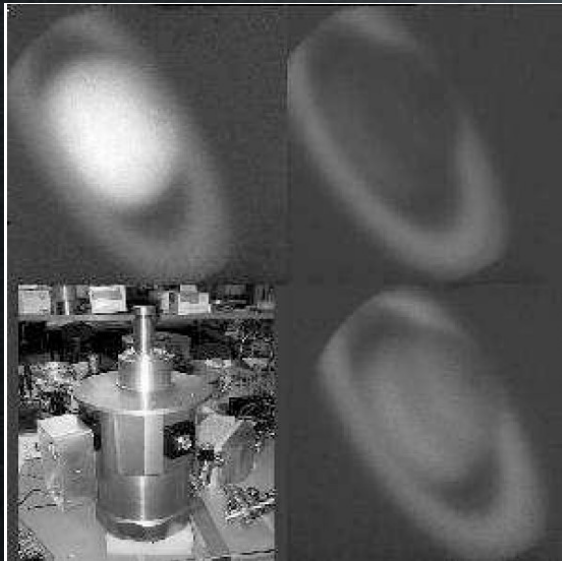
Imaging in multiple broadband filters is essentially the equivalent of low resolution spectroscopy as shown below:



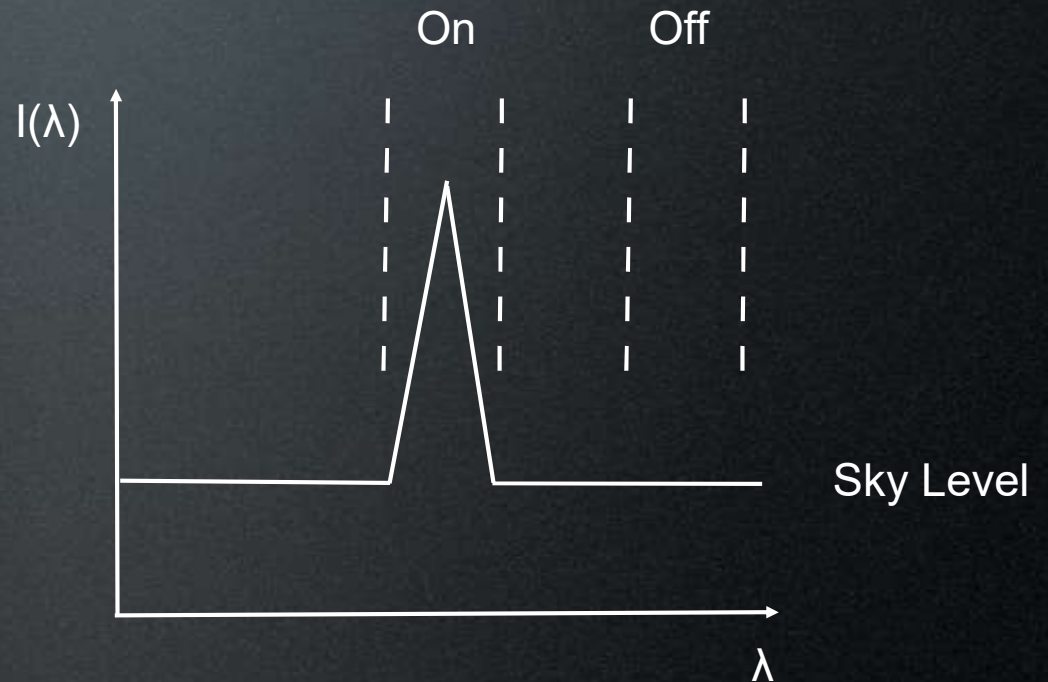
So why not just do plain spectroscopy? The advantage here is the huge spatial multiplexing factor because broad-band imaging produces a low-resolution spectrum at every pixel.

Narrowband imaging

Broadband imaging is not optimal when we are interested in a specific emission line from our target sources. Emission lines typically have widths that are much narrower than the bandpasses of broadband filters. Broadband observing would thus include more flux from the background (i.e., sky) than from the line of interest!!



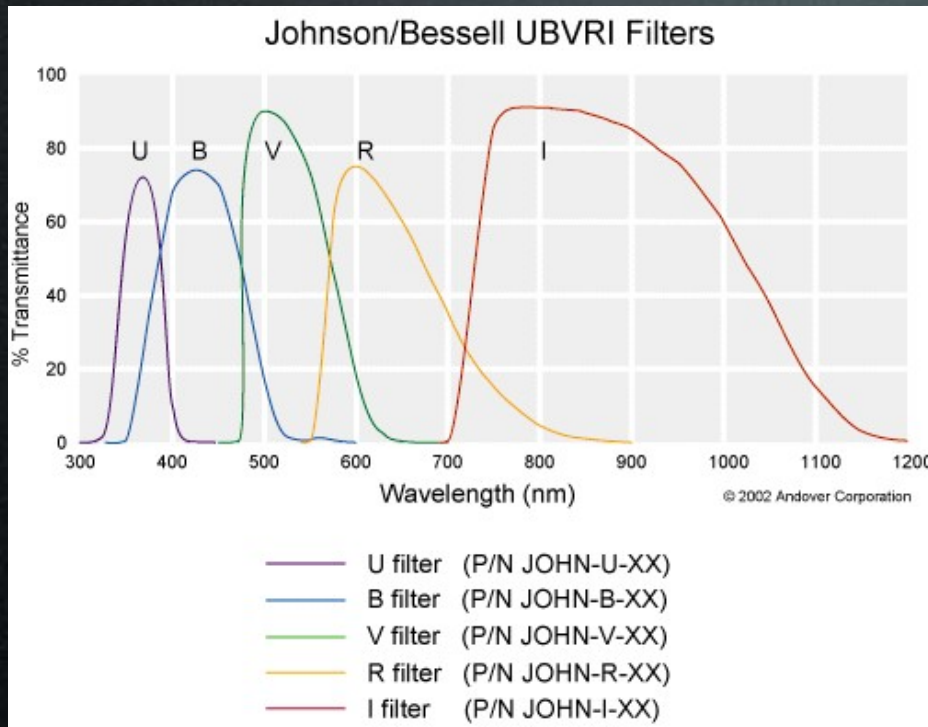
Imaging Saturn in one of its methane absorption bands



Other applications include Lyman-alpha emitters at very high redshifts and planetary nebulae in other galaxies

Flux Measurements - Johnson (Vega) Photometric System

The Johnson photometric system is defined such that the star Alpha Lyr (Vega) has $V = 0.03$, and all colours equal to zero.



Band	λ (um)	$\Delta\lambda/\lambda$	Flux @ m=0 (Jy)
U	0.36	0.15	1810
B	0.44	0.22	4260
V	0.55	0.16	3640
R	0.64	0.23	3080
I	0.79	0.19	2550

$$1 \text{ Jy} = 10^{-23} \text{ erg sec}^{-1} \text{ cm}^{-2} \text{ Hz}^{-1}$$

$$1 \text{ Jy} = 1.51 \times 10^7 \text{ photons sec}^{-1} \text{ m}^{-2} (\Delta\lambda/\lambda)^{-1}$$

Flux Measurements - AB Photometric System

The AB magnitude system is defined such that

$$m(\text{AB}) = -2.5 \log_{10} f_{\nu} - 48.60$$

where f_{ν} is measured in $\text{erg sec}^{-1} \text{cm}^{-2} \text{Hz}^{-1}$, and the value of the constant is selected to define $m(\text{AB}) = V$ for a flat-spectrum source. In this system, an object with constant flux per unit frequency interval has zero colour.

The AB system is more physical, and it has gained ground in recent years.

Noise Properties - Basic Equations

The variance of N measurements:

$$\sigma^2 = \frac{1}{N-1} \sum_{i=1}^N (x_i - \bar{x})^2$$

For a function f of N uncorrelated variables:

$$\sigma_f^2 = \left(\frac{df}{dx_1} \right)^2 \sigma_{x_1}^2 + \left(\frac{df}{dx_2} \right)^2 \sigma_{x_2}^2 + \dots + \left(\frac{df}{dx_N} \right)^2 \sigma_{x_N}^2$$

For a sum:

$$f = x_1 + x_2 + \dots + x_N$$

$$\sigma_f^2 = N\sigma_x^2$$

For an average:

$$f = (x_1 + x_2 + \dots + x_N)/N$$

$$\sigma_f^2 = (1/N)\sigma_x^2$$

Noise Properties - Sources of Noise in an Imaging Array

1. Photon Noise

Follows Poisson statistics. The probability $p(n,t)$ of n photons from a source crossing a given area in t seconds is given by

$$p(n, t) = (Nt)^n e^{-Nt} / n!$$

where N is the average flux in photons/sec from the source. The Poisson distribution has the interesting property that its variance is equal to N .

Photon noise comes from the source itself AND the (sky) background!

2. Readout noise

The charge transfer efficiency of an array readout is never 100%. Electrons get stochastically lost during transfer. The magnitude of this loss is described by an equivalent rms noise in electrons per sensing element .

Noise Properties - Basic Signal-to-Noise Ratio Calculation

The basic signal-to-noise ratio per sensing element for the observed flux from a source is:

$$S/N = \frac{C_{source}t}{(C_{source}t + C_{sky}t + N_R^2)^{1/2}}$$

where C_{source} and C_{sky} are observed count rates in photons s^{-1} pixel $^{-1}$ from the source and the sky respectively. N_R is the read-out noise in electrons. The observed rates depend on the quantum efficiency of the detector.

Note how the noise sources have been added in quadrature because they are uncorrelated.

Also note that the S/N goes as $t^{1/2}$ for bright sources, i.e., integrating twice as long does not increase the S/N ratio by a factor of two.

For calculating S/N over m pixels, the above equation must be modified such that the observed rates are now in photons s^{-1} , and the read-out noise term becomes mN_R^2 .

For a Gaussian PSF, the optimal extraction aperture radius is 1.6σ .

Depth

The “depth” of an image, i.e., the magnitude of the faintest, detectable objects, is an ambiguous metric. It depends on the intrinsic structure of the sources of interest, the significance (i.e., threshold) of the detection and the point-spread-function of the telescope (especially for ground-based telescope).

Point sources will be detected at greater depth than extended sources.

The detection limit for $3\text{-}\sigma$ significance will be brighter than the limit for $1\text{-}\sigma$ detections.

Survey	Area (deg x deg)	Filters	Depth for a point source SNR=5, 1.15"ap.,0.8"	Total integration per field	Observing strategy
Deep Synoptic: ~3 nights per run & 5 runs a year for each of the four fields					
	4	u*	28.7	33 hr (10%)	11 x 660 sec per run
		g'	28.9	33 hr (10%)	4.25 x 5 x 225 sec per run
		r'	28.5	66 hr (20%)	5.25 x 5 x 360 sec per run
		i'	28.4	132 hr (40%)	5.25 x 7 x 520 sec per run
		z'	27.0	66 hr (20%)	5.25 x 5 x 360 sec per run

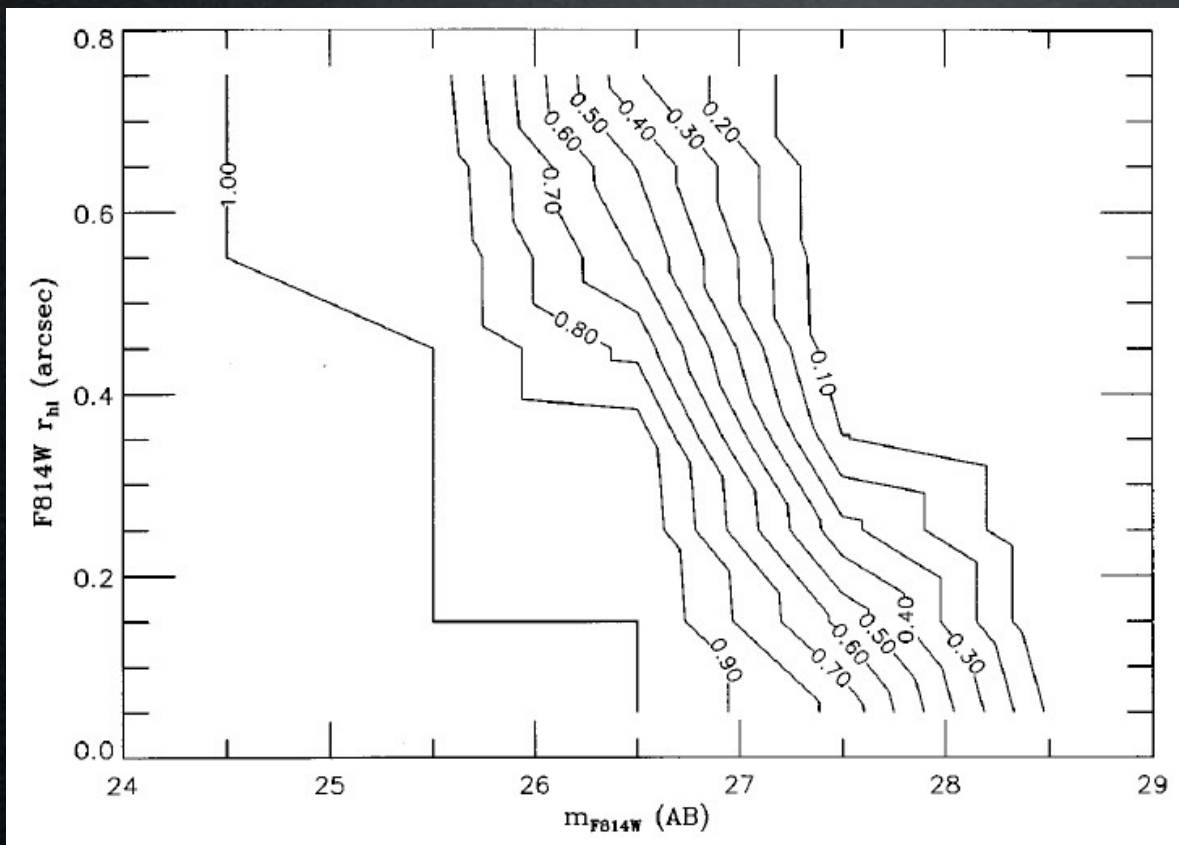
Note all the parameters (SNR, extraction aperture size and seeing) included here in the estimate of the depth of CFHTLS images.

Completeness

This is the detection efficiency of sources in an image. Typically, it will depend on both the apparent luminosity and size of a source in the sense.

At a given size, the detection efficiency will go down for fainter and fainter objects.

At a given luminosity, the detection efficiency will go down for larger and larger objects because the same amount of light is spread over a larger and larger area.



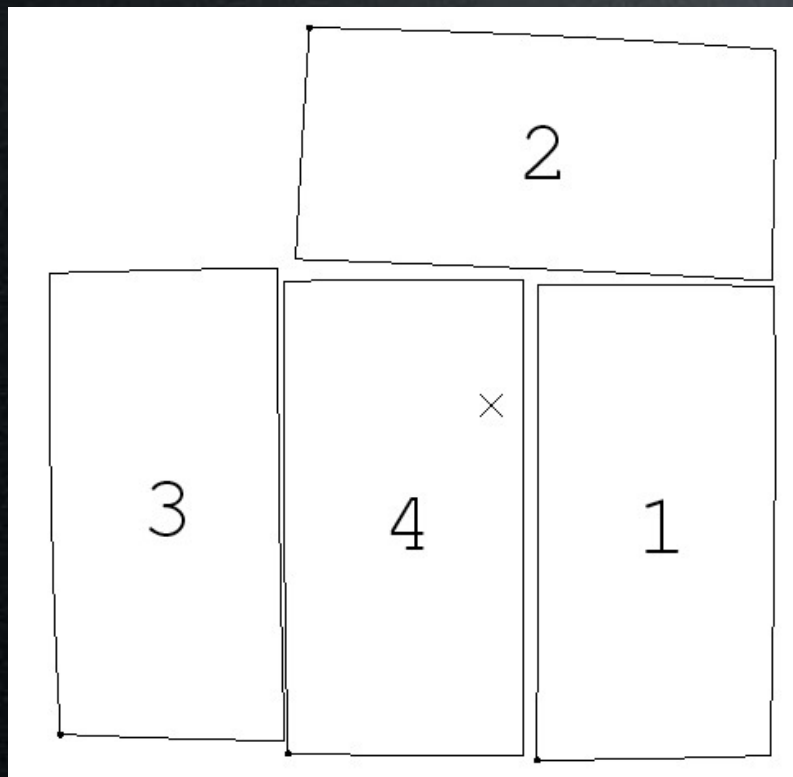
Luminosity-size completeness function for galaxies in the Hubble Deep Field North (Marleau and Simard 1998)

Positional Astrometry

The astrometric calibration consists of building a multivariate function that will map image pixel coordinates (x,y) onto coordinates on the sky (α,δ) .

Basic astrometric calibration will determine image position, image scale and rotation. Calibration fields with moderate target surface density are needed here.

Some imagers have higher-order geometric distortions such as “ripples” that require calibration fields with high target density such as open and globular clusters.



Once a good astrometric calibration has been derived, an image can be geometric-corrected through re-sampling.

Wide Field Camera on Isaac Newton Telescope

Spectrometers

Basic Nomenclature

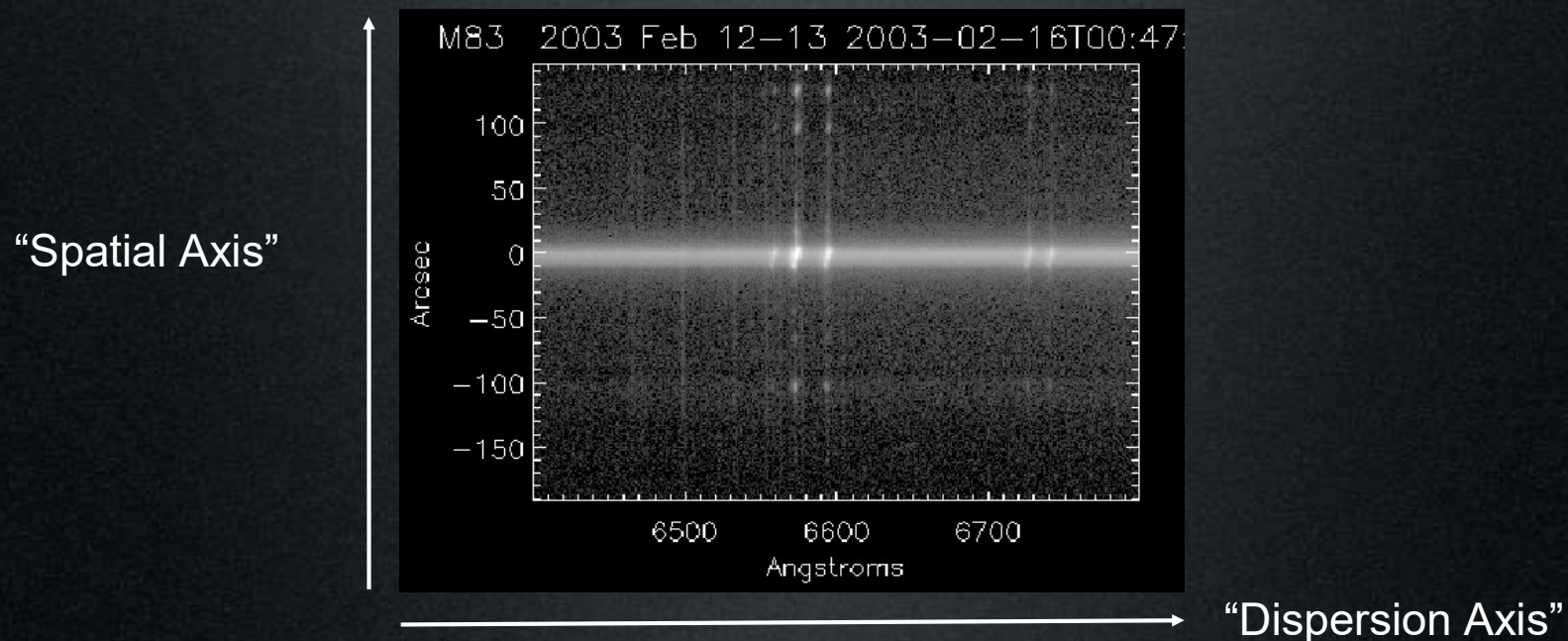
Dispersion: Wavelength interval per unit of length, i.e. angstroms/mm or angstroms/pixel

Resolution: Smallest wavelength interval that a spectrograph can distinguish. Usually expressed as

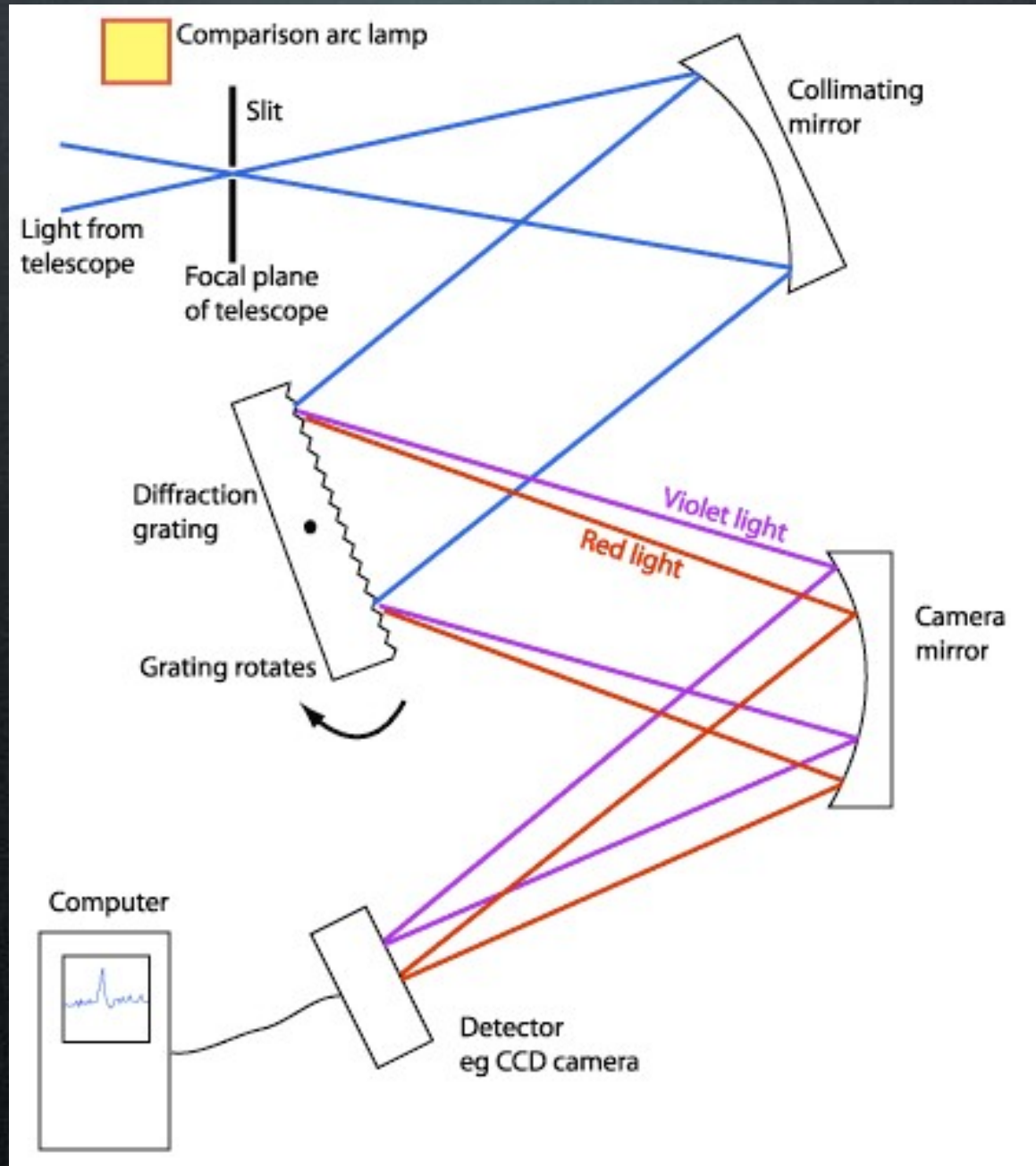
$$R \equiv \frac{\lambda}{\Delta\lambda}$$

A high resolution spectrograph will reach $R \sim 100,000$

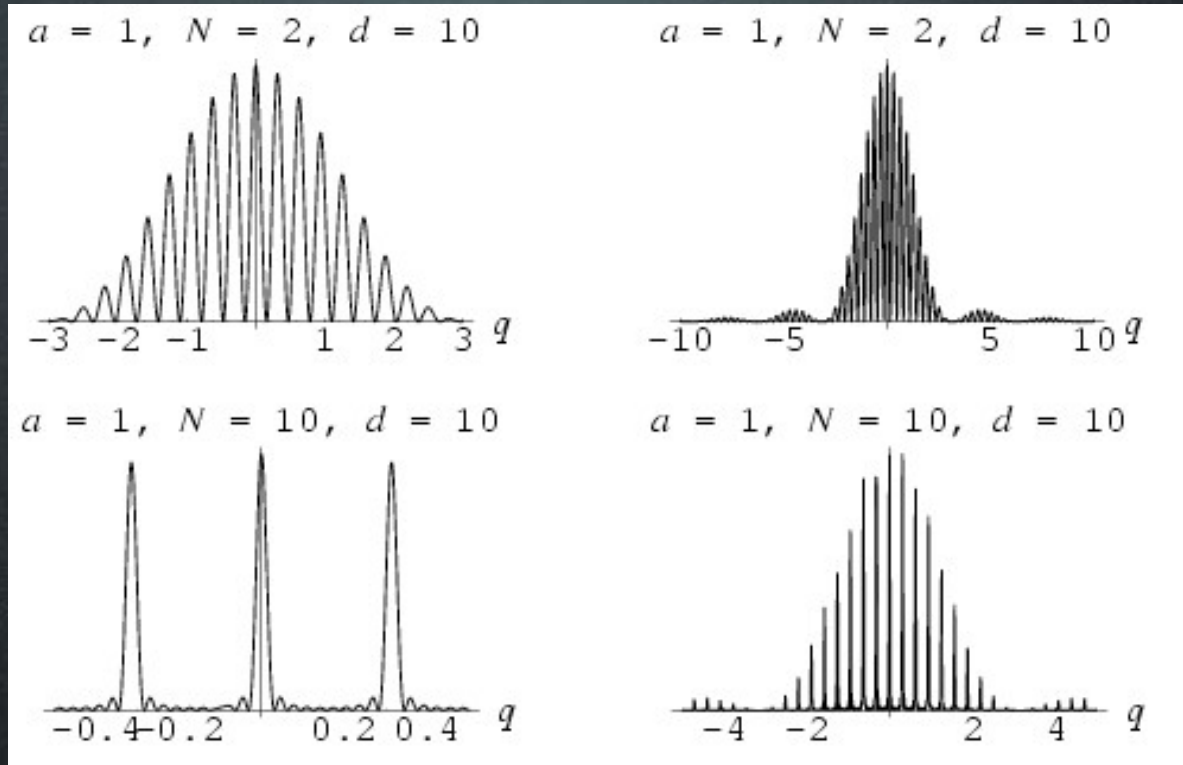
Wavelength coverage or bandwidth: Total span in wavelength covered by spectrum



Schematic Diagram of a Slit Spectrograph



Diffraction Gratings (see Chapter 4, C. R. Kitchin, Astrophysical Techniques)



For N apertures of width D separated by a distance d , the intensity of the pattern at some angle θ to the optical axis is given by:

$$I(\theta) = I(0) \left[\frac{\sin^2(\pi D \sin\theta / \lambda)}{(\pi D \sin\theta / \lambda)^2} \right] \left[\frac{\sin^2(N \pi d \sin\theta / \lambda)}{\sin^2(\pi d \sin\theta / \lambda)} \right]$$

Modulation of image by intensity structure for single aperture

Interference between N apertures

Diffraction Gratings (continued)

Let

$$\delta = \frac{\pi d \sin \theta}{\lambda}$$

Taking the limit

$$\lim_{\delta \rightarrow m\pi} \left(\frac{\sin(N\delta)}{\sin\delta} \right) = \pm N$$

Integer multiple of π give values of δ for which we have a principal fringe maximum. Angular positions of principal maxima is thus given by

$$\theta = \sin^{-1} \left(\frac{m\lambda}{d} \right)$$

where m is called the order of the fringe. Zero intensities in the fringe pattern are given by

$$N\delta = m'\pi$$

excluding cases where $m' = mN$. Their positions are given by:

$$\theta = \sin^{-1} \left(\frac{m'\lambda}{Nd} \right)$$

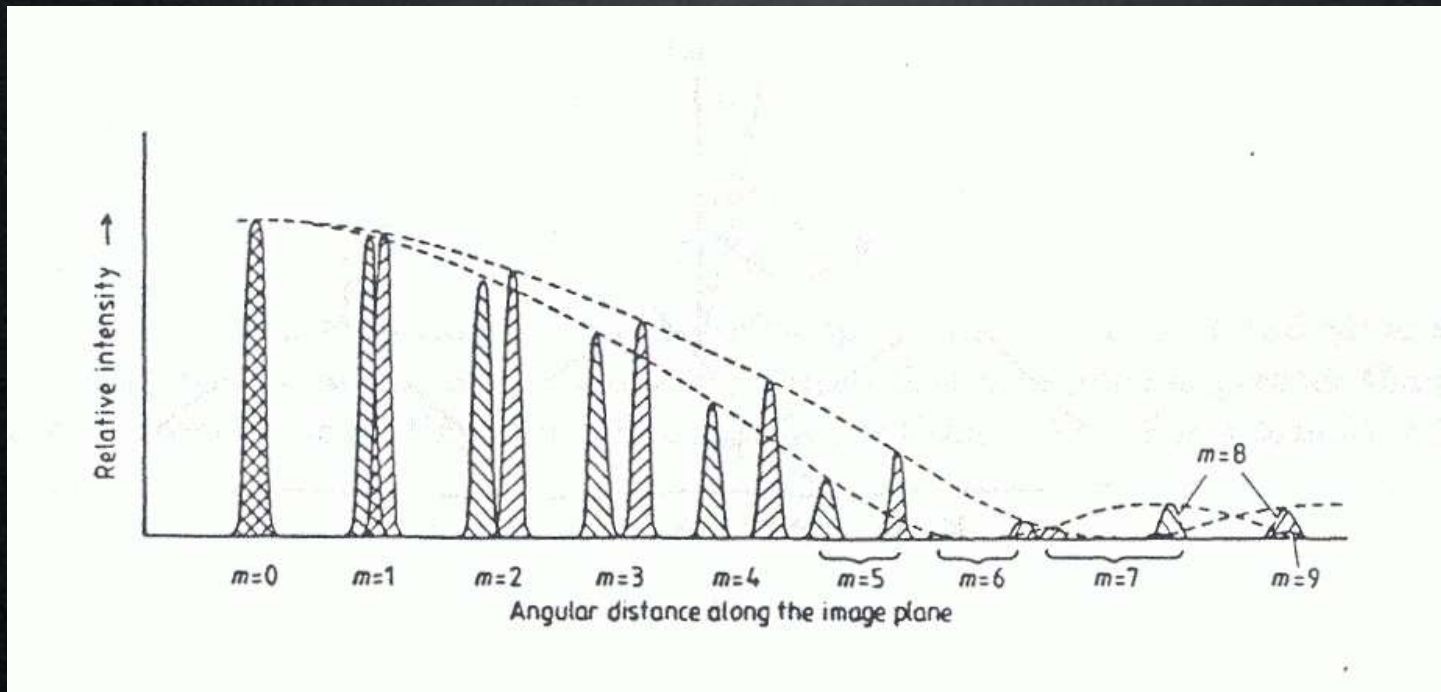
Diffraction Gratings (continued)

The angular width W of a principal maximum between the first zeroes on either side of it is thus

$$W = \frac{2\lambda}{Nd \cos \theta}$$

It is inversely proportional to the number of apertures and the peak intensity is proportional to the square of the number of apertures.

The angular separation of fringes of the same order for two wavelengths and small values of θ is proportional to both the wavelength and the order of the fringe. On the other hand, the fringe width is independent of the order.



Bichromatic
source pattern

Diffraction Gratings (continued)

The Rayleigh criterion

$$W' = \frac{\lambda}{Nd \cos \theta}$$

is independent of the fringe order. The spectral resolution increases directly with fringe order because the dispersion increases, i.e.,

$$\begin{array}{l} W_{\lambda} = W' \frac{d\lambda}{d\theta} \\ \frac{d\lambda}{d\theta} = \frac{d}{m} \cos \theta \end{array} \quad \longrightarrow \quad W_{\lambda} = \frac{\lambda}{Nm} \quad \longrightarrow \quad R = \frac{\lambda}{W_{\lambda}} = Nm$$

The linear dispersion within each spectrum is

$$\frac{dx}{d\lambda} = f \frac{d\theta}{d\lambda} = \pm \frac{mf}{d \cos \theta}$$

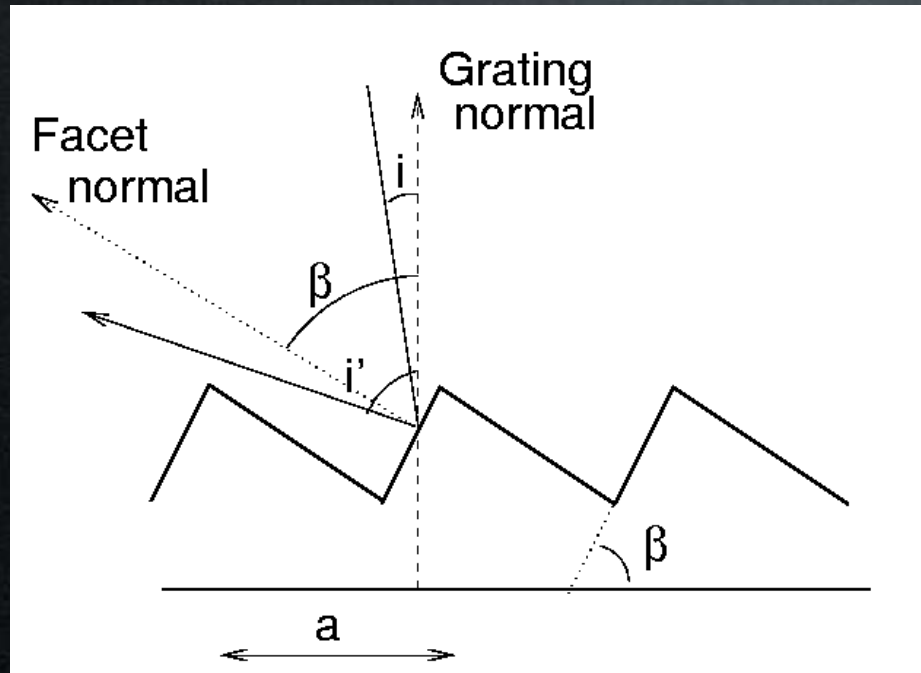
where f is the focal length of the imaging elements in the spectrometer.

Typical gratings have between 100 to 1800 grooves / mm

Diffraction Gratings (continued) - "Blaze"

One of the major disadvantages of a grating as a dispersing element is that light from the original source is spread over a large number of spectra (i.e., orders). The grating efficiency in terms of the fraction of light concentrated into the spectrum of interest is therefore very low ...

This disadvantage is mostly overcome by "blazing" the grating as shown here



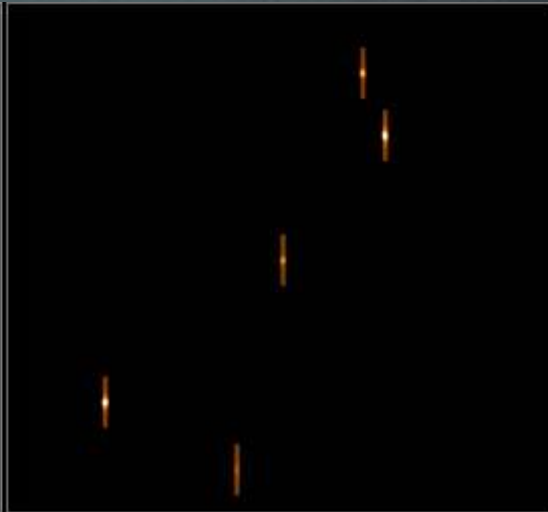
Blaze angle here is β .

Directions of constructive interference and specular reflection from grating coincide for a given order and wavelength.

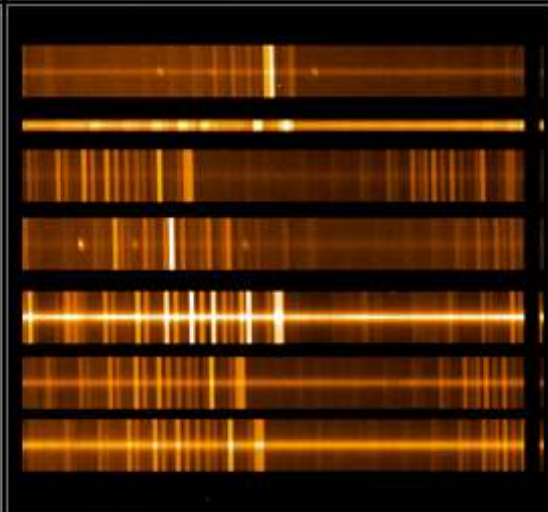
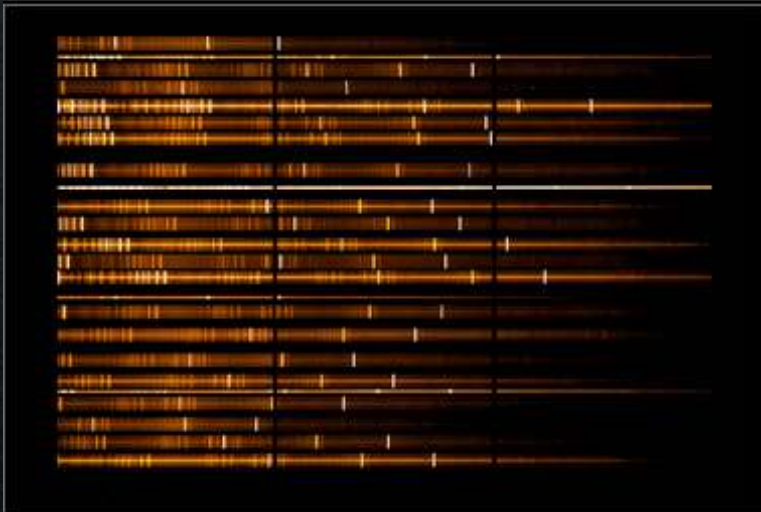
The blaze angle thus corresponds to a wavelength for which grating efficiency will be maximized.

Individual mirrors making up the grating are tilted so that they concentrate light into a narrow solid angle. Efficiency can be as high as 90% in low orders. Blazing still works for very high orders but light is concentrated into short segments of many different orders of spectra.

Multi-Object Spectroscopy



Direct exposure through mask



Grating is in - light is now dispersed

Note how different "slitlets" have different wavelength zero points

MOS can now achieve several hundreds of spectra in a single exposure through the use of band-limiting filters

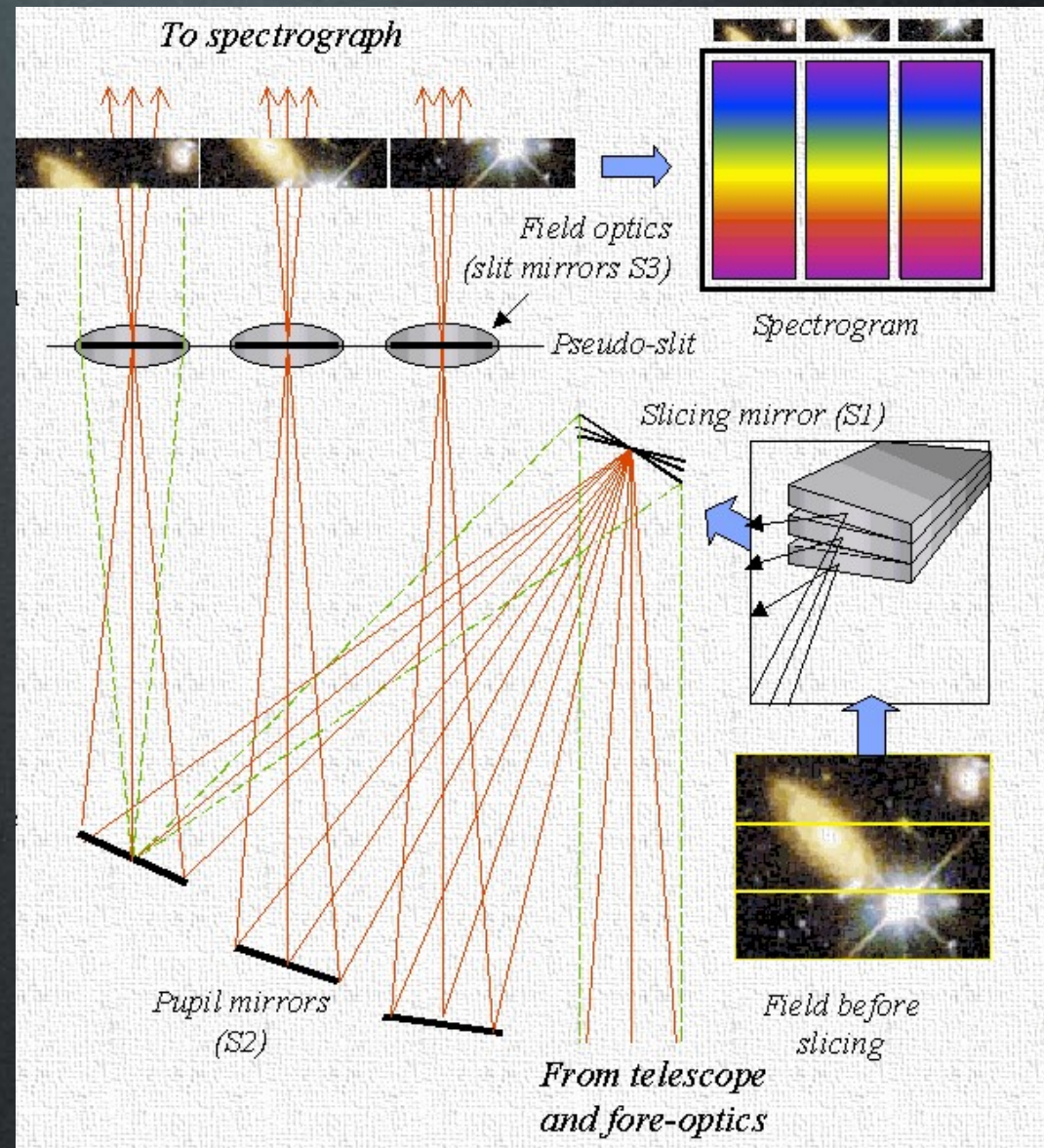
Image Slicers

Problem: Slit width must be kept as narrow as possible to preserve spectral resolution while minimizing light loss

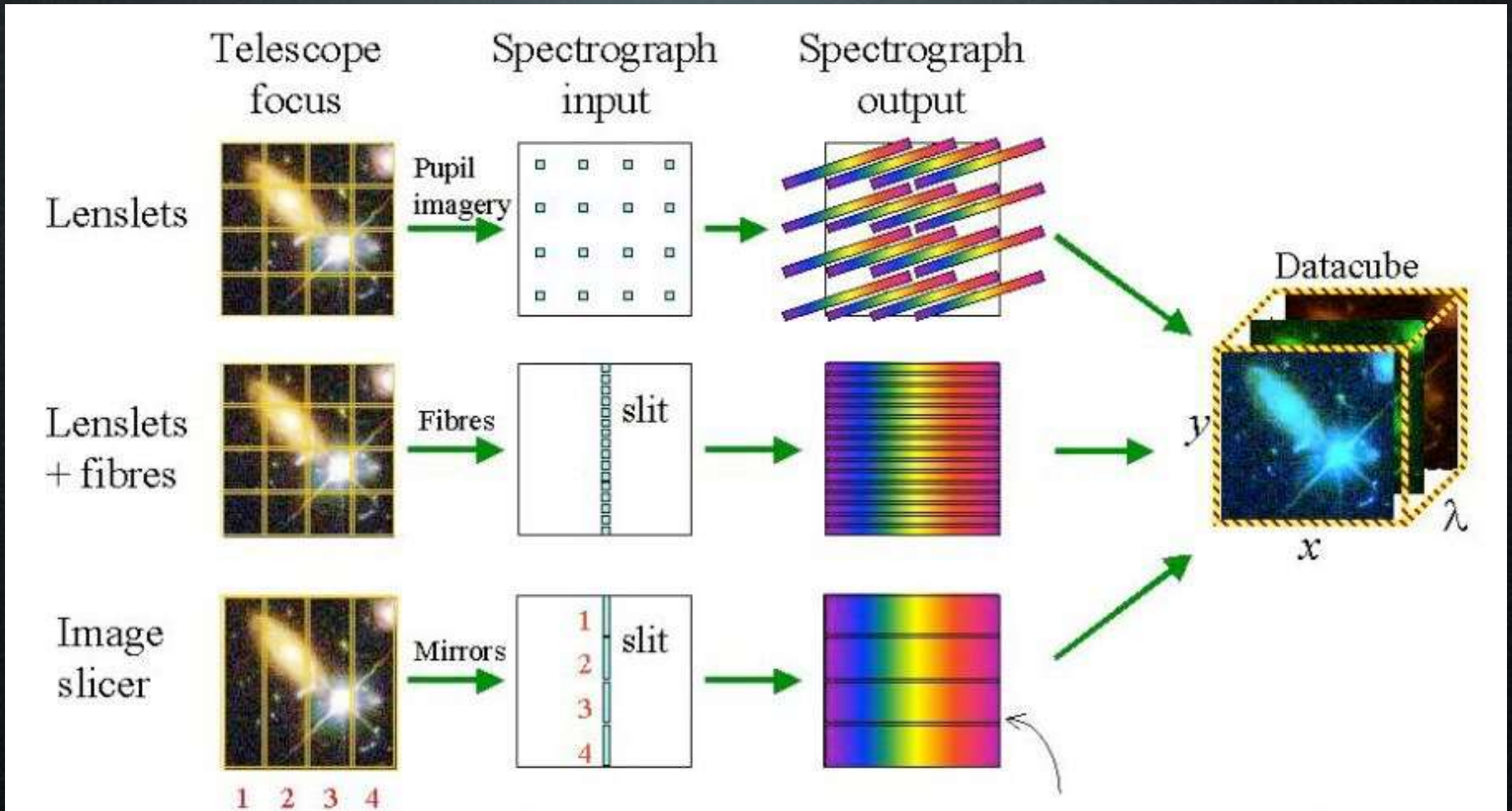
Solution: Slice it!

Durham Advanced Image Slicer Concept:

1. Optimum use of detector pixels
2. Correct spectral sampling with loss of spatial resolution in dispersion direction
3. Diffraction is only a 1D issue.



Integral Field Units



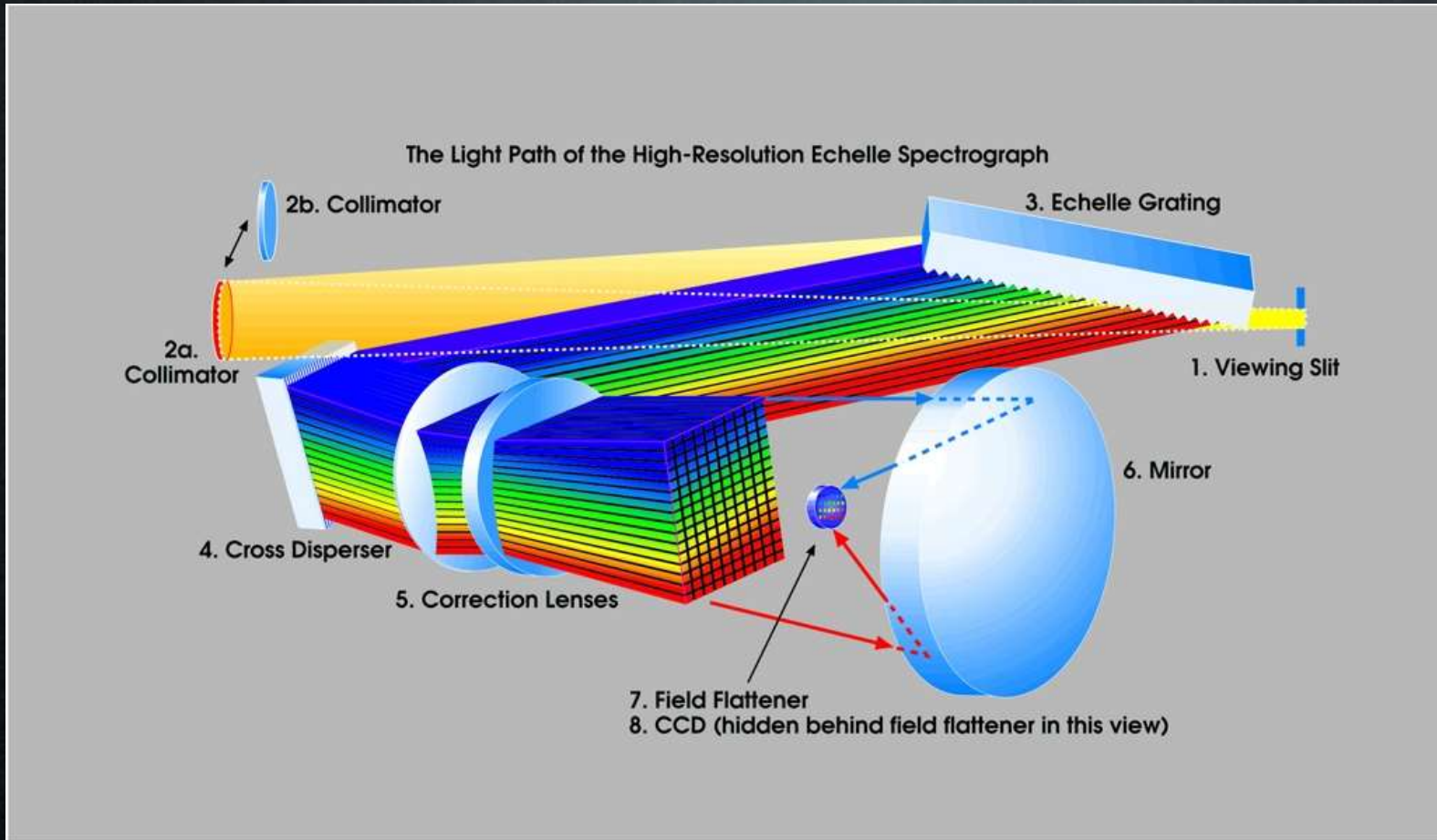
Lenslets provide good spatial sampling but spectrum packing on detector is a problem

Fibers+lenslets offer flexibility in building "pseudoslit", but fibers have problems.

Imager slicer IFUs offer best usage of detector "real estate"

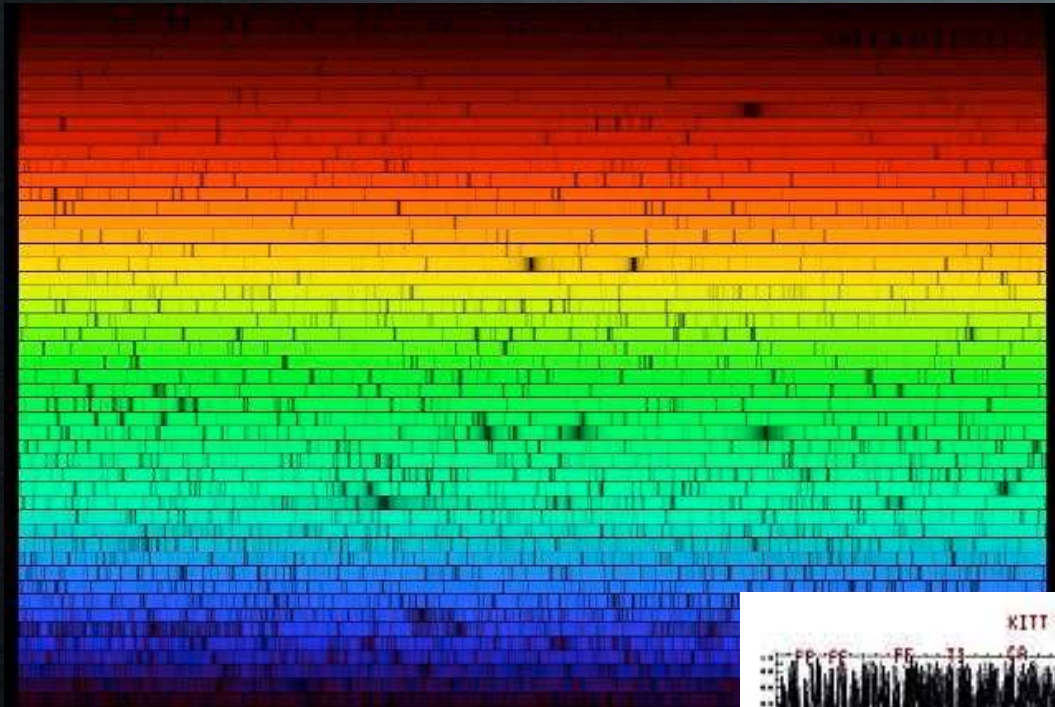
Echelle Spectrographs

Keck/HIRES
Echelle
Spectrograph

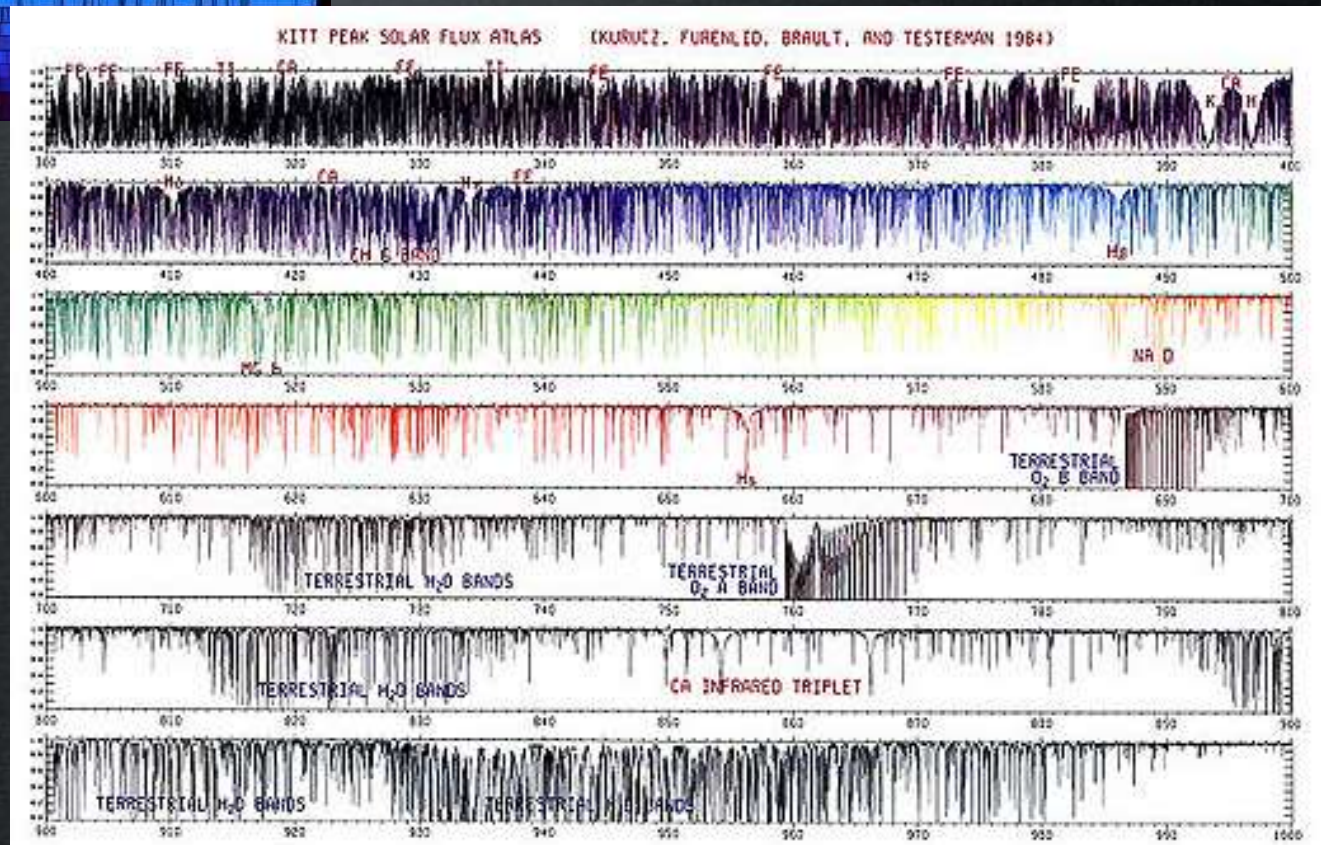


Operates in very high order for large R 's (50,000-100,000). This means that a cross-disperser is needed to separate strongly overlapping orders.

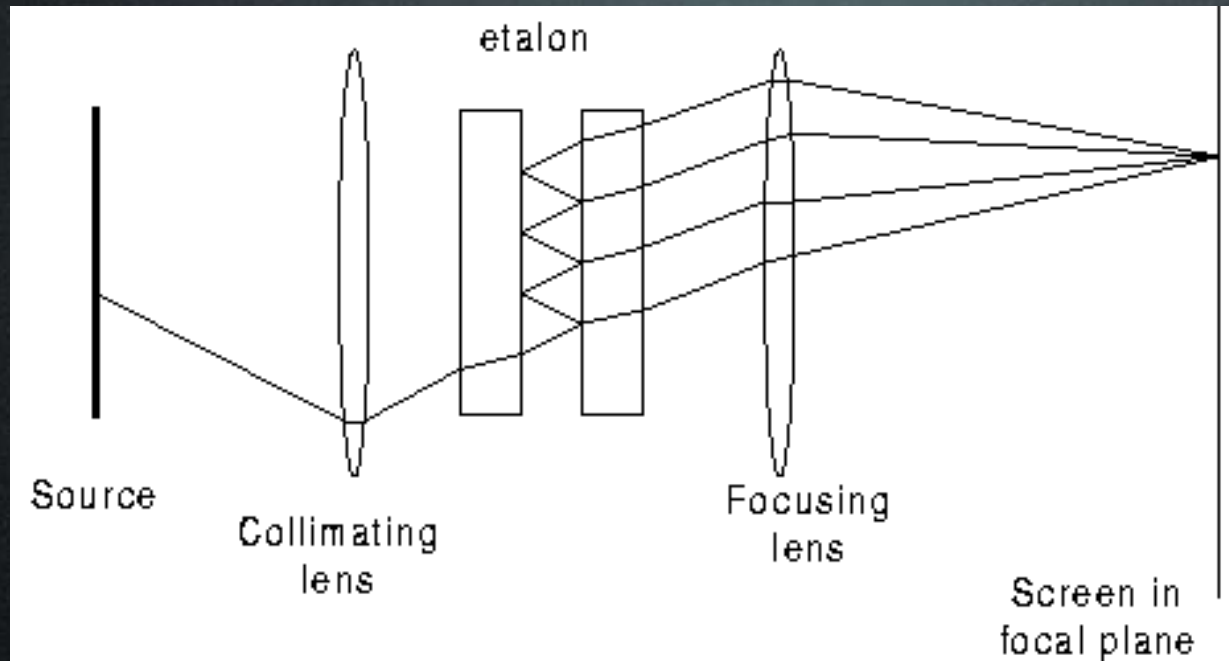
Echelle Spectrographs (continued)



Echelle spectra of the Sun



Fabry-Pérot Spectrograph (aka “circularly symmetric imaging spectrograph”)



Path difference between adjoining emergent rays is

$$\Delta P = 2t \cos \theta$$

Constructive interference occurs when

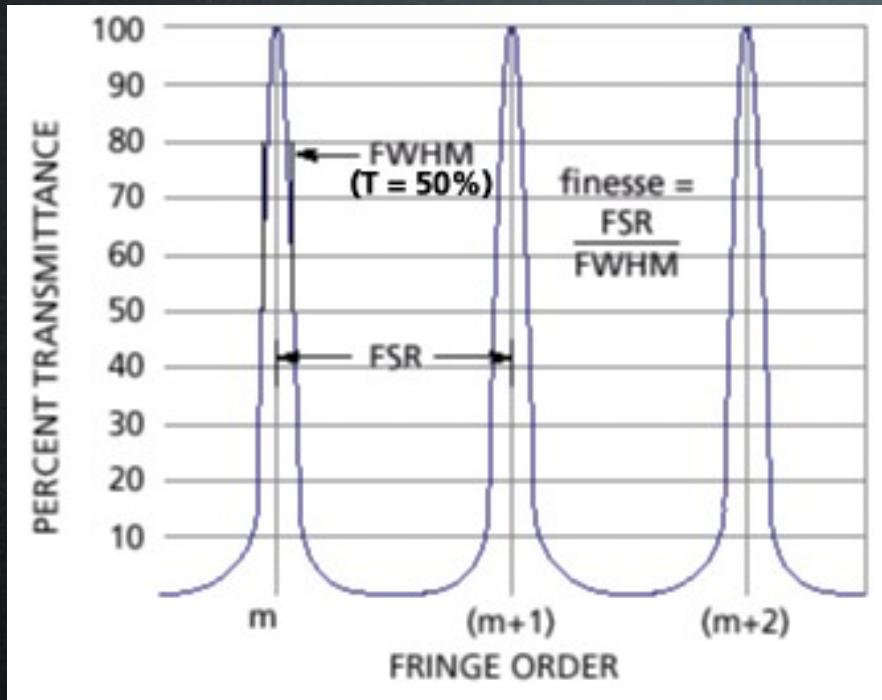
$$\mu \Delta P = m \lambda$$

where m is an integer. So,

$$\lambda = \frac{2t\mu \cos \theta}{m} \qquad \frac{d\lambda}{d\theta} = -\frac{2t\mu}{m} \sin \theta$$

Dispersion
relation

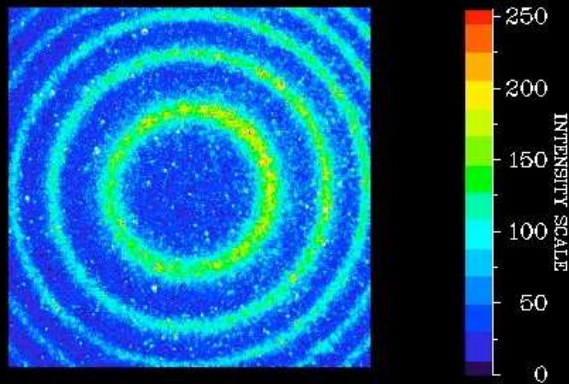
Fabry-Pérot Spectrograph (aka “circularly symmetric imaging spectrograph”)



Dual etalons (coarse + fine) becomes a powerful tunable, narrow-band filter!

Fabry-Perot Interferometer

Date = 19/03/99
Time = 02:50:19
Integration time = 20 sec
Mirror position = 4
Filter = 2



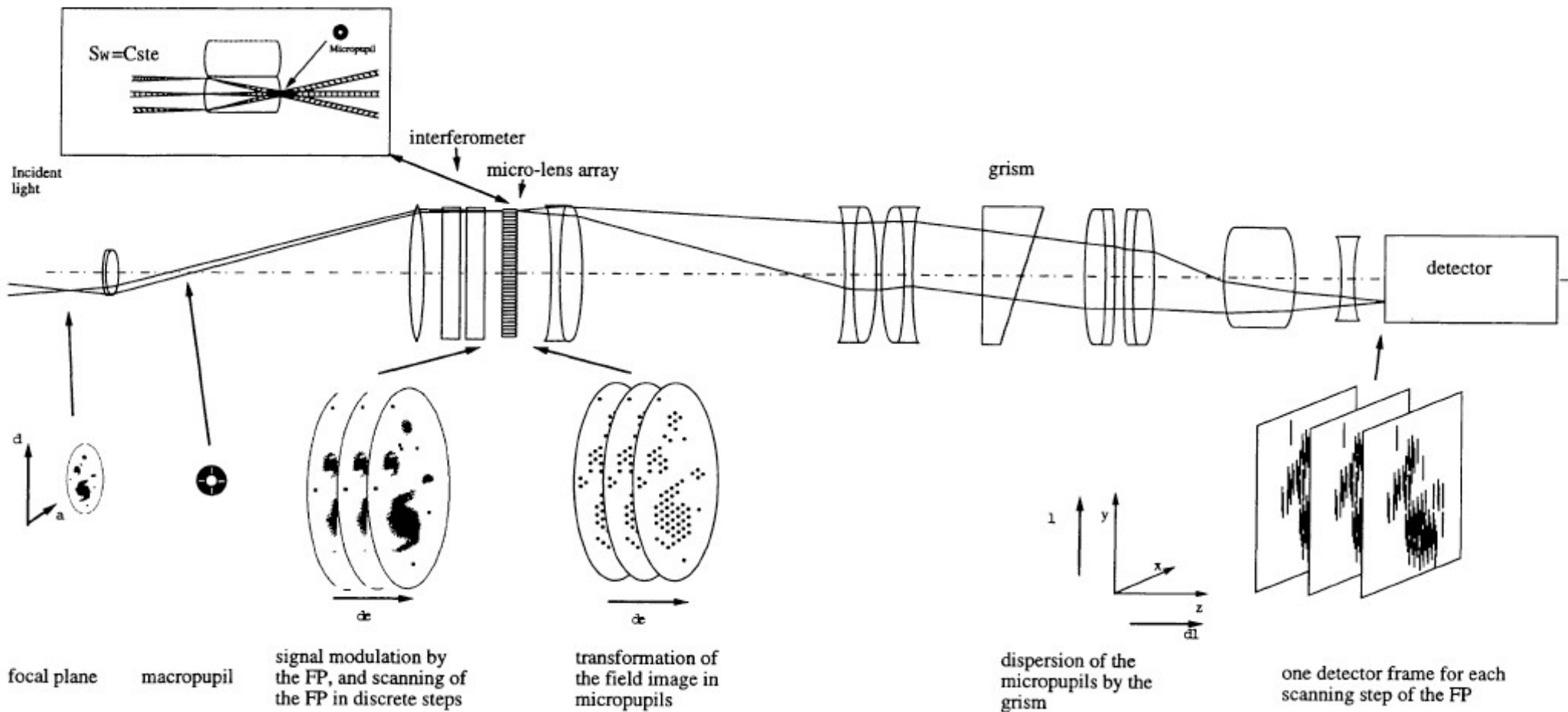
Must scan through free spectral range to build (x,y,λ) datacube.

Observing time intensive!

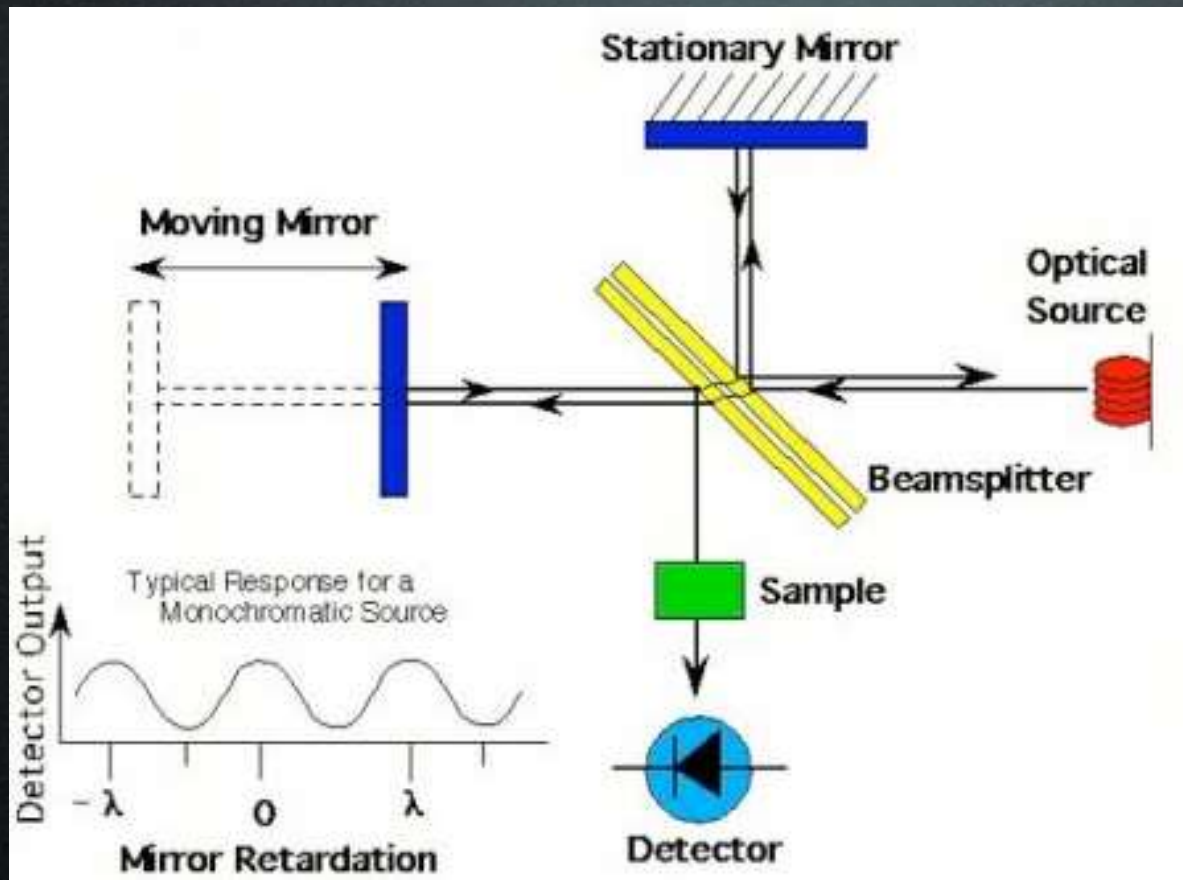
Multiplexing a Fabry-Pérot Spectrograph (!)

Since scanning takes up observing time, why not make the most of it by going from “datacubes to data hypercubes”? Enter PYTHEAS.

PYTHEAS



Fourier Transform Spectrograph (aka "Auto-correlator")



$$W_\lambda = \frac{\lambda^2}{2\Delta P}$$

$x \equiv$ Moving mirror displacement
 $\Delta P \equiv$ Path Difference

$$R = \frac{\lambda}{W_\lambda} = \frac{2x}{\lambda}$$

Given that x can be as long as 2m,
 then R can reach 1×10^6 !

Observations

Mapping Strategy - A possible Figure of Merit

For a fixed amount of observing time, the goal is to maximize the science return. Is it better to use a bigger aperture or a larger field of view?

Consider the following “figure of merit”

$$\frac{N}{t} = \frac{\phi_{obj}^2 A \Omega Q E \epsilon}{(SNR)^2 \phi_{sky} (\delta\Omega)}$$

where

$\epsilon \equiv$ observing efficiency	$\delta\Omega \equiv$ PSF footprint
$\phi_{sky} \equiv$ sky flux	$QE \equiv$ detection efficiency
$A \equiv$ aperture	$\Omega \equiv$ camera FOV

Science return here is the area surveyed (number of sources found) at a given signal-to-noise ratio down to some magnitude limit per unit time.

Mapping Strategy - Pointed Observations

Pointed observations are used when the nature of the targets (e.g., sky surface density, apparent size) is such that only one target can be observed at a time.

Examples include nearby galaxies, comets, active galaxies, bright stars, etc.

Pointed observations are inefficient by nature because they involve a lot of overheads. Every time the telescope goes to a different target, it has to:

1. Configure itself
2. Slew to the target position
3. Acquire target (not always a simple thing)
4. Perform some calibrations
5. Integrate on target

Mapping Strategy - Dithered Observations

A dither pattern is a set of images that overlap on the sky. The amount of overlap can vary quite a lot - from nearly 100% to 10%.

The overlap regions must be large enough so that the images can be astrometrically and photometrically tied together.

Dithered observations have a number of advantages:

1. Larger areal sky coverage than a single pointed observation
2. Improved flat-fielding
3. Improved global astrometry
4. Improved sky subtraction (IR observations)
5. Removal of gaps between detectors in a mosaic

Example:

2006A CFHT/WIRCAM observations of the GOODS-N field, 19 hours in K-band, PI: Yours truly.

Dither pattern is highly non-redundant:

16 positions (4x4 grid with 1'.2 separation)

--> 20 "random" sub-positions at each position (largest step is 1'.5)

--> 7 20-second exposures at each sub-position

Mapping Strategy - Drift-scanning

Drift scanning is used to image large strips of the sky.

If the telescope is held at a fixed position by turning off its tracking, objects will drift across the CCD at the sidereal rate. The sidereal rate is 15" per second at the celestial equator and varies as the cosine of the declination.

The trick is to read out the CCD at the same rate as the sidereal rate so that the images do not smear out.

The maximum exposure time is given by the angular extent of the detector along the drift axis divided by the sidereal rate.

All imaging data for the Sloan Digital Sky Survey has been acquired using drift-scanning (check out <http://cas.sdss.org/dr7/en/tools/scroll>).

In addition to observational simplicity, the main (and very attractive) advantage of this technique is that it produces images with very good flat-fielding because the total signal for each object has been recorded by many different pixels.

One difficulty with this technique is called "differential trailing". If the field of view of the detector is large enough, then the difference in drift rate between objects at the north and south ends will become significant.

Calibrations - Photometric

For a set of filters such as Johnson UBV, the standard photometric equations look like:

$$U = U_{inst} - A_u + Z_u + C_u(U - B) + \kappa_u X$$

$$B = B_{inst} - A_b + Z_b + C_b(B - V) + \kappa_b X$$

$$V = V_{inst} - A_v + Z_v + C_v(B - V) + \kappa_v X$$

where the instrumental magnitudes are $-2.5 \cdot \log_{10}(\text{counts})$, the A's are arbitrary constants added to the instrumental magnitudes, the Z's are the zeropoints between the instrumental and standard magnitudes, the C's are the color terms, the kappa terms are the extinction coefficients and X is the airmass (sec z)

Depending on the observing site, nightly calibrations must include standard observations for monitoring the zeropoint variations and observations of the same standard stars at different airmasses for computing kappa. On photometric nights at sites like Mauna Kea, a standard extinction coefficient can be used instead of empirically determining one (it saves observing time!).

Color terms are usually so stable (but not always!) that they do not have to be monitored on a nightly basis. They are usually provided by the Observatory.

Calibrations - CCD Instrumental Signatures

After being exposed to a sky flux of C_{ij} counts/sec for an integration time t , the $(i,j)^{\text{th}}$ pixel value F_{ij} will be given by:

$$F_{ij} = B_{ij} + D_{ij}t + C_{ij}q_{ij}t$$

where B_{ij} is the “bias” level, D_{ij} is the dark current, and q_{ij} is the response of the pixel to the incoming flux.

Current CCD detectors have negligible dark currents. However, owing to the smaller energy gap between their valence and conduction bands, calibrations of infrared array data must include a dark current correction.

The “bias” (or zeropoint) correction can be further decomposed as:

$$B_{ij} = B_0 + \Delta B_{ij}$$

where B_0 is called the “overscan” and ΔB_{ij} is the “bias structure”.

Calibrations - CCD Instrumental Signatures (continued)

The following calibrations should therefore be performed:

1. Bias frames

These are zero exposure images that have not been exposed to any outside light source. Overscan level is typically measured for every image as it can vary with temperature and time. The bias structure is quite stable, so bias frames can be acquired at the beginning of the night

2. Dark current

These are closed shutter exposures with the same integration times as the science images they will be used to correct.

3. Flat-Fields

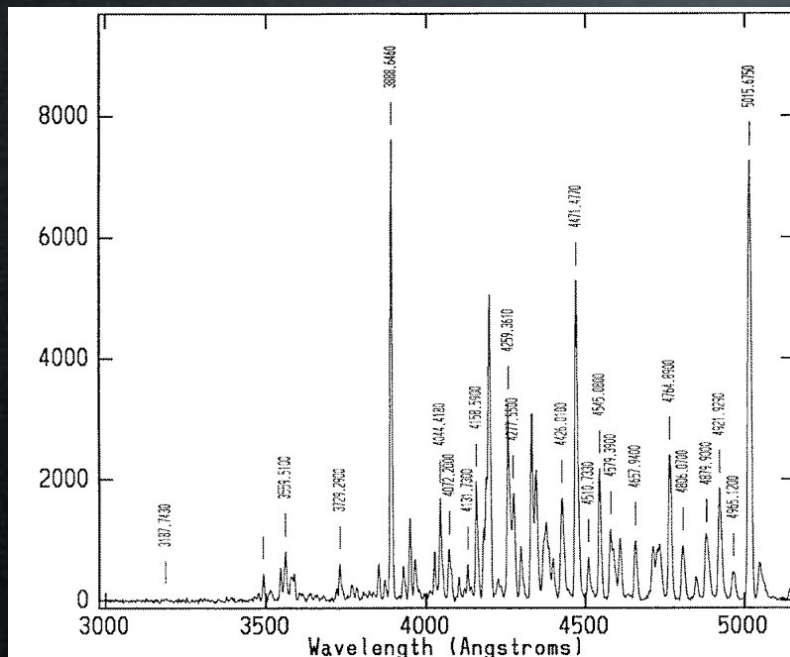
The pixel response q_{ij} must be mapped out using a light source that provides a uniform (i.e., flat) illumination of the CCD detector. CCD detectors have good linearity, so q_{ij} does not depend on the illumination level. Flat-field calibration images are acquired by either (1) illuminating the dome (good S/N for pixel-to-pixel variations) and/or (2) by taking images of the twilight sky (good for large scale response variations). Twilight flats have an illumination pattern which is obviously closer to the one for science images. They are tricky to acquire because their “acquisition window” can be quite short.

Calibrations - Wavelength

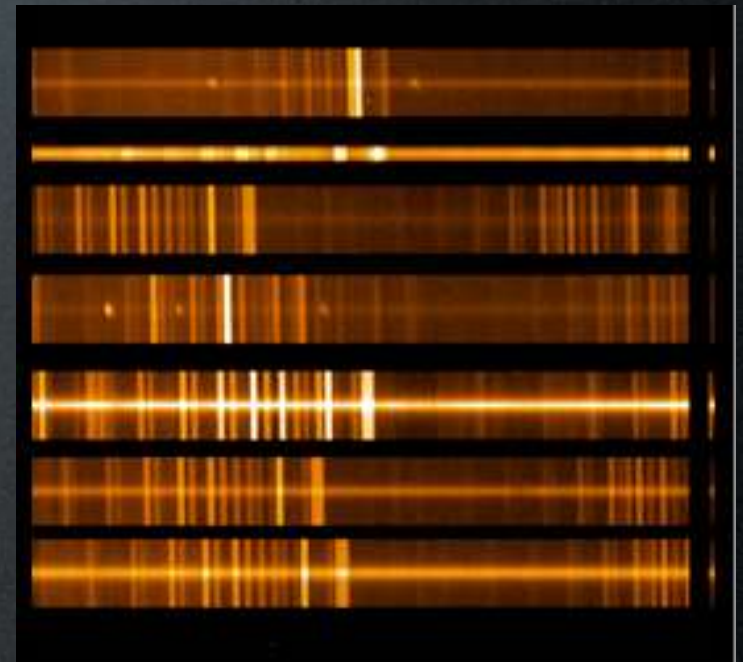
Wavelength calibrations are needed to determine both the dispersion (wavelength interval per unit length) and the zeropoint of the wavelength scale.

There are two sets of calibrations:

1. Arc lamp spectrum (e.g., HeNeAr)



2. Sky Spectrum



For spectra with a few sky lines (typically in the blue, i.e., blueward of 600 nm), the dispersion is determined with the arc lamp and the zeropoint is determined from one or more sky lines. One bright sky line will do.

For spectra with a lot of sky lines (typically in the red), both the dispersion and the zeropoint can be determined from these lines, and no arc spectra are needed.

Data Reduction

Image Reconstruction

Recall that the observed source surface brightness distribution on the sky is the convolution of the intrinsic source surface brightness distribution and the telescope point-spread-function (i.e., beam).

$$O(x, y) = I(x, y) * PSF(x, y)$$

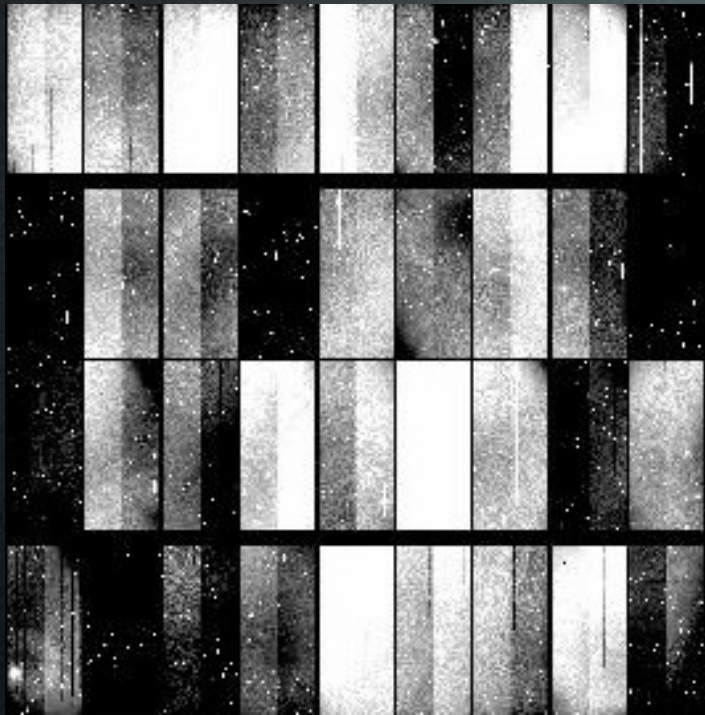
Given that the Fourier Convolution Theorem states that the Fourier transform of a convolution is equal to the product of the Fourier transforms of the convolved functions, it would seem (at first glance) that one could trivially solve for $I(x,y)$.

However, this is unfortunately never the case in practice. The Fourier transforms of $O(x,y)$ and $PSF(x,y)$ are never sampled at all spatial frequencies, i.e., their sampling bandwidth is never infinite. Just think about the incomplete $u-v$ plane coverage from an interferometer as an example.

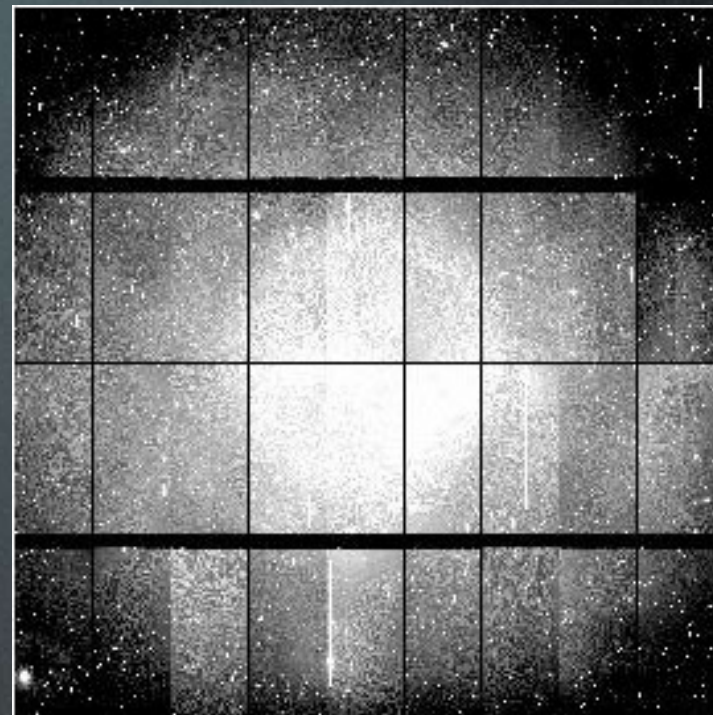
As a result, unknown Fourier coefficients at spatial frequencies outside the sampling bandwidth can introduce spurious features when solving for $I(x,y)$.

Deconvolution is almost an art, and many robust algorithms have been developed to tackle this difficult problem.

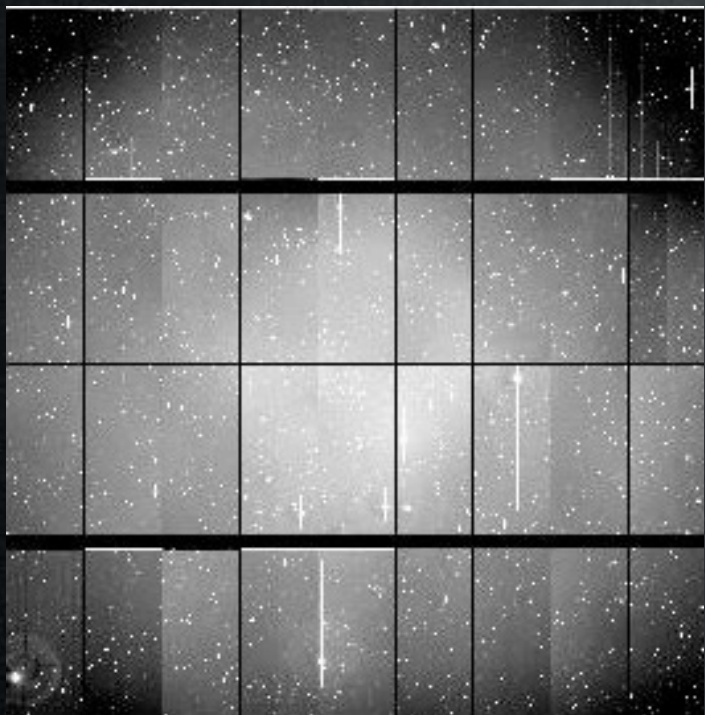
Removing Instrumental Signatures from CCD images - CFHT MegaPrime



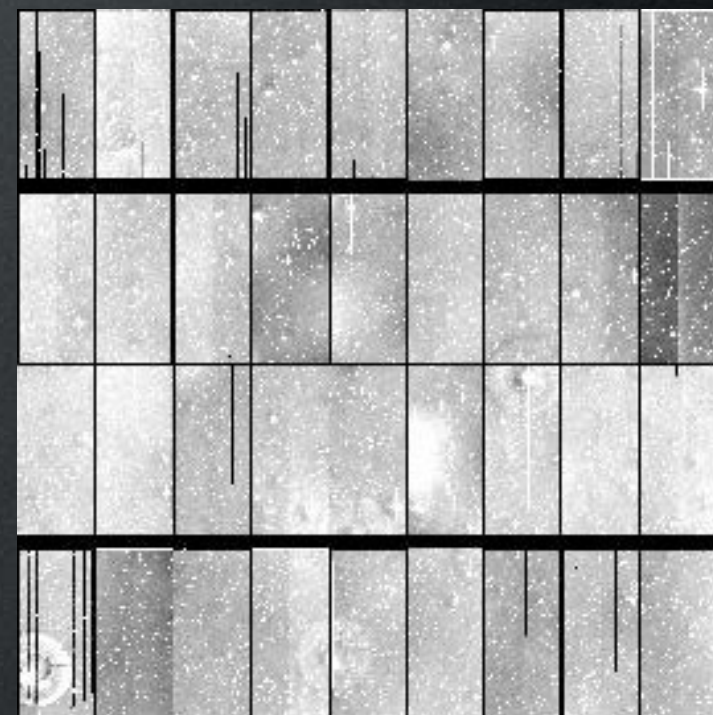
Raw



Flat-fielded

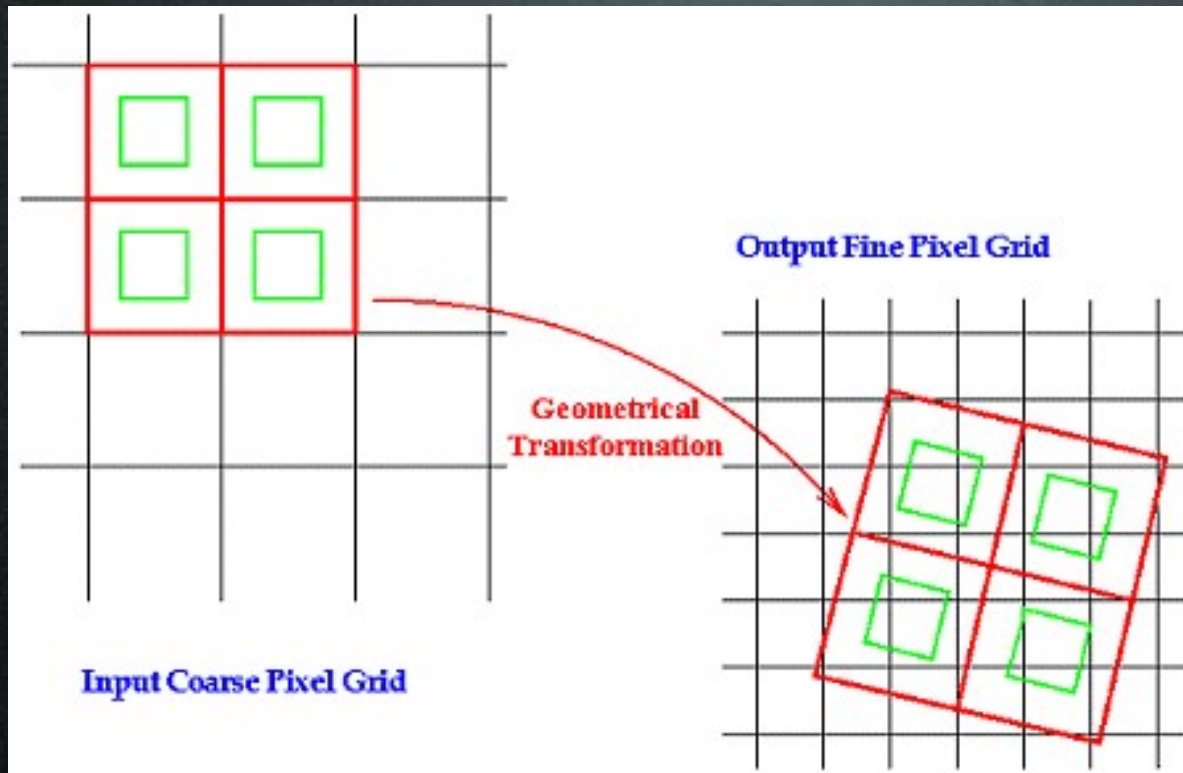


Fringe removal



Mode removal

Multidrizzling

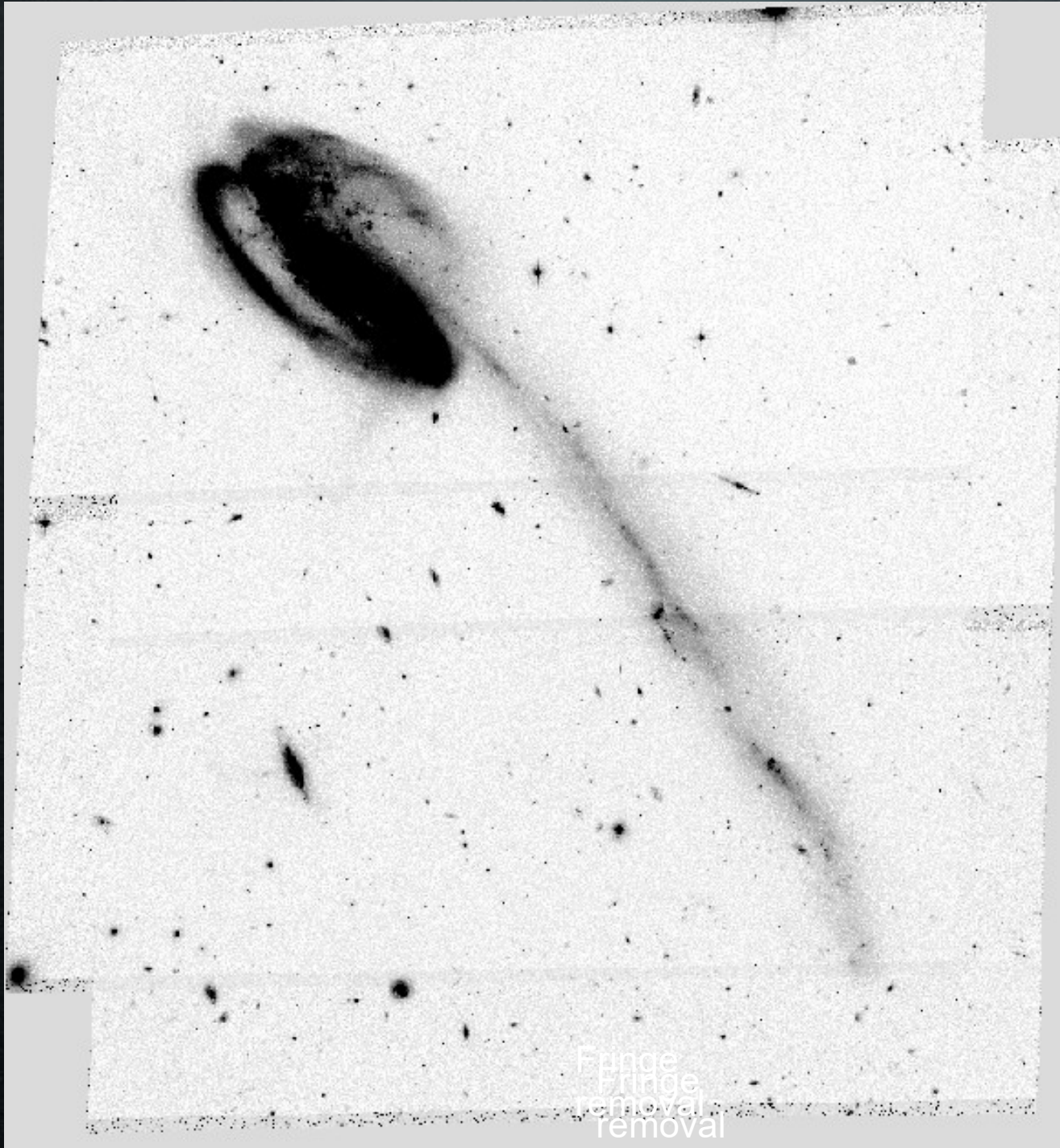


Given a deep stack of overlapping images on the sky with carefully-chosen dither offsets, it is possible to create an output, co-added image with a finer sampling by “dropping” a virtual grid through the stack and interpolating pixel fluxes at each layer.

Main disadvantage is that pixel-to-pixel noise is NO LONGER uncorrelated.

This technique has become widely known in astronomy when the Advanced Camera for Surveys onboard HST became operational.

Co-addition and Mosaicking



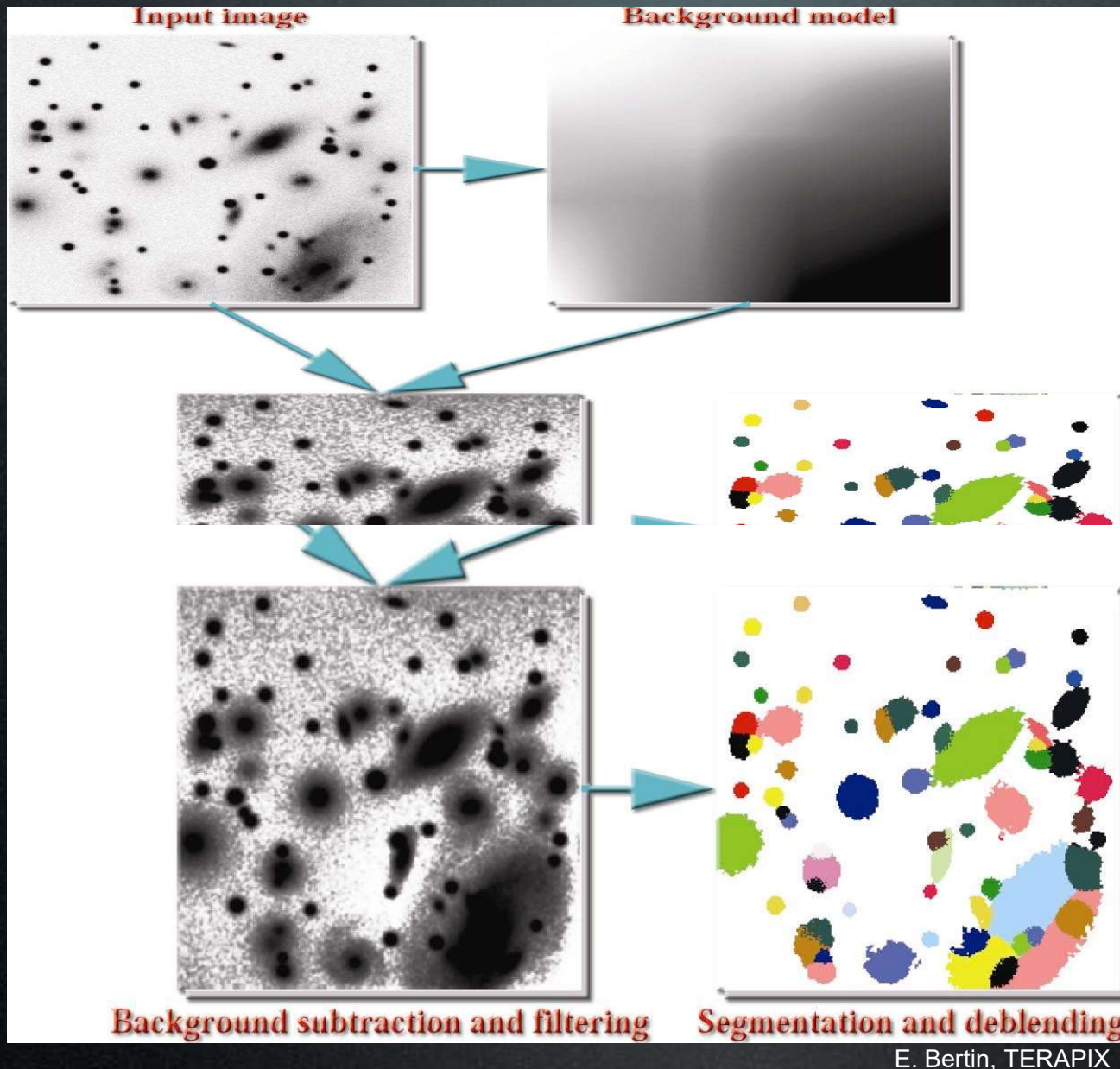
Six separate drizzled
HST/ACS of the
“Tadpole” Galaxy

Median combination
(effective way to
remove cosmic rays)

Required inputs:

1. Good astrometry
2. Data quality masks
3. Weight maps

Source Extraction



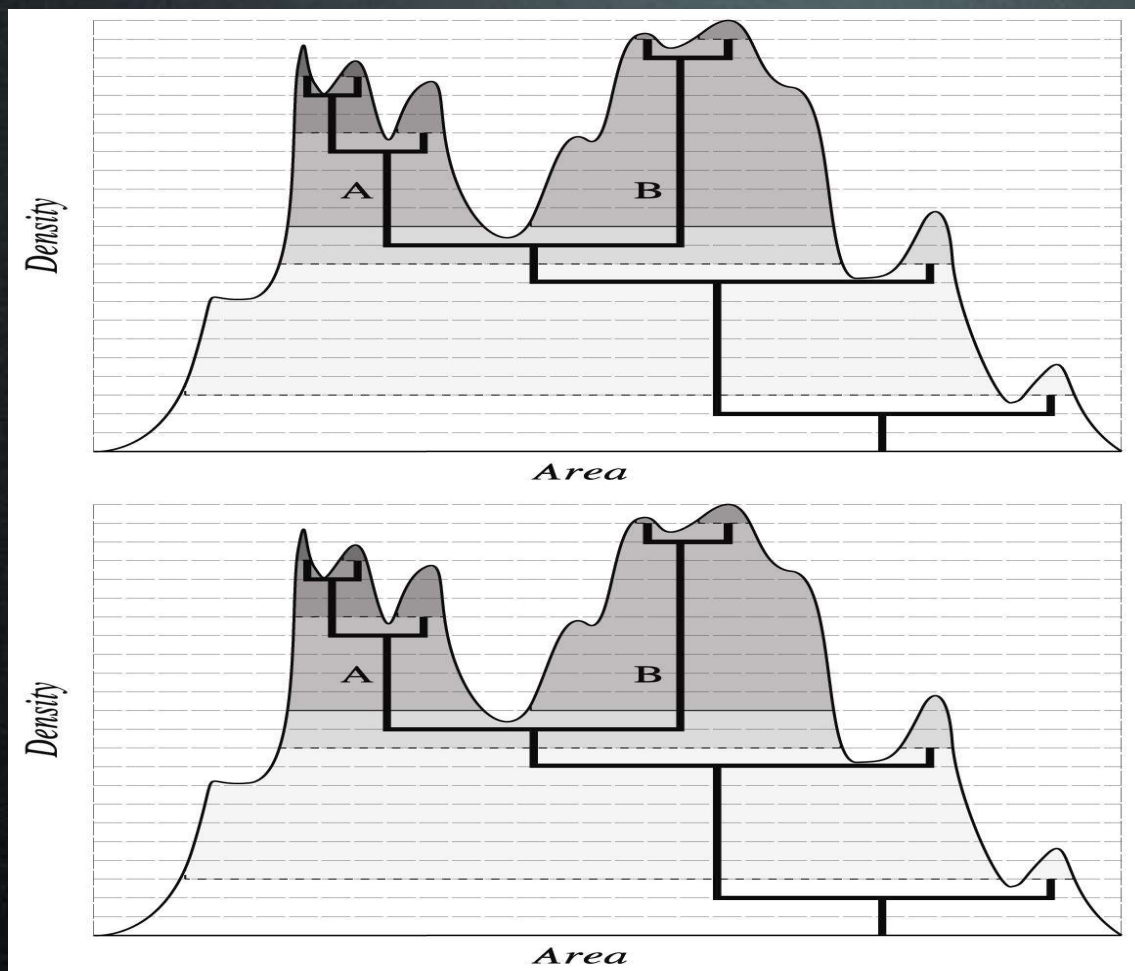
What is a source??

Procedure:

1. Sky background subtraction
2. Image filtering
3. Detection (sigma threshold + minimum area)
4. Segmentation

An image is said to reach the “confusion limit” when surface density of sources on the sky is so high that they cannot be meaningfully deblended.

Source Extraction (continued)



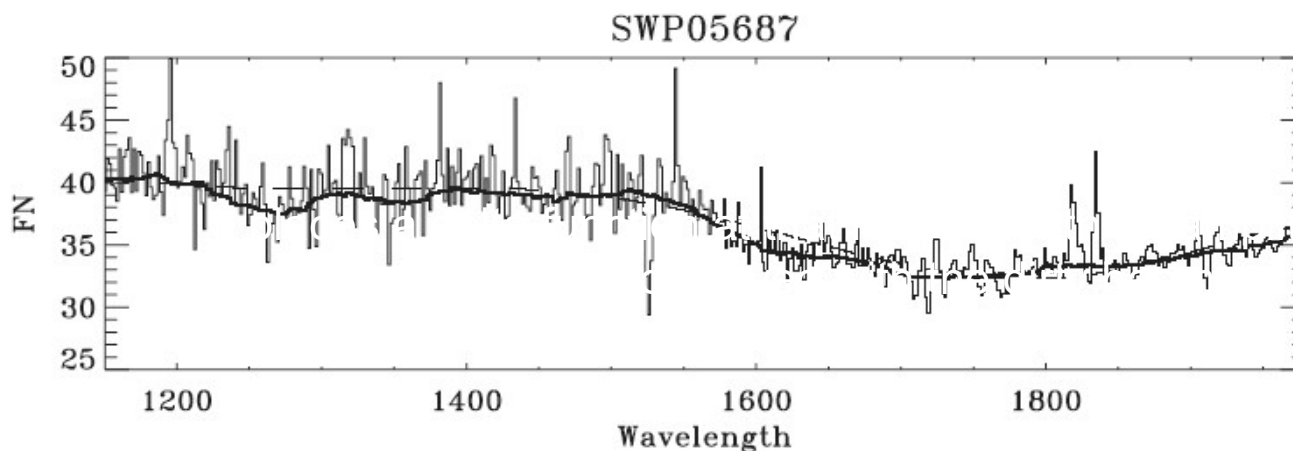
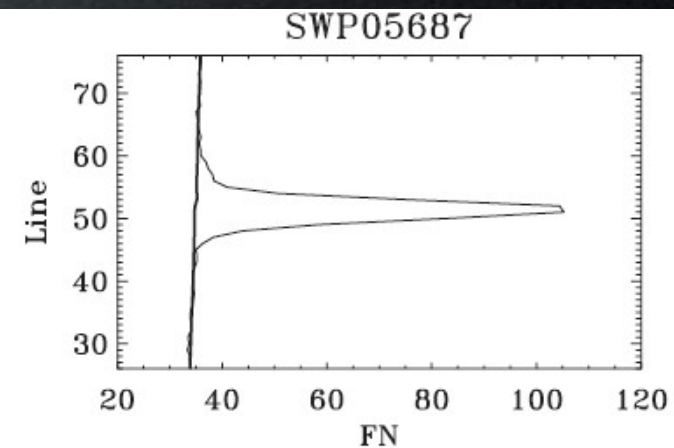
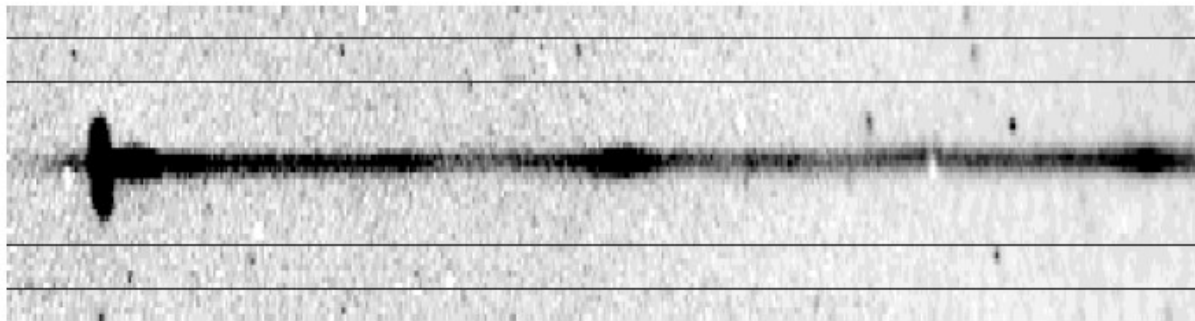
Source Deblending through multi-thresholding (e.g., SExtractor)

The definition of a source is operationally defined by the deblending threshold.

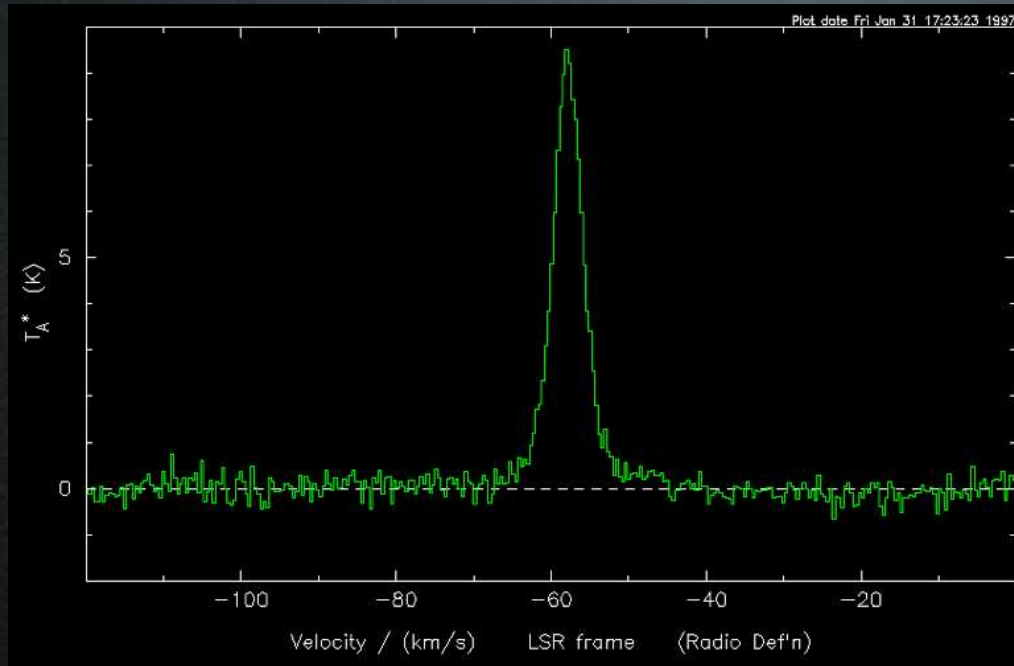
Spectral Extraction

Process by which 1D spectra are extracted from 2D data. The result is improved S/N, but all spatial information is lost. Spectral extraction involves:

1. Defining relative positions of sky windows
2. Tracing spectrum as a function of wavelength
3. Computing a weighted sum of the source flux at each wavelength IF noise spectrum is available - this is called "optimal extraction". Weights are $1/\sigma^2$



Spectral Line Flux



After carefully defining background windows, there are two ways to measure spectral line fluxes:

1. Direct summation
2. (Weighted) fit - should be guided by some a priori (physical) knowledge

A useful concept is the “EQUIVALENT WIDTH” of a line shown below:

